

Recurrent Dynamics of Nonsmooth Systems with Application to Human Gait

Petri Piiroinen

Doctoral Thesis Stockholm, 2002

Royal Institute of Technology Department of Mechanics

Recurrent Dynamics of Nonsmooth Systems with Application to Human Gait

by

Petri Piiroinen

November 2002
Technical Reports from
Royal Institute of Technology
Department of Mechanics
SE-100 44 Stockholm, Sweden



Recurrent Dynamics of Nonsmooth Systems with Application to Human Gait

Petri Piiroinen, 2002

Department of Mechanics, Royal Institute of Technology, 100 44 Stockholm, Sweden

Abstract

The focus of this thesis is on the development of methods of analysis and control of recurrent motions in nonsmooth dynamical systems, with particular emphasis on low-dimensional models of two-legged walking. In particular, passive walkers—bipedal rigid-body mechanisms that achieve sustained gait down incined planes with gravity as the only source of energy—are analyzed to demonstrate the existence of a variety of gait-like recurrent motions, such as periodic, quasiperiodic, and chaotic gait; and to establish the sensitivity of such motions to changes in system parameters and to small perturbations. As an example, the present study contains a careful analysis of the transition between gait motions prevented from exhibiting lateral dynamics and those of fully three-dimensional walkers. It is shown that instability mechanisms appear for the latter mechanisms that cannot be anticipated by a study of the constrained models, suggesting only limited applicability of a two-dimensional analysis to understanding actual human gait. To suggest ways to apply the present study to the clinical context, an idea on how to expand the three-dimensional passive walkers to include muscles is also discussed.

A control algorithm is presented that relies on the presence of discontinuities for controlling the local stability of periodic and other recurrent motions. The method allows one to predict the effects of the control strategy entirely from information about the uncontrolled system. This method is applied to the passive walkers to stabilize highly unstable periodic gait and to switch between different walking patterns. Finally, a method based on the discontinuity-mapping approach is derived to predict the characteristic changes in system behavior that occur following a grazing intersection of a quasiperiodic attractor with a state-space discontinuity. The method is applied to a simple model example representing a two-frequency, quasiperiodic oscillation of a forced van-der-Pol oscillator with a two-dimensional impact surface in a three-dimensional state space.

Descriptors: dynamical systems, nonsmooth dynamics, recurrent motions, stability analysis, solution continuation, Poincaré maps, passive walking, gait characteristics, musculoskeletal modeling

Preface

This thesis considers recurrent motions in dynamical systems with some applications on passive bipedal walkers and it is based on the papers as follow.

- **Paper1.** Petri Piiroinen, Harry Dankowicz, and Arne Nordmark., Breaking Symmetries and Constraints: Transitions from 2D to 3D in Passive Walkers, Accepted for publication in *Multibody System Dynamics*, 2002
- **Paper 2.** Petri Piiroinen, Harry Dankowicz, and Arne Nordmark., On a Normal-Form Analysis for a Class of Passive Bipedal Walkers, *International Journal of Bi-* furcation and Chaos, Vol. 11, No. 9, pp 2411-2425, 2001
- **Paper 3.** Harry Dankowicz, Petri Piiroinen, and Arne Nordmark., Low-velocity Impacts of Quasi-periodic Oscillations, *Chaos, Solitons and Fractals* **14**, pp 241-255, 2002
- **Paper 4.** Harry Dankowicz, Petri Piiroinen, and Arne Nordmark., Grazing Bifurcation of Initially Quasi-periodic System Attractors, In proceedings of *ASME 2001 DETC'01*, Pennsylvania, 2001
- **Paper 5.** Harry Dankowicz and Petri Piiroinen., Exploiting Discontinuities for Stabilization of Recurrent Motions., Accepted for publication in *Nonlinear Dynamics*, 2002
- **Paper 6.** Petri Piiroinen and Harry Dankowicz., Low-Cost Control of Repetitive Gait in Passive Bipedal Walkers, Submitted to *International Journal of Bifurcation and Chaos*, 2002
- **Paper 7.** Petri Piiroinen, Musculoskeletal Modeling of Two-Legged Bipedal Walkers, 2002

Contents

P	Preface			
1	Intr	roduction	1	
	1.1	Two-legged walking	2	
		1.1.1 Human walking	3	
		1.1.2 Artificial walkers	7	
	1.2	Thesis outline	8	
2	Ana	alysis of motion	9	
	2.1	Dynamical systems and Poincaré maps	Ĝ	
		2.1.1 Stability analysis for fixed points and Poincaré maps	11	
		2.1.2 Nonsmooth systems	14	
		2.1.3 Continuation of recurrent motions	16	
	2.2	Local bifurcations of the Poincaré map	18	
		2.2.1 Center manifold and normal forms for maps	18	
	2.3	On the derivation of the equations of motion	22	
	2.4	Linear control of dynamical systems	23	
	2.5	Conclusions	25	
3	Pas	sive walkers	27	
	3.1	Terminology	27	
	3.2	Model considerations	28	
	3.3	Modeling - deriving the equations of motion	30	
		3.3.1 Kinematics	31	
		3.3.2 Joints, foot points, and center of mass locations	32	
		3.3.3 Linear and angular momentum	34	
		3.3.4 Forces and torques	34	
		3.3.5 Dynamics	36	
	3.4	Gait patterns	36	
		3.4.1 2D walkers	37	
		3.4.2 3D walkers	40	
	3.5	Bifurcations and their effect on periodic gaits	41	
	3.6	Control of passive walkers	44	

	3.7 Numerics	44
4	Discussion and outlook	47
5	Summary of papers and authors contributions	49
A	cknowledgments	54
\mathbf{A}	Physical quantities	59
В	Numerical schemes	61
\mathbf{C}	Maple/Sophia code	63
Pa	aper 1 - Breaking Symmetries and Constraints: Transitions from 2D to 3D in Passive Walkers	
Pa	aper 2 - On a Normal-Form Analysis for a Class of Passive Bipedal Walkers	
Pa	aper 3 - Low-velocity Impacts of Quasi-periodic Oscillations	
Pa	aper 4 - Grazing Bifurcation of Initially Quasi-periodic System Attractors	
Pa	aper 5 - Exploiting Discontinuities for Stabilization of Recurrent Motions	
Pa	aper 6 - Low-Cost Control of Repetetive Gait in Passive Bipedal Walkers	
Pa	aper 7 - Musculoskeletal Modeling of Two-Legged Bipedal Walkers	

Chapter 1

Introduction

Most of us experience mechanical devices — cranes, office chairs, bicycles, and elevators — on a daily basis, often without reflecting on their presence or function. Their relatively simple construction leads us to expect these mechanisms to operate without complications with little or no understanding of the connection between performance, reliability, and ease of repair and the underlying details of the engineering design. To enhance our understanding of how these and other mechanical systems function as well as to be able to examine possible improvements to their design, engineers usually rely on the derivation and analysis of mathematical models, in recent times often with the aid of computer software. There are, at least, two characteristically different approaches to creating such mathematical models. In the development and testing of new or redesigned mechanical products, desirable models are usually intended to behave as closely to the actual mechanism as possible. In contrast, when there is a need for a detailed analysis of a specific device behavior, simplified models are used that still exhibit the same behavior as the actual mechanism. The latter approach is also that often used in basic research.

Two fields of research in which both modes of model development are used are biomechanics and robotics. The choice between the simplified and the comprehensive models is very subtle and usually requires significant experience. There are, typically, no general rules as to what approach to follow. In robotics, it is common to first create a comprehensive computer-based model and subsequently to build an actual mechanism. The limiting factor in this procedure is usually of a practical nature rather than at the level of the mathematical model. In biomechanics, on the other hand, computer-based models of one or several body parts of a living organism rely on the use of measurements (say of bone or soft-tissue properties) on the organism for arriving at suitable approximations. It is not hard to understand that the computer model of the robotic device usually agrees more closely with the actual device than the biomechanical model agrees with the biological mechanism.

The way in which the final mathematical models are used also differs significantly between the fields of robotics and biomechanics. For instance, control algorithms developed for the computer model of a robot can often be transferred to the real-world robot (with some modifications) and then implemented in industrial production. In biomechanics, on the other hand, a computer model often acts as a tool and a complement to the knowledge and experience of a practicing physician. As an example, computer-based anthropomorphic model mechanisms could be used to perform virtual surgeries in order assist in preoperative evaluation of the outcome of an actual surgery.

The focus of this thesis are mechanical systems and mathematical models that are influenced by and have implications to both robotics and biomechanics. A primary emphasis will be placed on a qualitative study of the dynamics of the human walking apparatus through a couple of different mathematical models. Even though the models studied here are very simple and far from being as complicated as the human legs, they still account for the key ingredients of the human locomotion, such as footto-ground impacts and the prevension of knee hyperextension. Several of the papers develop ways of analyzing the equations corresponding to these models establishing, among other things, the similarities between model behaviors and characteristics of human walking. That simple models of the walking apparatus are able to show complex anthropomorphic gait has obvious implications to the construction of humanoid robots as well as to explaining and exploring some characteristic features of human locomotion.

Before introducing the mathematical tools needed for the analysis of the equations describing the motion of the two-legged mechanisms modeled in this thesis a short background on two-legged walking will be presented. This introduction will focus on both human and artificial walking.

1.1 Two-legged walking

Humans and most legged mammals have similar locomotion strategies, namely to move themselves from one point to another by changing the leg configurations in a periodic-like way. There are many different characteristics and styles of locomotion that depend on where and how fast the motion is performed. The two main subgroups of locomotion are walking and running, distinguished primarily by the associated speed. In this thesis we will focus on walking, although running is also an interesting area that would be a subject for another thesis.

Another distinction between different kinds of gait is the number of legs used. Most mammals are four-legged (quadrupedal) and their motion patterns can be rather complex, at least when they are walking slowly. From a stability point of view quadrupedal walkers have the advantage over two-legged (bipedal) animals, since they usually have at least three feet in contact with the ground at any given moment. Bipedal walking is more simple in nature but is not typically statically stable and requires more (neural) control to sustain a decent gait.

1.1.1 Human walking

The development of human walking from gorilla-like gait to purely upright gait might have been one of the reasons of the rapid expansion of the humans population, both in size and distribution. This, of course, goes hand-in-hand with increased brain capacity, the ability to use tools, and the development of a language. At the same time, the ability to stand, walk, and run on two legs is pretty unique among mammals. The human walking apparatus can be seen as a very simple mechanism, an inverted double pendulum with a moving support, but so far there is no comprehensive understanding of how it works. What makes human gait so hard to master and analyze is the joint influence of the constitution of the legs, the nature of the muscles, and the local and global control accomplished by the spinal cord and the brain, respectively. At the same time, the complex nature of human gait makes it sensitive and an easy target for a diversity of problems and gait pathologies.

Gait pathologies

There are numerous well-understood processes leading to pathologies in humans gait. Some of them are caused by 'normal' accidents – leg fractures, sprained ankles, and so on. Other common causes of gait pathologies, and usually harder and more complicated to treat than those resulting from accidents, are diseases that generate problems of locomotion in the adult. Even more severe are problems that can be traced back to birth or fetal development and that occur already in the infant child, such as those of a neurological nature.

A common cause of gait problems and an illustrative example of methods used in classifying gait dysfunction is cerebral palsy (CP). Although the cause of CP is not completely understood, it is well-known that premature infants are more likely to develop the disorder than full-term infants. CP is most likely caused by an injury to the immature brain that usually occurs during or shortly after birth. It was originally described by William John Little in 1862, and is also referred to as Little's Disease. The ways in which CP is expressed varies from one patient to the next and therefore a classification of the symptoms is necessary. Cerebral palsy is usually classified by the type of movement problem or by the body parts involved. Spasticity refers to the inability of a muscle to relax, while athestosis refers to the an inability to control the movement of the muscle. Hemiplegia is cerebral palsy that involves one arm and one leg on the same side of the body, whereas diplegia primarily involves both legs. Quadriplegia refers to a CP-related dysfunction that involves all four extremities as well as trunk and neck muscles. A frequently used classification of CP is ataxia, which refers to balance and coordination problems. For more information on cerebral palsy, see Gage [15].

Analysis of walking

A wide-spread method to analyze normal and pathologic gait is to use a video-based motion-capture system based on a set of video cameras that track markers attached to the various body segments of the subject of the experiment coupled with force plates and electromyography (see Whittle [45]). There are a number of different gaitanalysis systems and associated computer software on the market (for example, the Vicon system [44]). The typical setup for professional gait analysis consists of six video cameras, two force plates, and electrodes for detecting neuronal activity. A computer with suitable software performs data analysis on the signals obtained from the video-recording devices to generate quantitative information on the positions and orientations of the various body segments. The force plates (usually one or two) measure the ground-reaction forces on the feet. Together with the data from the video system, it is possible to calculate the forces and torques acting on the different joints. Electromyography is used to measure which muscle is active at different times. A good complement to the video system, the force plates, and electromyography is a calorimeter that calculates the amount of energy used during gait. This is done by measuring the amount of carbon dioxide that the subject exhales in every breath.

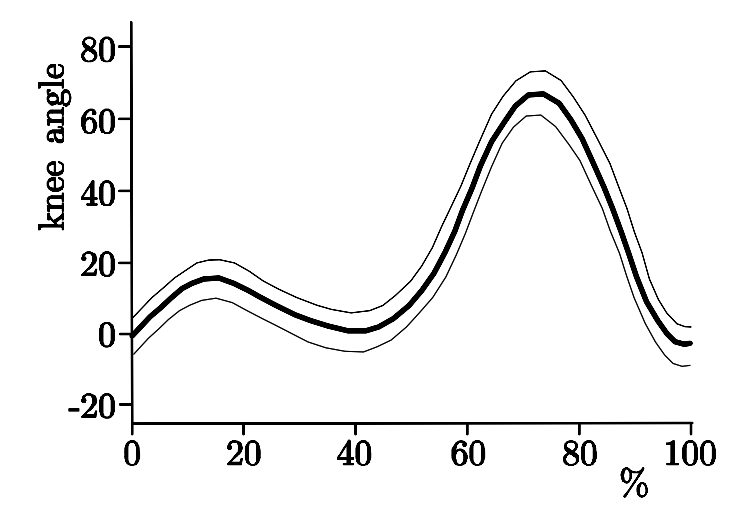


Figure 1.1: The knee angle (in degrees) during one full stride averaged from 30 subject, where the upper and lower curves about the ideal curve show the standard deviation for this sample. The data is from Murray M P, American J Physical Medicine, 46(1), p.290, 1967

There are some fundamental problems that are often encountered when using gait analysis for diagnosis and evaluation of treatment of pathologic gait. The main problem is the great variability in gait pattern between different individuals making it difficult to establish a 'normal' gait. Gait characteristics for an ideal human are instead based on averages across large sample populations. Clinical gait analysis is

then used to see whether the subject's gait differs significantly from normal gait. Figure 1.1 shows the time history of the knee angle during one stride averaged over a sample of 30 subjects. The area (formed by the thin curves) about the ideal curve corresponds to the standard deviation of the time histories of the knee angles.

Reliable gait data is also important and needed when creating models mimicking human or robotic gait. Here, an additional problem occurs, namely the difficulty in correctly measuring body-segment parameters like lengths, masses, moments of inertia, and locations of the corresponding centers of mass. These parameter values are needed for describing dynamical behaviors (deriving equations of motion) of biomechanical models of humans. Historically, body segments of cadavers have been weighed to find the masses and to locate the centers of mass. Moments of inertia of body segments have been determined by finding the natural periods of oscillation, by using both cadavers and living individuals. Another technique to find masses of body parts is to first find their volumes and then using densities averaged over bone and soft tissue. For more information on this issue see [9], [20], [21], [23], [24], and [12].

We conclude this discussion with a summary of some of the applications of gait analysis, gait data, and the measurements of body-segment parameters, namely

- the analysis of the kinematics, kinetics, and energy consumption of human gait;
- pre- and postsurgical evaluation as well as long-term monitoring of the development of gait pathologies; and
- the development of biomechanical models of humans.

1.1.2 Artificial walkers

There are almost as many ideas for how to reproduce human-like gait in an artificial mechanism as there are researchers in the field of robotics. The ideas cover everything from totally unactuated few-degree-of-freedom walkers to completely controlled, highly complex robots. While the ultimate desire in constructing two-legged robots capable of sustained locomotion is to mimic human gait, no perfect human-like gait has yet been performed by a robot.

In this thesis, a distinction is made between unactuated and actuated two-legged walkers, with primary emphasis on the former type to be discussed in greater detail in section 3. To put this in perspective, however, let us take a glimpse into the field of controlled walkers. There are a number of different ongoing projects dealing with controlled two-legged robots, of which we will mention only a few.

• The MIT Leg Laboratory has a long history of constructing a variety of bipedal robots. One of their most well-known bipeds is the Spring Turkey. This three-dimensional mechanism is constrained by an unactuated boom, thus restricting its motion to a two-dimensional gait pattern. The Spring Turkey is actuated in

the hips and knees and walking algorithms are implemented to achieve a desired gait. A successor of the Spring Turkey, the Spring Flamingo, has an increased number of degrees of freedom, but is still constrained by a boom. For both robots, force actuation is achieved through servo motors located in the upper body and coupled to the body segments by elastic springs.

Current work at the LegLab focuses on the M2 robot. It is a three-dimensional, bipedal mechanism with 12 degrees of freedom (3 in each hip, 1 in each knee, and 2 in each ankle). To date, the mechanism has been built and gait has been successfully simulated on a computer. For more information see [33]

- An ongoing project at Laboratoire de Mécanique des Solides and INRIA Rhône-Alpes in France is the construction of two BIP 2000 Robots (see [4]). The first robot, BIP1, has 8 degrees of freedom, while BIP2 has 15 degrees of freedom including a pelvis and a 3-degrees-of-freedom trunk. BIP1 took its first steps in March 2000.
- One of the greatest technological achievements in this area is the Honda humanoid robot project, with the robots P2, P3 and ASIMO. In 1996, Honda developed the human-like robot P2, which is 182 cm tall and weighs 210 kg. It has cameras in its head, an on-board power supply and can perform a variety of walking motions. The P3 robot is 22 cm smaller than P2 and weighs 130 kg. The P3 robot possesses 16 joints that can be individually actuated. In 2000, Honda launched their latest robot, ASIMO, which is 122 cm tall, weighs 52 kg and has 26 degrees of freedom (distributed over 16 joints). Since these are commercial products, a fair amount of secrecy obscures the details of the construction (see [22]).
- Two Swedish humanoid robots called Elvis and Elvina are being developed at Chalmers Institute of Technology (see Nordin et al. [37] and [41]). Their fundamental control algorithms are developed through a learning process, where genetic algorithms allow optimization based on previous errors and successes.

Experimental observations on human gait suggest that almost no muscle activity is present during the swing phase. Instead, the natural pendulum motion of the swing leg appears to make bipedal gait energetically efficient and reasonably robust against external perturbations. This discovery has given impetus to ideas on how to model walking mechanisms with passive elements, such as springs and dampers, using gravity as the only energy source. Such mechanisms are usually referred to as passive. By allowing the passive mechanisms to descend down an incline, the energy dissipated in ground contact and in the joints is balanced by that gained from the descending motion. Most attempts to model passive walkers try to mimic the human body constitution, i.e. with a torso, upper legs, and lower legs connected through joints with varying number of degrees of freedom.

One of the main goals in the analysis of these somewhat simplified models of bipedal walkers is an improved understanding of human gait. As discussed above, this could be used to construct more energy efficient two-legged robots. A separate area of application is the design of new leg prostheses with dynamical behavior more like human legs, and that enable faster and easier recovery after accidents.

As in the case of controlled two-legged robots, there are some projects worth mentioning.

- Tad McGeer [31], [32] was the first to show that a passive bipedal mechanism could walk stably down an incline with gravity as its only energy source. As we will indicate in later sections, this was an *a priori* unexpected result, that has provided a breeding ground for all subsequent work in passive walking. As an aside, McGeer also studied passive running, differentiated from walking by repeated flight phases. For more details see McGeer [30] and Mochon et al. [36].
- Following McGeer's example, Andy Ruina and his group at Cornell University has further studied the gait patters of passive bipedal walkers, both numerically and experimentally. One of the areas of interest has been the existence of periodic gait in the limit of zero slope (see, for instance, Chatterjee et al. [5]). A separate focus has been on achieving stable gait in models with as few degrees of freedom as possible and with as simple ground interactions as possible. For instance, a Tinkertoy model has been successfully constructed that performs stable periodic gait both in experiments and simulations (see Coleman et al. [6] and [7]). In 2000, a passive walker with arm-like limbs was built. The inclusion of passive arms served to reduce the side-to-side rocking by transferring some of the associated angular momentum to an out-of-phase swinging of the arms (see [8]).
- Another approach to the analysis of passive walkers is ballistic walking. In ballistic walking, an impulse is given to the mechanism at each double-support phase, such that the mechanism returns to its initial configuration after one step with the left and right feet shifted. Ballistic walking has been studied by Mochon et al. [35] and Formal'sky [13].

Analysis

There are significant differences between the analysis of human gait and that of human-like models, such as passive walkers and bipedal robots. While the methods for studying human gait are mainly experimental and of a practical nature (see section 1.1.1), the analysis of artificial walkers in general, and of computer-based models of passive walkers in particular, is more theoretical in nature. Such analysis includes mathematical modeling and approximations of biomechanical systems, deriving equations of motion, and numerical computations. Much research is also

devoted to active control of bipedal mechanisms, of obvious importance in robotics. Such research is both focused on the understanding of how muscles work as well as on creating proper control algorithms.

1.2 Thesis outline

The intent of the work presented here is

- to further investigate the passive dynamics of bipedal mechanisms;
- to study the dynamics of a more general class of systems with sudden and abrupt changes in system characteristics, such as the collisions between the feet and the ground in the case of the passive walkers;
- and to develop means for using such sudden and abrupt changes in the design of low-cost control of system dynamics.

The outline of the thesis is as follows. Chapter 2 introduces the mathematical tools and concepts used in this thesis. In chapter 3, we discuss the modeling of the passive walkers, the derivation of the equations of motion, the different gait patterns exhibited by the walkers, and gait bifurcations under parameter variations. The practical implementation of the numerical algorithms is described briefly in chapter 3.7. In chapter 4, a concluding discussion of the subject of the thesis is presented. A presentation of the seven papers constituting the brunt of the thesis and the contributions of the present author is given in chapter 5, which is followed by the seven papers.

Chapter 2

Analysis of motion

In this chapter we will introduce some mathematical concepts and tools used in the analysis of motion in general and for the passive walkers discussed in detail in section 3 in particular. Following a general discussion of dynamical systems, we turn to the important concept of a Poincaré mapping and its use for analyzing the stability of recurrent motions in smooth as well as nonsmooth dynamical systems. We present a useful method for locating and continuing recurrent motions under parameter variations, followed by a discussion about bifurcations and their analysis using normal forms. Finally, we review a general methodology for deriving the equations of motion of a multi-body mechanical systems as well as some fundamental notions involving the of control of such systems. The chapter concludes with a summary of the mathematical techniques introduced here.

2.1 Dynamical systems and Poincaré maps

Dynamical systems are convenient tools for describing systems that evolve in time. When the emphasis is on continuous changes in time, the dynamical system is typically represented by a (system of) differential equation(s). Similarly, iterated maps model systems with discrete time evolution. In many cases, however, such as mechanical systems with impacts, the dynamical-system description incorporates both continuous and discrete states. It is convenient to differentiate between *non-autonomous* systems, for which the changes depend explicitly on time, and *autonomous* systems for which any changes are independent of the current time.

A continuous dynamical system can usually be represented by a system of firstorder differential equations

$$\dot{\mathbf{x}} = \mathbf{f}(\mathbf{x}, t) \quad \mathbf{x} \in \mathbb{R}^n, \tag{2.1}$$

where \mathbf{x} is the state vector and \mathbb{R}^n is known as the state space. The complexity of the dynamical system depends on the dimensionality of the system and degree of nonlinearity and smoothness of the function \mathbf{f} . While a low-dimensional system is

easier to visualize, the possible dynamics are limited relative to the high-dimensional systems. Similarly, nonlinear systems can exhibit nontraditional behaviors, such as sensitive dependence on initial conditions (generally known as chaos) that are not possible for linear systems. Moreover, while general formula exists for the analysis of linear systems, nonlinear systems are typically only analysable through perturbation methods and numerical approximation. This will be discussed later in section 2.1.2.

Example 1 A large class of dynamical systems originates from equations of motion of mechanical systems. For instance, the equations of motion for the forced, onedimensional pendulum can be written

$$\ddot{x} + h(x, \dot{x}) = f(t). \tag{2.2}$$

where x represents the angle of the pendulum. This second-order ordinary differential equation can easily be rewritten as an autonomous system of first order differential equations:

$$\dot{x} = y \tag{2.3}$$

$$\dot{y} = f(\theta) - h(x, y) \tag{2.4}$$

$$\dot{\theta} = 1. \tag{2.5}$$

$$\dot{\theta} = 1. \tag{2.5}$$

As shown in the example, it is always possible to reformulate a non-autonomous system as an autonomous one, at the expense of introducing an additional state variable. Thus, without loss of generality, we restrict attention to systems of the form

$$\dot{\mathbf{x}} = \mathbf{f}(\mathbf{x}), \quad \mathbf{x} \in \mathbb{R}^n. \tag{2.6}$$

Some well-known examples with complex dynamics are the van-der-Pol oscillator, the Lorenz attractor, the Volterra-Lotka predator-prey model and, of course, passive walkers.

If we imagine x as representing the position of a particle in state space, then $\dot{\mathbf{x}}$ represents the particle's velocity. Since Eq. (2.6) is time-independent, the size and direction of the velocity $\dot{\mathbf{x}}$ is given by the unique vector function \mathbf{f} of $\mathbf{x} \in \mathbb{R}^n$. The trajectory followed by the particle through state space is a curve whose tangent direction at any given point x is parallel to f(x). Now imagine that the entire state space is filled with such trajectories, setting up a flow of particles (like in a fluid). We may represent this collection of trajectories by a flow function Φ , such that $\Phi(\mathbf{x}_0, t - t_0)$ corresponds to the point at time t on the trajectory that passes through \mathbf{x}_0 at time t_0 . While it is generally impossible to find an explicit representation for the solutions of Eq. (2.6), and similarly for the flow function Φ , classical theory of ordinary differential equations guarantees the existence of the function Φ with as much smoothness as the vector field \mathbf{f} . In particular one easily shows that

$$\frac{\partial}{\partial t} \Phi(\mathbf{x}, t) = \mathbf{f} (\Phi(\mathbf{x}, t))$$

$$\Phi(\mathbf{x}, 0) = \mathbf{x},$$
(2.7)

$$\Phi\left(\mathbf{x},0\right) = \mathbf{x},\tag{2.8}$$

for all \mathbf{x} and t.

The focus of the modern theory of dynamical systems is the exploration of the qualitative properties of Φ . In particular, emphasis is placed on the existence of recurrent motion, such as equilibria, periodic orbits, and quasi-periodic motions, their stability properties, and their persistence under changes in the system description. Here, recurrent motions are those trajectories that are bounded to a finite volume of state space and that approximately revisit any arbitrary point on the trajectory infinitely many times in forward and backward time.

Equilibria are special examples of state space trajectories that consist of a single point. In particular, an equilibrium \mathbf{x}^* is characterized by

$$\Phi\left(\mathbf{x}^*, t\right) = \mathbf{x}^* \tag{2.9}$$

for all t. It follows that

$$\mathbf{f}\left(\mathbf{x}^*\right) = \mathbf{0},\tag{2.10}$$

i.e., equilibria are zero points of the vector field. Similarly, periodic solutions are state space trajectories that form closed curves. It follows that there exists at least one point \mathbf{x}^* , such that

$$\Phi\left(\mathbf{x}^*, T\right) = \mathbf{x}^*,\tag{2.11}$$

for some T > 0. In fact, since

$$\Phi\left(\Phi\left(\mathbf{x}^{*},t\right),T\right) = \Phi\left(\mathbf{x}^{*},\mathbf{t}\right), t \in [0,T), \tag{2.12}$$

any point on the trajectory may be chosen to represent \mathbf{x}^* .

The existence of a unique period T of a periodic motions shows that the time evolution of any state variable can be written as a Fourier expansion with a single fundamental frequency. In contrast, a quasiperiodic solution is a state space trajectory for which the time evolution of any state variable is characterized by a Fourier expansion with several incommensurable fundamental frequencies.

2.1.1 Stability analysis for fixed points and Poincaré maps

An important concept in dynamical-system analysis is that of *stability* of a state-space trajectory. The stability of a reference trajectory is a measure of its sensitivity to perturbations, i.e., the extent to which nearby trajectories will remain in the vicinity of the original trajectory or deviate from it in forward time. Explorations of the stability characteristics of a reference trajectory are performed by looking at the local flow in the vicinity of the trajectory. In a first approximation, such a local analysis is achieved by a linear approximation of the flow about the reference trajectory.

Specifically, let \mathbf{x} be an initial condition in the vicinity of a point \mathbf{x}^{ref} on the reference trajectory. Then,

$$\Phi(\mathbf{x},t) - \Phi(\mathbf{x}^{\text{ref}},t) \approx \partial_{\mathbf{x}}\Phi(\mathbf{x}^{\text{ref}},t)(\mathbf{x} - \mathbf{x}^{\text{ref}}),$$
 (2.13)

where the Jacobian $\partial_{\mathbf{x}}\Phi\left(\mathbf{x}^{\mathrm{ref}},t\right)$ can be shown to satisfy the linear initial-value problem

$$\dot{\mathbf{X}} = \partial_{\mathbf{x}} \mathbf{f} \left(\Phi \left(\mathbf{x}^{\text{ref}}, t \right) \right) \mathbf{X}, \ \mathbf{X} \left(0 \right) = \mathbf{I}, \tag{2.14}$$

where the differential equation is known as the *variational equation* and \mathbf{I} is an *n*-by-*n* identity matrix.

As an example, consider the stability analysis for an equilibrium \mathbf{x}^* . It follows that the coefficient matrix in the variational equation $\partial_{\mathbf{x}}\mathbf{f}(\mathbf{x}^*)$ is a constant matrix. From the elementary theory of linear differential equations with constant coefficients, it follows that stability is determined by the sign of the real part of the eigenvalues λ_i , $i=1,\ldots,n$, of $\partial_{\mathbf{x}}\mathbf{f}(\mathbf{x}^*)$. Specifically, if the real part of every eigenvalue is less than 0, then the solution is asymptotically stable, i.e. all nearby initial conditions are attracted to the equilibrium as $t\to\infty$. On the other hand, if at least one eigenvalue has a positive real part, it is unstable. Typically, some nearby initial conditions will deviate substantially from the equilibrium in forward time. The linear analysis falls short, however, of predicting stability when all eigenvalues have non-positive real parts and at least one lies on the imaginary axis. In the discussion below, we will refer to equilibria with all eigenvalues off of the imaginary axis as hyperbolic. Non-hyperbolic equilibria are also said to be degenerate.

Although the variational equation may be employed for the stability analysis of periodic solutions, we will use a slightly different approach that has a more geometric appeal, namely that of a Poincaré map. This concept allows us to treat a periodic solution as a fixed point of an iterated map. Similarly, stability properties of the periodic solution correspond to those of the fixed point. To facilitate the analysis, it is convenient to introduce a codimension-one surface in state space, also known as a Poincaré section, for example given by the zero-level surface of a scalar function h, such that a point \mathbf{x} lies on the section if

$$h(\mathbf{x}) = 0. \tag{2.15}$$

In particular, we pick h, such that the periodic solution intersects the corresponding Poincaré section Σ_h transversally at a point \mathbf{x}^* . We define the Poincaré map, \mathbf{P} , for points near \mathbf{x}^* , such that \mathbf{P} maps a point on Σ_h to the subsequent intersection of the corresponding trajectory with Σ_h near \mathbf{x}^* , provided such an intersection can be found (see left panel in Figure 2.1). In particular, it follows that $\mathbf{P}(\mathbf{x}^*) = \mathbf{x}^*$. The Poincaré map is sometimes also referred to as the first return map. As with the flow mapping, it is generally impossible to find a closed formula for \mathbf{P} .

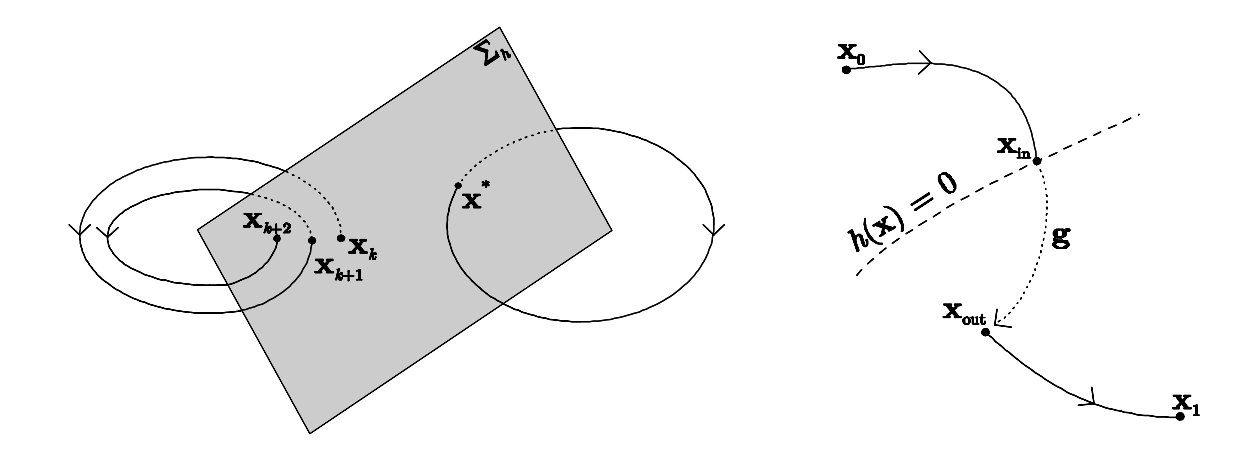


Figure 2.1: Left: Three consecutive intersections $(\mathbf{x}_k, \mathbf{x}_{k+1}, \text{ and } \mathbf{x}_{k+2})$ with the Poincaré section Σ_h and a fixed point \mathbf{x}^* of a Poincaré mapping. Right: A schematic drawing of a discontinuity jump.

The stability of a discrete trajectory of \mathbf{P} based at \mathbf{x}^* is given by the deviation (cf. Eq. 2.13)

$$\underbrace{\mathbf{P} \circ \cdots \circ \mathbf{P}}_{i \text{ times}}(\mathbf{x}) - \underbrace{\mathbf{P} \circ \cdots \circ \mathbf{P}}_{i \text{ times}}(\mathbf{x}^*) \approx \underbrace{\partial_{\mathbf{x}} \mathbf{P}(\mathbf{x}^*) \cdots \partial_{\mathbf{x}} \mathbf{P}(\mathbf{x}^*)}_{i \text{ times}}(\mathbf{x} - \mathbf{x}^*). \tag{2.16}$$

It follows that, to first approximation, the stability of a periodic orbit is given by the eigenvalues of $\partial_{\mathbf{x}} \mathbf{P}(\mathbf{x}^*)$. Specifically, we know that for maps, fixed points are asymptotically stable if all eigenvalues have a magnitude less than 1, and unstable if at least one eigenvalue falls outside the unit circle. Again we refer to a fixed point with all its eigenvalues off of the unit circle as hyperbolic and, similarly, for the corresponding periodic solution. In the degenerate case, the linear analysis fails to predict the local stability behavior.

To compute $\partial_{\mathbf{x}} \mathbf{P}(\mathbf{x}^*)$, let $\tau(\mathbf{x})$ be the time of flight for the orbit through $\mathbf{x} \in \Sigma_h$ to the next intersection with Σ_h , i.e.,

$$h\left(\Phi\left(\mathbf{x},\tau\left(\mathbf{x}\right)\right)\right) = 0. \tag{2.17}$$

Then the Poincaré map can be written

$$\mathbf{P}(\mathbf{x}) = \Phi(\mathbf{x}, \tau(\mathbf{x})), \qquad (2.18)$$

where Φ is the flow introduced above. In particular, $\tau(\mathbf{x}^*) = T$, the period of the periodic motion. From the implicit function theorem, it follows that, for \mathbf{x} near \mathbf{x}^* , τ is a differentiable function of \mathbf{x} provided that

$$\partial_{\mathbf{x}} h\left(\mathbf{x}^*\right) \partial_t \Phi\left(\mathbf{x}^*, T\right) \neq 0.$$
 (2.19)

It is easy to see that this condition is satisfied provided that the intersection of the periodic motion with Σ_h is transversal. It is then possible to show that

$$\partial_{\mathbf{x}}\tau\left(\mathbf{x}^{*}\right) = -\frac{\partial_{\mathbf{x}}h\left(\mathbf{x}^{*}\right)\partial_{\mathbf{x}}\Phi\left(\mathbf{x}^{*},T\right)}{\partial_{\mathbf{x}}h\left(\mathbf{x}^{*}\right)\partial_{t}\Phi\left(\mathbf{x}^{*},T\right)}.$$
(2.20)

By the chain rule, differentiating Eq. (2.18) with respect to \mathbf{x} and evaluating at \mathbf{x}^* , we find

$$\partial_{\mathbf{x}} \mathbf{P} \left(\mathbf{x}^* \right) = \partial_{\mathbf{x}} \Phi \left(\mathbf{x}^*, T \right) + \partial_t \Phi \left(\mathbf{x}^*, T \right) \partial_{\mathbf{x}} \tau \left(\mathbf{x}^* \right). \tag{2.21}$$

Substituting Eq. (2.20) in Eq. (2.21) yields

$$\partial_{\mathbf{x}} \mathbf{P}(\mathbf{x}^*) = \partial_{\mathbf{x}} \Phi(\mathbf{x}^*, T) - \partial_t \Phi(\mathbf{x}^*, T) \frac{\partial_{\mathbf{x}} h(\mathbf{x}^*) \partial_{\mathbf{x}} \Phi(\mathbf{x}^*, T)}{\partial_{\mathbf{x}} h(\mathbf{x}^*) \partial_t \Phi(\mathbf{x}^*, T)}$$
(2.22)

$$= \left(I - \frac{\partial_t \Phi\left(\mathbf{x}^*, T\right) \partial_{\mathbf{x}} h\left(\mathbf{x}^*\right)}{\partial_{\mathbf{x}} h\left(\mathbf{x}^*\right) \partial_t \Phi\left(\mathbf{x}^*, T\right)}\right) \partial_{\mathbf{x}} \Phi\left(\mathbf{x}^*, T\right). \tag{2.23}$$

It is easy to show that at least one eigenvalue of $\partial_{\mathbf{x}}\Phi(\mathbf{x}^*,T)$ must equal 1, namely the eigenvalue corresponding to deviations tangential to the periodic orbit. By Eq. (2.23), this corresponds to a zero eigenvalue of $\partial_{\mathbf{x}}\mathbf{P}(\mathbf{x}^*)$.

The Poincaré-mapping concept is also useful in the analysis of quasiperiodic motions. Contrary to periodic solutions that result in finitely many discrete intersections with Σ_h , quasiperiodic orbits typically intersect the Poincaré section along closed curves. This allows for characterizing quasiperiodic solutions by invariant curves of the Poincaré mapping and for studying the local stability of the solutions in terms of the corresponding behavior of the Poincaré mapping near such curves although the analysis is generally more complicated.

To numerically study the stability characteristics of quasiperiodic motions as well as more complicated recurrent motions, it is convenient to calculate the Lyapunov exponents (see [39], [26], and [19]). This technique is used in paper 3 for a system that exhibits both quasiperiodic and chaotic behaviors.

2.1.2 Nonsmooth systems

So far the focus of the discussion has been on smooth dynamical systems, i.e. systems that are everywhere differentiable. If the system instead experiences sudden changes in the state variables or the vector field, the dynamical system is said to be nonsmooth. The most typical example in mechanics is afforded by the almost instantaneous change in a the relative velocity of two colliding objects, whether modelled by a truly instantaneous jump in state space or by a discontinuous change in forcing. Guided by this observation, Leine [27] classifies nonsmooth dynamical systems into three different categories, namely

1. Non-smooth continuous systems with a discontinuous Jacobian, i.e. systems with a continuous but nonsmooth vector field. $\partial_{\mathbf{x}} \mathbf{f}(\mathbf{x}, t)$ is discontinuous.

Example: Systems with a purely elastic one-sided supports.

2. Filippov systems, i.e., systems with discontinuous vector field. $\mathbf{f}(\mathbf{x},t)$ is discontinuous

Example: Systems with a visco-elastic support and dry friction. This is the model chosen to represent ground impacts for the passive walkers studied in this thesis.

3. Systems with jumps in the state.

Example: Impacting systems with reversing velocities, like a bouncing ball. The hopping mechanism and the Braille printer in paper 5 fall into this category.

In the previous section, the stability of a periodic motion of a smooth dynamical system was determined. As seen below, a special treatment is needed to determine the stability of a trajectory in a dynamical system including discontinuities.

Again, assume we have the dynamical system

$$\dot{\mathbf{x}} = \mathbf{f}(\mathbf{x}), \quad \mathbf{x} \in \mathbb{R}^n \tag{2.24}$$

where \mathbf{f} is a continuous vector field and suppose that there exists a discontinuity surface (or event surface) given by the zero-level surface of a function h, such that an incoming state on the surface is mapped by a jump function \mathbf{g} to another point in state space (see right panel in Figure 2.1). Finally, introduce a Poincaré section Σ_H given by the zero-level surface of a function H, such that the periodic trajectory intersections the section at the point \mathbf{x}^* . In particular, suppose that

$$h\left(\Phi\left(\mathbf{x}^*, t_{\text{disc}}\right)\right) = 0, \tag{2.25}$$

i.e., $t_{\rm disc}$ is the time of flight along the trajectory through \mathbf{x}^* until the discontinuity is reached and there exists a $T > t_{\rm disc}$, such that

$$\mathbf{x}^* = \Phi\left(\mathbf{x}^*, T\right) = \Phi\left(\mathbf{g}\left(\Phi\left(\mathbf{x}^*, t_{\text{disc}}\right)\right), T - t_{\text{disc}}\right). \tag{2.26}$$

To calculate the stability characteristics of the periodic trajectory, consider the Poincaré map

$$\mathbf{P}(\mathbf{x}) = \Phi\left(\mathbf{g}\left(\Phi\left(\mathbf{x}, \tau_{\text{disc}}\left(\mathbf{x}\right)\right)\right), \tau_{\text{ret}}\left(\mathbf{x}\right)\right), \tag{2.27}$$

where \mathbf{x} is a point on Σ_H near \mathbf{x}^* , $\tau_{\text{disc}}(\mathbf{x})$ is the time of flight along the trajectory through \mathbf{x} until the discontinuity is reached and $\tau_{\text{ret}}(\mathbf{x})$ is the time of flight along the same trajectory until the next intersection with Σ_H . From the previous section, it follows that

$$\partial_{\mathbf{x}} \mathbf{P}(\mathbf{x}^*) = \left(I - \frac{\partial_t \Phi\left(\mathbf{x}^*, T\right) \partial_{\mathbf{x}} H\left(\mathbf{x}^*\right)}{\partial_{\mathbf{x}} H\left(\mathbf{x}^*\right) \partial_t \Phi\left(\mathbf{x}^*, T\right)} \right) \partial_{\mathbf{x}} \Phi\left(\mathbf{x}^*, T\right). \tag{2.28}$$

In contrast with the smooth case, however, it is possible to show that

$$\partial_{\mathbf{x}}\Phi\left(\mathbf{x}^{*},T\right) = \partial_{\mathbf{x}}\Phi\left(\mathbf{g}\left(\Phi\left(\mathbf{x}^{*},t_{\mathrm{disc}}\right)\right),T-t_{\mathrm{disc}}\right)\cdot C\left(\Phi\left(\mathbf{x}^{*},t_{\mathrm{disc}}\right)\right)\cdot\partial_{\mathbf{x}}\Phi\left(\mathbf{x}^{*},t_{\mathrm{disc}}\right), \quad (2.29)$$

where the correction term is given by

$$C\left(\Phi\left(\mathbf{x}^{*}, t_{\text{disc}}\right)\right) = \mathbf{g}_{\mathbf{x}}\left(\Phi\left(\mathbf{x}^{*}, t_{\text{disc}}\right)\right) + G, \tag{2.30}$$

where

$$G = \frac{\left(\mathbf{f}\left(\mathbf{g}\left(\Phi\left(\mathbf{x}^{*}, t_{\text{disc}}\right)\right)\right) - \mathbf{g}_{\mathbf{x}}\left(\Phi\left(\mathbf{x}^{*}, t_{\text{disc}}\right)\right)\mathbf{f}\left(\Phi\left(\mathbf{x}^{*}, t_{\text{disc}}\right)\right)\right) h_{\mathbf{x}}\left(\Phi\left(\mathbf{x}^{*}, t_{\text{disc}}\right)\right)}{h_{\mathbf{x}}\left(\Phi\left(\mathbf{x}^{*}, t_{\text{disc}}\right)\right)\mathbf{f}\left(\Phi\left(\mathbf{x}^{*}, t_{\text{disc}}\right)\right)}$$
(2.31)

(cf. Adolfsson et al. [2], Aizerman & Ganthmakher [3], and Müller [34]). More details on the derivation of the correction term and some applications are found in Paper 5 and paper 6.

2.1.3 Continuation of recurrent motions

Before one can study the persistence of recurrent motions under the variation of some system parameter it is essential to first be able to locate such motions. Consider, as a special case, the following methodology for locating periodic trajectories.

Suppose that the periodic orbit is known to transversally intersect a Poincaré section corresponding to the zero-level surface of a function h at some unknown point \mathbf{x}^* . It follows that

$$h(\mathbf{x}^*) = 0 \tag{2.32}$$

and

$$\Phi\left(\mathbf{x}^*, T\right) = \mathbf{x}^* \tag{2.33}$$

for some unknown period T. These two equations correspond to a system of n+1 scalar equations in n+1 unknowns, namely \mathbf{x}^* and T. We can now formulate the multi-dimensional Newton-Raphson method to solve Eqs. (2.32 - 2.33):

$$\begin{pmatrix} \mathbf{x}_{k+1} \\ T_{k+1} \end{pmatrix} = \begin{pmatrix} \mathbf{x}_k \\ T_k \end{pmatrix} - D^{-1} \begin{pmatrix} \Phi(\mathbf{x}_k, T_k) - \mathbf{x}_k \\ h(\mathbf{x}_k) \end{pmatrix}, \tag{2.34}$$

where

$$D = \begin{pmatrix} \partial_{\mathbf{x}} \Phi(\mathbf{x}_k, T_k) - I & \partial_t \Phi(\mathbf{x}_k, T_k) \\ \partial_{\mathbf{x}} h(\mathbf{x}_k) & 0 \end{pmatrix}.$$
 (2.35)

Given a sufficiently good initial guess $\mathbf{x}_0 \approx \mathbf{x}^*$ and $T_0 \approx T$, we expect the above iterations to converge at a rate quadratic in the remaining error to the correct values. Alternatively, reformulating this problem in terms of the corresponding Poincaré mapping, (section 2.1.1), Eqs. 2.34 and 2.35 can be reduced to

$$\mathbf{x}_{k+1} = \mathbf{x}_k - \partial_{\mathbf{x}} \mathbf{P} \left(\mathbf{x}_k \right)^{-1} \mathbf{P} \left(\mathbf{x}_k \right), \tag{2.36}$$

where

$$\partial_{\mathbf{x}} \mathbf{P}(\mathbf{x}_{k}) = \left(\mathbf{I} - \frac{\partial_{t} \Phi\left(\mathbf{x}_{k}, \tau\left(\mathbf{x}_{k}\right)\right) \partial_{\mathbf{x}} h\left(\Phi\left(\mathbf{x}_{k}, \tau\left(\mathbf{x}_{k}\right)\right)\right)}{\partial_{\mathbf{x}} h\left(\Phi\left(\mathbf{x}_{k}, \tau\left(\mathbf{x}_{k}\right)\right)\right) \partial_{t} \Phi\left(\mathbf{x}_{k}, \tau\left(\mathbf{x}_{k}\right)\right)} \right) \partial_{\mathbf{x}} \Phi\left(\mathbf{x}_{k}, \tau\left(\mathbf{x}_{k}\right)\right). \tag{2.37}$$

For example, if a hyperbolic periodic orbit with a transversal intersection with the Poincaré section has been found for a given set of parameter values, then standard persistence theory guarantees the continued presence under small variations in the parameters of such a periodic orbit in the vicinity of the original orbit, with qualitatively identical stability characteristics. We can thus employ a continuation algorithm to follow stable as well as unstable periodic solutions under parameter variations until either hyperbolicity is lost (i.e., in a bifurcation - se further below in section 2.2) or transversality is lost (in which case we should change to a different Poincaré section). As with any iterative method, convergence relies on a satisfactory initial guess. In the implementation of the Newton-Raphson scheme described here, we let the initial guess be determined by extrapolation taking into account solutions found for nearby parameter values. For instance, the most simple method is to use linear extrapolation, in which two previously found fixed points $\mathbf{x}_{p_1}^*$ and $\mathbf{x}_{p_2}^*$ (for the parameters p_1 and p_2 , respectively) are used to find an initial guess \mathbf{x}_{p_3} , such that

$$\mathbf{x}_{p_3} = 2\mathbf{x}_{p_2}^* - \mathbf{x}_{p_1}^*, \tag{2.38}$$

where it is assumed that $p_3 - p_2 = p_2 - p_1$. Other, more complex extrapolation methods are certainly possible and may improve convergence when the periodic solution changes rapidly in state space under variations of some state parameter.

If the recurrent motion includes a discontinuity, the Jacobian $\partial_{\mathbf{x}}\Phi(\mathbf{x}_k, T_k)$ has to be modified so that

$$\partial_{\mathbf{x}}\Phi\left(\mathbf{x}_{k},T_{k}\right) = \partial_{\mathbf{x}}\Phi\left(\mathbf{g}\left(\Phi\left(\mathbf{x}_{k},t_{c}\right)\right),T_{k}-t_{c}\right)\cdot C\left(\Phi\left(\mathbf{x}_{k},t_{c}\right)\right)\cdot\partial_{\mathbf{x}}\Phi\left(\mathbf{x}_{k},t_{c}\right),\tag{2.39}$$

where t_c is the time of flight from \mathbf{x}_k to the discontinuity. The correction term $C\left(\Phi\left(\mathbf{x}_k,t_c\right)\right)$ (cf. Eq. (2.39)) is calculated as described in section 2.1.2.

Continuation methods for quasiperiodic motions require a somewhat different approach than the one presented above for periodic motions. As suggested above, a

quasiperiodic motion corresponds to an invariant curve for the Poincaré mapping. The continuation algorithm will consequently have to follow closed curves under the variation of some system parameter. One way to complete this is to make a discretization of the curve and use splines to build up the closed curve. Then the Newton-Raphson scheme could be used for each discretization point, but instead of trying to locate fixed points - points that are mapped onto themselves - each point used for discretization should be mapped onto the closed curve. The number of unknowns for this method is significantly larger than when finding fixed points, since large number of discretization points are necessary to ensure good accuracy.

2.2 Local bifurcations of the Poincaré map

Most dynamical systems representing mechanical systems have several parameters affecting their behavior. Clearly, the existence and stability of the types of motions discussed in the previous section depend on the values of the system parameters. We are especially interested in classifying changes due to small parameter variations. In particular, we will denote a change in the number of solutions or their stability as a bifurcation and the corresponding point in parameter space as a bifurcation point. A point on a particular branch of equilibria, fixed points, or periodic solutions in a combined parameter and state space is said to be regular if no bifurcation occurs. As an example, it is possible to show that points in this space corresponding to hyperbolic equilibria or periodic orbits are regular.

The above conclusions are only valid for systems with a continuous vector field. As already discussed, many dynamical systems possess state-space discontinuities, for example, modeling impacts or friction in mechanical systems. Bifurcations can occur due to interactions with these discontinuities, even in the presence of hyperbolicity. For example, in the case of the walking mechanism, foot scuffing may occur during the swing phase (see chapter 3.4), resulting in a rapid change in existence and stability characteristics of recurrent gait and subsequent collapse.

In the vicinity of a bifurcation point, a nonlinear treatment is necessary since the linear analysis predicts a degenerate solution at the bifurcation point. As we will show below, it is possible to derive a reduced description of the dynamics, a normal form, which allows a complete unfolding of the local bifurcation behavior. The number of free parameters of the normal form is known as the codimension of the bifurcation. In this thesis, we restrict attention to codimension-one bifurcations. However, codimension-m bifurcations do occur for passive walkers and might be a focus of another thesis.

2.2.1 Center manifold and normal forms for maps

Since our main concern are periodic and other recurrent motions the following discussion is limited to Poincaré maps. Similar results can be found for the continuous

case. Given a fixed point \mathbf{x}^* of the Poincaré map, we can associate three disjoint subspaces corresponding to direct sums of the generalized eigenspaces for eigenvalues of $\partial_{\mathbf{x}} \mathbf{P}(\mathbf{x}^*)$ inside, outside, and on the unit circle. These are denoted by

 $E^s = \operatorname{span}\{n_s \text{ generalized eigenvectors whose eigenvalue has modulus } < 1\},$

 $E^u = \operatorname{span}\{n_u \text{ generalized eigenvectors whose eigenvalue has modulus } > 1\},$

 $E^c = \operatorname{span}\{n_c \text{ generalized eigenvectors whose eigenvalue has modulus } = 1\},$

where $n_s + n_u + n_c = n$, the dimensionality of the discrete dynamical system. These are invariant for the linearized dynamics near \mathbf{x}^* . In particular, for the linearized map, solutions lying on E^s decay exponentially (monotonically or oscillatory) to \mathbf{x}^* , since a general solution is given by

$$\mathbf{P}^{i}(\mathbf{x}) = \sum_{j} \mathbf{p}_{j}(i)\lambda_{j}^{i}, \tag{2.40}$$

where the \mathbf{p}_j s are vectorial polynomials in i, and the λ_j s are the corresponding eigenvalues. Similarly, solutions in E^u grow exponentially in discrete time and solutions in E^c grow at most polynomially fast in discrete time.

For hyperbolic fixed points, E^c is empty and by the stable-manifold theorem (see e.g. Guckenheimer & Holmes [19] and Strogatz [43]), we can guarantee the existence of locally invariant (for the full nonlinear dynamics) manifolds W^s_{loc} and W^u_{loc} close to x_0 . The dynamics on W^s_{loc} and W^u_{loc} are qualitatively identical to those on the linear spaces E^s and E^u , respectively. From this we can conclude that the stability derived for the linearized Poincaré map also holds for the original map in a neighborhood of the fixed point.

In addition to local stable and unstable manifolds, for degenerate fixed points and sufficiently smooth Poincaré maps, the center-manifold theorem ensures the existence of an invariant manifold W_{loc}^c , known as a center manifold, that is tangent to the center eigenspace E^c at the fixed point. While W_{loc}^s and W_{loc}^u are unique, W_{loc}^c need not be. Since W_{loc}^c is a manifold and its dimension equals n_c , there exists a linear coordinate transformation such that W_{loc}^c is parameterized by the first n_c coordinates

$$\mathbf{x} = \mathbf{h}(\mathbf{z}, \boldsymbol{\mu}),\tag{2.41}$$

where $\mathbf{x} = (q_1, \dots, q_n)$, $\mathbf{z} = (q_1, \dots, q_{n_c})$, and $\boldsymbol{\mu} = (\mu_1, \dots, \mu_k)$. Without loss of generality, assume that $\mathbf{x} = \mathbf{x}^*$ corresponds to $\mathbf{z} = \mathbf{0}$ and the bifurcation point is given by $\boldsymbol{\mu} = \mathbf{0}$. Then, since W_{loc}^c is tangential to E^c ,

$$\mathbf{x}^* = \mathbf{h}(\mathbf{0}, \mathbf{0}) \tag{2.42}$$

and

$$\partial_{\mathbf{z}}\mathbf{h}(\mathbf{0},\mathbf{0}) = \mathbf{0}.\tag{2.43}$$

We now make a Taylor-expansion ansatz, which we eventually truncate at some low order:

$$\mathbf{x} = \mathbf{h}(\mathbf{z}, \boldsymbol{\mu}) = \sum_{i_1, \dots, i_k > 0} \mathbf{x}_{[i_1, \dots, i_k]}(\mathbf{z}) \frac{1}{i_1! \dots i_k!} \mu_1^{i_1} \dots \mu_k^{i_k}, \tag{2.44}$$

where

$$\mathbf{x}_{[i_1,\dots,i_k]}(\mathbf{z}) = \frac{\partial^m \mathbf{h}(\mathbf{z}, \boldsymbol{\mu})}{\partial^{i_1} \mu_1 \cdots \partial^{i_k} \mu_k} \text{ and } m = i_1 + \dots + i_k.$$
 (2.45)

Since $\mathbf{x} = \mathbf{x}^*$ for $\mathbf{z} = \mathbf{0}$ and $\boldsymbol{\mu} = \mathbf{0}$, it must hold that $\mathbf{x}_{[0,\dots,0]}(\mathbf{0}) = \mathbf{x}^*$. Since the manifold is invariant, we write the dynamics in \mathbf{z} as

$$\mathbf{z}_{n+1} = \mathbf{c}(\mathbf{z}_n, \boldsymbol{\mu}) = \sum_{i_1, \dots, i_k \ge 0} \mathbf{c}_{[i_1, \dots, i_k]}(\mathbf{z}_n) \frac{1}{i_1! \cdots i_k!} \mu_1^{i_1} \cdots \mu_k^{i_k}.$$
 (2.46)

where

$$\mathbf{c}_{[i_1,\dots,i_k]}(\mathbf{z}_n) = \frac{\partial^m \mathbf{c}(\mathbf{z}, \boldsymbol{\mu})}{\partial^{i_1} \mu_1 \cdots \partial^{i_k} \mu_k} \text{ and } m = i_1 + \dots + i_k.$$
 (2.47)

Since $\mathbf{z} = \mathbf{0}$ and $\boldsymbol{\mu} = \mathbf{0}$ is a fixed point, we must have $\mathbf{c}_{[0,\dots,0]}(\mathbf{0}) = \mathbf{0}$. To find the coefficient functions, we substitute Eqs. (2.44) and (2.46) in

$$\mathbf{x}_{n+1} = \mathbf{P}\left(\mathbf{x}_n, \boldsymbol{\mu}\right) \tag{2.48}$$

and obtain

$$P(h(\mathbf{z}_n, \boldsymbol{\mu}), \boldsymbol{\mu}) - h(\mathbf{c}(\mathbf{z}_n, \boldsymbol{\mu}), \boldsymbol{\mu}) = 0. \tag{2.49}$$

This can be Taylor expanded about $\mu=0$ to yield the equations for the coefficient functions.

Let us look at the following simple example (taken from Guckenheimer & Holmes [19]) that shows how to derive the center manifold and the corresponding dynamics:

Example 2 Consider the map

$$x_{n+1} = x_n + x_n y_n, (2.50)$$

$$y_{n+1} = \mu y_n - x_n^2, \quad 0 < \mu < 1.$$
 (2.51)

The Jacobian at the fixed point $(x_n, y_n) = (0, 0)$ is

$$J|_{(0,0)} = \begin{pmatrix} 1 & 0 \\ 0 & \mu \end{pmatrix}, \tag{2.52}$$

with the eigenvalues $\lambda_1 = 1$ and $\lambda_2 = \mu$. The center eigenspace corresponds to the x-axis. The center manifold is thus one-dimensional and parameterized by x, i.e., $y = h(x, \mu)$. The tangency conditions imply that $h(0, \mu) = h'(0, \mu) = 0$. If we Taylor expand $h(x, \mu)$ in x we get

$$y = a(\mu) x^{2} + b(\mu) x^{3} + \mathcal{O}(x^{4}), \tag{2.53}$$

where $a(\mu) = h''(0, \mu)$ and $b(\mu) = h'''(0, \mu)$. Substituting (2.53) into Eq. (2.51) and using Eq. (2.50) we get

$$a(\mu)(x + x(a(\mu)x^{2} + \dots))^{2} + b(\mu)(x + x(a(\mu)x^{2} + \dots))^{3} -\mu(a(\mu)x^{2} + b(\mu)x^{3}) + x^{2} = \mathcal{O}(x^{4})$$
(2.54)

or

$$a(\mu) x^{2} + b(\mu) x^{3} - \mu a(\mu) x^{2} - \mu b(\mu) x^{3} + x^{2} = \mathcal{O}(x^{4})$$
 (2.55)

so that

$$a(\mu) = \frac{1}{\mu - 1},$$
 (2.56)

and

$$b\left(\mu\right) = 0. \tag{2.57}$$

Thus we obtain

$$y = \frac{x^2}{\mu - 1} + \mathcal{O}(x^4) \tag{2.58}$$

for the center manifold, and

$$x_{n+1} = x_n + \frac{x_n^3}{\mu - 1} + \mathcal{O}(x_n^4)$$
 (2.59)

for the corresponding dynamics. It is straightforward to show that for $x_0 < \sqrt{1-\mu}$, $x_n \to 0$ as $n \to \infty$, i.e., the fixed point $(x_n, y_n) = (0, 0)$ is locally asymptotically stable for the full dynamics.

While the analysis above applies to sufficiently smooth systems, many interesting application involve singularities of some sort. For example, an interesting limit of our walker corresponds to infinitely wide feet, for which the dynamics in certain degrees of freedom become infinitely fast. This resembles the singularly perturbed dynamical systems

$$\dot{x} = f(x, y) \tag{2.60}$$

$$\varepsilon \dot{y} = g(x, y), \tag{2.61}$$

where for small ε the changes in y occur on a time scale much shorter than the corresponding time scale for x. Nevertheless, as discussed in great detail in paper 1 and paper 2, the center-manifold approach appears to work even near the singular limit. For a nice paper on singular limits of dynamical systems, see Guckenheimer [18].

2.3 On the derivation of the equations of motion

To derive the equations of motion (EOM) of mechanical systems in general and the passive walkers described in section 3 in particular, *Kane's method* (see Kane & Levinsson [25] and Lesser [29]) is used here. Kane's method is based on *d'Alemberts principle of virtual work*. The idea behind this is that the total power consumed by the constraint forces during allowable motions is zero. This assumption allows the elimination of the unknown constraint forces from the analysis through a projection of the full Newtonian equations of motion onto the possible directions of allowable motions.

Assume we have a mechanical system consisting of k rigid bodies. Then the position vector of the center of mass, the corresponding velocity vector, and the angular velocity vector of the ith body relative to some inertial reference frame \mathcal{N} can be written $\mathbf{r}_i^{CM} = \mathbf{r}_i(q,t)$, $\mathbf{v}_i^{CM} = \mathbf{v}_i^{CM}(u,q,t)$, and $\boldsymbol{\omega}_i = \boldsymbol{\omega}_i(u,q,t)$, respectively. Here $q = (q_1, \ldots, q_g)^T$ is a set of configuration coordinates collected in a column matrix and $u = (u_1, \ldots, u_d)^T$ is a minimal set of independent velocity coordinates, also known as generalized speeds, such that

$$\dot{q} = K(q,t)u + k(q,t). \tag{2.62}$$

These equations are known as the kinematic differential equations and allow the complete integration of the motion given the time-dependence of the generalized speeds. Following the notation of Dankowicz [10], the linear and angular velocity vectors can be collected in a column matrix v such that

$$v = \begin{pmatrix} \mathbf{v}_1^{CM} & \boldsymbol{\omega}_1 & \cdots & \mathbf{v}_k^{CM} & \boldsymbol{\omega}_k \end{pmatrix}^T = \beta(q, t)u + \beta_t(q, t)$$
 (2.63)

where

$$\beta = (\boldsymbol{\beta}_1 \cdots \boldsymbol{\beta}_d) \text{ and } \beta_t = (\boldsymbol{\beta}_{t,1} \cdots \boldsymbol{\beta}_{t,k})^T$$
 (2.64)

and the β_i s are linearly independent tangent vectors to the configuration manifold. The momentum description of the mechanical system is given by the row matrix

$$p = (m_1 \mathbf{v}_1^{CM} \quad \mathbf{I}_1^{CM} \cdot \boldsymbol{\omega}_1 \quad \cdots \quad m_k \mathbf{v}_k^{CM} \quad \mathbf{I}_k^{CM} \cdot \boldsymbol{\omega}_k). \tag{2.65}$$

where m_i is the mass of the *i*th rigid body and \mathbf{I}_i^{CM} is moment of inertia dyad of the same body. From Newton's second law of motion it is given that

$$F_a + F_c + \dot{p} = 0, (2.66)$$

where \dot{p} is the rate of change of the momentum description (2.65) relative to the inertial reference frame and where

$$F_a = \begin{pmatrix} \mathbf{F}_{a,1} & \mathbf{T}_{a,1}^{CM} & \cdots & \mathbf{F}_{a,k} & \mathbf{T}_{a,k}^{CM} \end{pmatrix}$$
 (2.67)

and

$$F_c = \begin{pmatrix} \mathbf{F}_{c,1} & \mathbf{T}_{c,1}^{CM} & \cdots & \mathbf{F}_{c,k} & \mathbf{T}_{c,k}^{CM} \end{pmatrix}$$
 (2.68)

are force descriptions of the applied and constraint forces and torques, respectively. d'Alemberts principle, in this context, states that

$$F_c \bullet \beta = 0, \tag{2.69}$$

i.e. that the constraint force descriptions are 'perpendicular' to the tangent vectors $\boldsymbol{\beta}_i$. Here the \bullet denotes a regular vector dot product distributed across a matrix product. From Newton's second law of motion (2.66) and Eq. (2.69), we get the final form of the equations of motion

$$0 = (F_a + F_c - \dot{p}) \bullet \beta \tag{2.70}$$

$$= (F_a - \dot{p}) \bullet \beta. \tag{2.71}$$

This form of the equations of motion of the mechanisms studied in this thesis has been implemented numerically with great success. Other methods to derive the EOM are certainly possible, but the final results should always be the same, regardless of the method used.

2.4 Linear control of dynamical systems

Most interesting dynamical control systems are nonlinear and normally require nonlinear control methods. By using linearization techniques it is still possible to control such systems, as we will se below.

Consider the continuous nonlinear control system

$$\dot{\mathbf{X}} = \mathbf{f} \left(\mathbf{X}, \mathbf{U} \right), \tag{2.72}$$

where \mathbf{X} is the state and \mathbf{U} is the control input. Let $\hat{\mathbf{X}}$ be a solution of (2.72) generated by the input $\hat{\mathbf{U}}$. By writing

$$\mathbf{x}(t) = \mathbf{X}(t) - \hat{\mathbf{X}}(t) \text{ and}$$
 (2.73)

$$\mathbf{u}\left(t\right) = \mathbf{U}\left(t\right) - \hat{\mathbf{U}}\left(t\right) \tag{2.74}$$

the linearized control system can be written

$$\dot{\mathbf{x}} = A(t)\,\mathbf{x} + B(t)\,\mathbf{u},\,\mathbf{x} \in \mathbb{R}^n \tag{2.75}$$

where

$$A(t) = \frac{\partial \mathbf{f}}{\partial \mathbf{X}} \left(\hat{\mathbf{X}}(t), \hat{\mathbf{U}}(t) \right) \text{ and } B(t) = \frac{\partial \mathbf{f}}{\partial \mathbf{U}} \left(\hat{\mathbf{X}}(t), \hat{\mathbf{U}}(t) \right)$$
(2.76)

if $\mathbf{X}(t)$ is sufficiently close to $\hat{\mathbf{X}}(t)$. The goal of the control algorithm may be to develop a feedback law whereby \mathbf{u} is computed in order to ensure an asymptotic behavior arbitrarily close to $\hat{\mathbf{X}}(t)$.

In the special case where $\hat{\mathbf{X}}$ and $\hat{\mathbf{U}}$ are independent of time, the matrices A and B are constant. There are a numerous of different choices and approaches to find a feedback \mathbf{u} for the corresponding linearized control system (2.75). The most simple control is given by the state feedback

$$\mathbf{u} = C\mathbf{x} \tag{2.77}$$

where C is a constant gain matrix. Substituting (2.77) into (2.75) then yields

$$\dot{\mathbf{x}} = A\mathbf{x} + BC\mathbf{x} = F\mathbf{x},\tag{2.78}$$

where F = A + BC. As discussed in an earlier section, the stability of (2.78) is given by the eigenvalues λ_i of F. Under suitable conditions on the matrices A and B, it is possible to assign arbitrary eigenvalues to F by choosing the elements of C appropriately.

For a discrete nonlinear dynamical system the same approach as above can be applied, such that

$$\mathbf{x}_{n+1} = A\mathbf{x}_n + B\mathbf{u}_n \tag{2.79}$$

and the state feedback can again be given the form

$$\mathbf{u}_n = C\mathbf{x}_n \tag{2.80}$$

yielding

$$\mathbf{x}_{n+1} = A\mathbf{x}_n + BC\mathbf{x}_n = F\mathbf{x}_n,\tag{2.81}$$

The eigenvalues of F are the given by solving

$$\det\left(A + BC - \lambda I\right) = 0,\tag{2.82}$$

and the discrete system (2.79) is stable when all eigenvalues lie within the unit circle in the complex plane, i.e., $|\lambda_i| \leq 1$ for all i.

In papers 5 and 6, a control algorithm is developed that shares some features in common with the discrete version of the control discussed above. There, the feedback achieves only an indirect influence on the system dynamics by affecting the timing of subsequent impacts of a mechanism with its surrounding environment. The method is based on the ability to calculate the stability of discontinuous systems (cf. section 2.1.2).

2.5 Conclusions

In conclusion, we can employ the methods of dynamical-systems analysis to

- identify relevant features of the system dynamics,
- study their stability characteristics,
- evaluate their persistence under parameter variations, and
- predict local dynamics in the vicinity of bifurcations.

However, we generally have no a priori methods for

- arguing the existence of periodic orbits in the first place,
- locating them if we have reason to believe they exists, or
- evaluating the persistence of such orbits that approach grazing incidence with discontinuity surfaces.

In light of these observations, it is quite unexpected to find periodic solutions for the mechanisms studied in this thesis, particularly the passive walkers. Having found one such periodic solution we can use the continuation methods discussed above to find additional motions for nearby parameter values. Even more surprising, however, is the persistence of periodic solutions over large parameter ranges. After all, solution branches could terminate in saddle-node bifurcations or through foot-scuffing. In fact, quite frequently this is the fate for many solution branches. Methods for studying the influence of foot scuffing of periodic gait patterns can be found in the literature. Some attempts to predict the influence of such scuffing on initially quasiperiodic gait patterns are described in papers 3 and 4.

Chapter 3

Passive walkers

In this chapter, we discuss aspects of the modeling of passive walkers, such as model kinematics, forces, torques, and the derivation of the equations of motion as well as different gait patterns and bifurcations under parameter variations for both two- and three-dimensional passive walkers.

3.1 Terminology

Since the emphasis of this thesis is the dynamics of two-legged passive walkers, we will here introduce some of the terminology commonly used in both medical and engineering disciplines. Most of these terms are used by a majority of the researchers in the field of walking but some were previously introduced by the present author and collaborators in Adolfsson [1] and Piiroinen [40].

The term walking implies locomotion for which at least one of the two feet is in contact with the ground at any given moment. Walking is made up from of a number of gait cycles or steps that follow each other. A step is completed once both legs have performed a full revolution. A gait cycle can be divided into two distinct phases, namely, the single-support phase and the double-support phase. In the single support phase, one leg—the stance leg—is in contact with the ground while the other leg—the swing leg—performs a pendulum-like motion about its (moving) support. The time interval during which both legs are simultaneously in contact with the ground is referred to as the double-support phase. A gait is period-n if n is the smallest integer, such that the configuration of the legs is identical to their initial configuration after n steps. There are (at least) two different periodic gaits that need some further explanations. In symmetric gait, the left and right legs perform the same motion with a time shift of half a period, while in asymmetric gait or limping gait, the left and right legs do not perform the same motion.

If the swing-leg foot hits the ground during its pendulum phase prior to the swing-leg knee reaching its full extension, the gait experiences a foot scuff. For the passive walkers studied here foot scuffing typically has a negative effect, resulting in a discontinued gait and subsequent collapse. Humans, on the other hand, use their muscles to overcome the retarding action of the premature ground contact and the gait can be continued as if nothing ever happened. The limiting case, when the swing-leg foot barely touches the ground during its pendulum motion, is called *grazing*. While humans hardly notice such light ground touches, the gait of passive walkers might turn chaotic (see section 3.4).

Three planes are referred to repeatedly in our discussions, namely

- the ground the inclined plane restricting the motion of the mechanism,
- the sagittal plane the symmetry plane of the mechanism (this assumes that the right and left legs as well as the torso are identical under reflection), and
- the nominal plane any plane perpendicular to the ground that contains the gravity vector.

We conclude this section by a discussion of the different walkers analyzed in this thesis. The simplest walker model is the 2D walker, whose motion and geometry is constrained to a nominal plane and lacks side-to-side motion. Interactions of the walker feet with the ground are modeled through a single contact point per foot. A relative of the 2D walker is the planar walker that has zero hip width, but infinitely wide feet with one contact point on either end. While a planar walker is able to move freely in space, the foot geometry effectively constrains its motion to some plane perpendicular to the ground, i.e., the motion has constant heading relative to the nominal plane. An extended 2D walker differs from the planar walker in that the feet have finite width but remain symmetric about the zero-width hip. This removes the effective planar constraint, allowing it to exhibit side-to-side motion. Because of their design, extended 2D walkers may exhibit all the motions of the regular 2D walkers. We have mainly studied two types of 3D walkers, namely the 3D walker with toe line and the 3D walkers with heels. Both types have three-dimensional characteristics and a nonvanishing hip width, but while the former type has a similar foot geometry to the extended 2D walker, the latter type has two additional foot points on each foot forming a heel.

3.2 Model considerations

As with the modeling of an arbitrary complex mechanical system, a number of modeling considerations need to be accounted for prior to actual analysis.

Choice of mechanical model for constituent bodies.

We have the option of modeling the bodies as rigid or deformable. An advantage of using deformable elements is the possibility of estimating the growth of cracks, likeli-

hood of failure, etc. On the other hand, the resulting mathematical model is infinite-dimensional, requires solving PDEs, and is prohibitively hard to analyze. Since, in the present study, any deformations are expected to be small, rigid bodies provide a first stab at modeling the dynamics of the mechanism. In Appendix A, we have listed the different parameters (such as masses, lengths, and inertia matrices) used in the numerical analyses reported here.

Choice of model geometry.

The walkers discussed here consist of a torso, two upper limbs, and two lower limbs (except in paper 7, where two articulated feet are included). Throughout this thesis, the torso center of mass coincides with the mid-point of the line connecting the hip joints. In addition to being symmetric about the sagittal plane, its mass properties are chosen such that the torso has rotational symmetry about the hip line. A more anthropomorphic torso would likely require active control, which lies outside of this analysis. One might certainly imagine allowing the foot to move relative to the lower legs. In this situation, however, it is unclear if gait could be sustained without active control (cf. paper 7). As mentioned in section 3.1, we differentiate between two- (2D) and three-dimensional (3D) walkers. While a 2D walker is constrained to move in a nominal plane, the 3D walkers are free to move in the entire physical space. 2D walkers are relatively easier to analyze due to their fewer degrees of freedom, but may not capture motion exhibited by actual walkers. On the other hand, actual bipedal walking appears to be fairly two-dimensional in nature.

Previous work on passive walkers used curved feet to allow for rolling motion of the stance foot during the swing phase, thereby mimicking the shift of the pressure point on the foot during human gait (cf. Coleman et al. [6]). In Dankowicz et al. [11] and Adolfsson et al. [2], it was shown that stable gaits persisted even when the radius of the foot was decreased to zero. In this thesis, we model each foot to be made up of two (see illustration in paper 1) or four contact points (paper 6 and 7). The first case mimics a human walking on her toes. Actually, many mammals (such as cats and dogs) walk entirely on their toes.

Joint mobility.

Human joints possess a considerable number of degrees of freedom (DOF). The hip joints each have three DOF, the knees have one DOF each, and the ankles have at least two DOF each. Our models, however, are limited to hinge joints at the hips and knees and completely locked ankles (except paper 7). Similar considerations as in the choice between 2D and 3D walkers apply. Additional DOF might necessitate active control for stabilization.

Force interactions at joints and with the external environment.

Theoretically we could allow the joints to be totally unactuated. Of course, in the human knee, muscles, tendons and ligaments constrain the motion to prevent hyperextension. In the passive walkers originally proposed by McGeer (see McGeer [32] and Garcia et al. [17]), the knees are modeled with plastic stops. These grab on to the leg when it reaches full extension and release the leg from its locked mode at the beginning of the next single-support phase. In our model, we replace the plastic stops with springs and dampers, active only during hyperextension.

The symmetry assumptions on the torso and the two-dimensional character of the gait result in a weak coupling between the torso rotation about the hip line and the motion of the rest of the mechanism. Thus, to avoid free rotation of the torso, dampers are added to the hip joints.

As with the knee, the ground contact can be modeled in a number of different ways. Impact models are easier to simulate and have fewer parameters than a model with springs, dampers, and some kind of friction. The latter models, however, may be better adapted to real contact. In this thesis, the ground contact is modeled with springs and dampers, where the former try to bring the toe point back to its original point of contact.

As the walker proceeds down the incline, the forces due to the springs and dampers in the knees and the ground are turned on and off at discrete events triggered by changes in the configuration. Some of these events also include discrete jumps in the state variables. The resulting dynamical description is a hybrid system involving both continuous and discrete dynamics. For a detailed explanation of this see Adolfsson et al. [2] and paper 6.

3.3 Modeling - deriving the equations of motion

The modeling of passive walkers throughout this thesis is based largely on the work by Adolfsson [1]. The implementation in papers 1 and 2 differs somewhat from this model in order to better fit the present problem statement. A further extension to this model is also presented in paper 7. The discussion below is more or less complete, and should read as a complement to the Maple code given in Appendix C, containing the derivation of the equations of motion for a 3D passive walker with heels.

The derivation of the equations of motion is done as follows. First a kinematical description of the walker is developed. This involves the introduction of configuration coordinates and independent velocity coordinates (generalized speeds). We continue by establishing a description of the distribution of mass for each rigid-body segment. This is needed for the calculation of the linear and angular momenta. The positions of the foot contact points are also defined. Finally, the applied forces and torques are defined and the dynamical differential equations are derived.

3.3.1 Kinematics

In this section, we describe a standard model for a 3D passive walker. This model is a result of the model considerations made in the previous section and based mainly on the work presented in Adolfsson [1]. Walkers that differs significantly from the model presented here, such as 2D passive walkers, have been discussed briefly in section 3.1 and will be treated later in section 3.4.

We begin by introducing some useful notation that will be used throughout the thesis. Let N be an inertial reference frame with reference point N and right-handed, orthonormal reference basis n relative to which the ground is stationary. Specifically, the ground is spanned by \mathbf{n}_1 and \mathbf{n}_2 , where \mathbf{n}_1 is pointing downhill in the direction of the largest slope, and \mathbf{n}_3 is perpendicular to the ground in the direction opposite to gravity. The passive walker model consists of five rigid bodies, namely a torso, two upper limbs, and two lower limbs. Each rigid body is associated with a body-fixed reference frame. Specifically, \mathcal{T} , $\mathcal{U}^{(L)}$, $\mathcal{U}^{(R)}$, $\mathcal{L}^{(L)}$, and $\mathcal{L}^{(R)}$ are the reference frames corresponding to the torso, the left upper limb, the right upper limb, the left lower limb, and the right lower limb, respectively. In a similar way as for the inertial reference frame, each body-fixed reference frame consists of a reference point and a reference basis, e.g., the torso-fixed reference frame \mathcal{T} consists of the reference point T and the reference basis t.

The torso is assumed to have three translational and three rotational degrees of freedom. The position of the reference point T on the torso relative to the point N can now be written

$$\mathbf{r}^T = q_1 \mathbf{n}_1 + q_2 \mathbf{n}_2 + q_3 \mathbf{n}_3. \tag{3.1}$$

The orientation of the torso relative to the ground can be given by the sequence of simple rotations $\{n,t^{(1)},1,q_4\}$, $\{t^{(1)},t^{(2)},3,q_5\}$, and $\{t^{(2)},t,2,q_6\}$, where the notation $\{a,b,i,\theta\}$ is used to mark that the reference basis b is rotated an angle θ relative to the reference basis a about their common i-axis, i.e. $\mathbf{a}_i = \mathbf{b}_i$. The hip joints connecting the torso and the upper limbs and the knee joints connecting the upper and lower limbs are modeled as simple hinge joints. It follows that the orientation of the limbs can be described by the sequence $\{t^{(2)},u^{(L)},2,q_7\}$, $\{u^{(L)},l^{(L)},2,q_8\}$, $\{t^{(2)},u^{(R)},2,q_9\}$, and $\{u^{(R)},l^{(L)},2,q_{10}\}$. The 10 configuration coordinates $q_i, i=1,\ldots,10$ are necessary and suffice to describe an arbitrary configuration of the walker. It follows that the general 3D passive walker model discussed here has ten degrees of freedom.

Since there are no additional kinematic constraints, 10 independent velocity coordinates (generalized speeds) \mathbf{u}_i , $i=1,\ldots,10$ are necessary and suffice to describe the linear and angular velocities of all rigid-body segments of the walker. These are introduced as follows. Let the linear and angular velocities of the torso relative to the inertial reference frame be given by

$$\mathbf{v}^T = u_1 \mathbf{n}_1 + u_2 \mathbf{n}_2 + u_3 \mathbf{n}_3 \tag{3.2}$$

and

$${}^{\mathcal{N}}\boldsymbol{\omega}^{\mathcal{T}} = u_4 \mathbf{t}_1^{(2)} + u_6 \mathbf{t}_2^{(2)} + u_5 \mathbf{t}_3^{(2)}. \tag{3.3}$$

Similarly, let the angular velocities of the left and right upper limbs relative to the torso be expressed as

$$\mathcal{U}^{(2)}\boldsymbol{\omega}^{\mathcal{U}^{(L)}} = u_7 \mathbf{t}_2^{(2)} \tag{3.4}$$

$$T^{(2)}\omega^{\mathcal{U}^{(R)}} = u_9 \mathbf{t}_2^{(2)},$$
 (3.5)

and the angular velocities of the left and right lower limbs relative to the upper limbs be expressed as

$$\mathcal{U}^{(L)} \boldsymbol{\omega}^{\mathcal{L}^{(L)}} = u_8 \mathbf{t}_2^{(2)}$$

$$\mathcal{U}^{(R)} \boldsymbol{\omega}^{\mathcal{L}^{(R)}} = u_{10} \mathbf{t}_2^{(2)}.$$
(3.6)

$$\mathcal{U}^{(R)}\boldsymbol{\omega}^{\mathcal{L}^{(R)}} = u_{10}\mathbf{t}_2^{(2)}. \tag{3.7}$$

It follows that the independent velocity coordinates are related to the rates of change of the configuration coordinates by the kinematical differential equations

$$\dot{q} = K(q)u \tag{3.8}$$

where $q = (q_1 \cdots q_{10})^T$, $\dot{q} = (\dot{q}_1 \cdots \dot{q}_{10})^T$, $u = (u_1 \cdots u_{10})^T$ (cf. Eq. 2.62),

and $s_i = \sin(q_i)$, $c_i = \cos(q_i)$, and $t_i = \tan(q_i)$.

3.3.2 Joints, foot points, and center of mass locations

The positions of the left and right hip joints relative to the torso reference point T (see Eq. 3.1) are given by

$$\mathbf{r}_{\text{left hip joint}} = r_{\text{lhj},2}\mathbf{t}_2 \tag{3.10}$$

$$\mathbf{r}_{\text{right hip joint}} = r_{\text{rhj},2}\mathbf{t}_2.$$
 (3.11)

Similarly, the positions of the knee joints relative to the corresponding hip joints are given by

$$\mathbf{r}_{\text{left knee joint}} = r_{\text{lkj},3} \mathbf{u}_{3}^{(L)}$$

$$\mathbf{r}_{\text{right knee joint}} = r_{\text{rkj},3} \mathbf{u}_{3}^{(R)}.$$
(3.12)

$$\mathbf{r}_{\text{right knee joint}} = r_{\text{rki},3} \mathbf{u}_3^{(R)}. \tag{3.13}$$

Recall that interactions between the lower limbs and the ground are modeled with a number of foot contact points. Specifically, the foot points of the left and right feet relative to the corresponding knee joints are given by

$$\mathbf{r}_{\text{left foot point } i} = r_{\text{lfp}i,1} \mathbf{l}_{1}^{(L)} + r_{\text{lfp}i,2} \mathbf{l}_{2}^{(L)} + r_{\text{lfp}i,3} \mathbf{l}_{3}^{(L)}, i = 1, \cdots, m$$
 (3.14)

$$\mathbf{r}_{\text{right foot point } i} = r_{\text{rfp}i,1} \mathbf{l}_{1}^{(R)} + r_{\text{rfp}i,2} \mathbf{l}_{2}^{(R)} + r_{\text{rfp}i,3} \mathbf{l}_{3}^{(R)}, i = 1, \dots, m.$$
 (3.15)

Note that m=1 for the 2D walker, m=2 for the 3D walkers with toe lines, and m=4 for the 3D walkers with heels.

Next we focus on the centers of mass (COM) of the torso and upper and lower legs. Their positions will be given relative to the reference point N. The center of mass of the pelvis is given by

$$\mathbf{r}_{\text{torso}}^{CM} = \mathbf{r}^T + r_{\text{t},1}\mathbf{t}_1 + r_{\text{t},2}\mathbf{t}_2 + r_{\text{t},3}\mathbf{t}_3.$$
 (3.16)

Throughout the thesis (except paper 7) $r_{t,1} = r_{t,2} = r_{t,3} = 0$, i.e., the torso reference point T coincides with the torso center of mass. The positions of the COM of the left and right upper limbs are

$$\mathbf{r}_{\text{left upper limb}}^{CM} = \mathbf{r}^T + \mathbf{r}_{\text{left hip joint}} + r_{\text{lul},1} \mathbf{u}_1^{(L)} + r_{\text{lul},2} \mathbf{u}_2^{(L)} + r_{\text{lul},3} \mathbf{u}_3^{(L)}$$
(3.17)

$$\mathbf{r}_{\text{right upper limb}}^{CM} = \mathbf{r}^T + \mathbf{r}_{\text{right hip joint}} + r_{\text{rul},1} \mathbf{u}_1^{(R)} + r_{\text{rul},2} \mathbf{u}_2^{(R)} + r_{\text{rul},3} \mathbf{u}_3^{(R)}.$$
 (3.18)

In a similar way the COM of the left and right lower limbs are given by

$$\mathbf{r}_{\text{left lower limb}}^{CM} = \mathbf{r}^T + \mathbf{r}_{\text{left hip joint}} + \mathbf{r}_{\text{left knee joint}} +$$
 (3.19)

$$\mathbf{r}_{\text{right lower limb}}^{CM} = \mathbf{r}_{\text{right hip joint}}^{(L)} + r_{\text{lil},2} \mathbf{l}_{2}^{(L)} + r_{\text{lil},3} \mathbf{l}_{3}^{(L)}$$

$$\mathbf{r}_{\text{right lower limb}}^{CM} = \mathbf{r}^{T} + \mathbf{r}_{\text{right hip joint}} + \mathbf{r}_{\text{right knee joint}} + r_{\text{right knee joint}} + r_{\text{right lower limb}}^{(R)} + r_{\text{right lower limb}}^{(R)} + r_{\text{right lower limb}}^{(R)} + r_{\text{right lower limb}}^{(R)}$$

$$(3.20)$$

3.3.3 Linear and angular momentum

The linear momenta of the torso, left and right upper limbs, and left and right lower limbs relative to the inertial reference frame are given by

$$\mathbf{P}_{\text{torso}} = m_{\text{torso}} \mathbf{v}_{\text{torso}}^{CM}, \tag{3.21}$$

$$\mathbf{P}_{\text{left upper limb}} = m_{\text{left upper limb}} \mathbf{v}_{\text{left upper limb}}^{CM}, \tag{3.22}$$

$$\mathbf{P}_{\text{right upper limb}} = m_{\text{right upper limb}} \mathbf{v}_{\text{right upper limb}}^{CM}, \tag{3.23}$$

$$\mathbf{P}_{\text{left lower limb}} = m_{\text{left lower limb}} \mathbf{v}_{\text{left lower limb}}^{CM}, \tag{3.24}$$

and

$$\mathbf{P}_{\text{right lower limb}} = m_{\text{right lower limb}} \mathbf{v}_{\text{right lower limb}}^{CM}, \tag{3.25}$$

where, e.g., m_{torso} is the mass of the torso and $\mathbf{v}_{\text{torso}}^{CM}$ is the velocity of the center of mass of the torso relative to N. The angular momenta of the torso, left and right upper limbs, and left and right lower limbs relative to the inertial reference frame are given by

$$\mathbf{H}_{\text{torso}} = \mathbf{I}_{\text{torso}} \bullet^{\mathcal{N}} \boldsymbol{\omega}^{\mathcal{T}},$$
 (3.26)

$$\mathbf{H}_{\text{left upper limb}} = \mathbf{I}_{\text{left upper limb}} \bullet^{\mathcal{N}} \boldsymbol{\omega}^{\mathcal{U}^{(L)}},$$
 (3.27)

$$\mathbf{H}_{\text{right upper limb}} = \mathbf{I}_{\text{right upper limb}} \bullet^{\mathcal{N}} \boldsymbol{\omega}^{\mathcal{U}^{(R)}},$$
 (3.28)

$$\mathbf{H}_{\text{left lower limb}} = \mathbf{I}_{\text{left lower limb}} \bullet^{\mathcal{N}} \boldsymbol{\omega}^{\mathcal{L}^{(L)}},$$
 (3.29)

and

$$\mathbf{H}_{\text{right lower limb}} = \mathbf{I}_{\text{right lower limb}} \bullet^{\mathcal{N}} \boldsymbol{\omega}^{\mathcal{L}^{(R)}}, \tag{3.30}$$

where, e.g., \mathbf{I}_{torso} is the moment of inertia of the torso and ${}^{\mathcal{N}}\boldsymbol{\omega}^{\mathcal{U}^{(L)}} = {}^{\mathcal{N}}\boldsymbol{\omega}^{\mathcal{T}^{(2)}} + {}^{\mathcal{T}^{(2)}}\boldsymbol{\omega}^{\mathcal{U}^{(L)}}$.

3.3.4 Forces and torques

As mentioned above, the only forces and torques acting on the passive walker are those of gravity, dampers in the hips, springs and dampers in the knees, and springs and dampers between the ground and foot contact points. Specifically, let $\gamma \in [0, \pi)$ be the inclination of the ground relative to the local direction of gravity. Then, the direction of gravitational acceleration can be written

$$\gamma = \sin(\gamma) \mathbf{n}_1 - \cos(\gamma) \mathbf{n}_3. \tag{3.31}$$

The only forces acting on the torso and the upper limbs are due to gravity, which we can write as

$$\mathbf{F}_{\text{torso}} = m_{\text{torso}} g \boldsymbol{\gamma},$$
 (3.32)

$$\mathbf{F}_{\text{left upper limb}} = m_{\text{left thigh}} g \gamma, \text{ and}$$
 (3.33)

$$\mathbf{F}_{\text{right upper limb}} = m_{\text{right thigh}} g \gamma,$$
 (3.34)

where $q \approx 9.81 \text{ ms}^{-2}$ is the gravity constant. In addition to the gravitational forces the lower limbs experience ground reaction forces whenever one or more of the foot contact points are in contact with the ground, i.e.

$$\mathbf{F}_{\text{left lower limb}} = m_{\text{left lower limb}} g \boldsymbol{\gamma} + \sum \mathbf{F}_{\text{left foot point } i}$$
 (3.35)

$$\mathbf{F}_{\text{right lower limb}} = m_{\text{right lower limb}} g \gamma + \sum_{i} \mathbf{F}_{\text{right foot point } i}$$
 (3.36)

where, e.g., the ground reaction force on the *i*th foot point on the left foot is

$$\mathbf{F}_{\text{left foot point } i} = F_{\text{lfp}i,1}\mathbf{n}_1 + F_{\text{lfp}i,2}\mathbf{n}_2 + F_{\text{lfp}i,3}\mathbf{n}_3 \tag{3.37}$$

and

$$F_{\mathrm{lfp}i,j} = \begin{cases} -k_{\mathrm{ground},\ j} \left(p_{\mathrm{lfp}i,j} - s_{\mathrm{l}i,j} - q_{j} \right) - c_{\mathrm{ground},j} \dot{p}_{\mathrm{lfp}i,j} & p_{\mathrm{lfp}i,3} \leq 0, j = 1, 2\\ -k_{\mathrm{ground},3} p_{\mathrm{lfp}i,3} - c_{\mathrm{ground},3} \dot{p}_{\mathrm{lfp}i,3} & p_{\mathrm{lfp}i,3} \leq 0, \dot{p}_{\mathrm{lfp}i,3} \leq 0, j = 3\\ -k_{\mathrm{ground},3} p_{\mathrm{lfp}i,3} & p_{\mathrm{lfp}i,3} \leq 0, \dot{p}_{\mathrm{lfp}i,3} \leq 0, j = 3\\ 0 & p_{\mathrm{lfp}i,3} \geq 0, \dot{p}_{\mathrm{lfp}i,3} > 0, j = 3 \end{cases},$$

$$(3.38)$$

where $k_{\text{ground}, j}$ and $c_{\text{ground}, j}$ are the spring and damper constants in the \mathbf{n}_j -direction, respectively. The variables $p_{\text{lfp}i,j}$ and $s_{\text{l}i,j}$ describe the position of the present foot point and its initial point of contact with the ground (see further Paper 1).

Let k_{knee} and c_{knee} be the spring and damper constants of the knee model and c_{hip} be the damper constant in the hip joint models. The corresponding torques are

$$\mathbf{T}_{\text{torso}} = c_{\text{hip}} \left(\dot{q}_7 + \dot{q}_9 - 2\dot{q}_6 \right) \mathbf{t}_2^{(2)}, \tag{3.39}$$

$$\mathbf{T}_{\text{left upper limb}} = \mathbf{T}_{\text{left knee}} + c_{\text{hip}} \left(\dot{q}_6 - \dot{q}_7 \right) \mathbf{t}_2^{(2)}, \tag{3.40}$$

$$\mathbf{T}_{\text{right upper limb}} = \mathbf{T}_{\text{right knee}} + c_{\text{hip}} \left(\dot{q}_6 - \dot{q}_9 \right) \mathbf{t}_2^{(2)}, \tag{3.41}$$

$$\mathbf{T}_{\mathrm{left\ lower\ limb}} = -\mathbf{T}_{\mathrm{left\ knee}} + \sum \left(\mathbf{r}_{\mathrm{cm} \to \mathrm{lfp}i,j} \times \mathbf{F}_{\mathrm{left\ foot\ point\ }i} \right), \qquad (3.42)$$

and

$$\mathbf{T}_{\text{right lower limb}} = -\mathbf{T}_{\text{right knee}} + \sum_{i} \left(\mathbf{r}_{\text{cm} \to \text{rfp}i,j} \times \mathbf{F}_{\text{right foot point }i} \right), \tag{3.43}$$

where $\mathbf{r}_{\text{cm}\to\text{lfp}i}$ and $\mathbf{r}_{\text{cm}\to\text{rfp}i}$ are the position vectors of the ith foot point relative to the corresponding foot COM, respectively. The torques in the left and right knees are given by

$$\mathbf{T}_{\text{left knee}} = \begin{cases}
(k_{\text{knee}}q_8 + c_{\text{knee}}\dot{q}_8)\mathbf{t}_2^{(2)} & q_8 \leq 0 \\
\mathbf{0} & q_8 > 0
\end{cases}$$

$$\mathbf{T}_{\text{right knee}} = \begin{cases}
(k_{\text{knee}}q_{10} + c_{\text{knee}}\dot{q}_{10})\mathbf{t}_2^{(2)} & q_{10} \leq 0 \\
\mathbf{0} & q_{10} > 0
\end{cases}$$
(3.44)

$$\mathbf{T}_{\text{right knee}} = \begin{cases} (k_{\text{knee}} q_{10} + c_{\text{knee}} \dot{q}_{10}) \mathbf{t}_{2}^{(2)} & q_{10} \leq 0 \\ \mathbf{0} & q_{10} > 0 \end{cases}, \tag{3.45}$$

respectively.

3.3.5 Dynamics

Using the methodology (Kane's method) introduced in section 2.3, the dynamical differential equations are given by

$$(F_a - \dot{p}) \cdot \beta = 0, \tag{3.46}$$

where the momentum description is (using Eq. (3.21-3.30))

$$p = \begin{bmatrix} \mathbf{P}_{\text{torso}} & \mathbf{H}_{\text{torso}} & \mathbf{P}_{\text{left upper limb}} & \mathbf{H}_{\text{left upper limb}} & \mathbf{P}_{\text{right upper limb}} & \cdots & (3.47) \\ \mathbf{H}_{\text{right upper limb}} & \mathbf{P}_{\text{left lower limb}} & \mathbf{H}_{\text{left lower limb}} & \mathbf{P}_{\text{right lower limb}} & \mathbf{H}_{\text{right lower limb}} \end{bmatrix}$$

and the applied force description is (from Eq. (3.32-3.45))

$$F_a = \begin{bmatrix} \mathbf{F}_{\text{torso}} & \mathbf{T}_{\text{torso}} & \mathbf{F}_{\text{left upper limb}} & \mathbf{T}_{\text{left upper limb}} & \mathbf{F}_{\text{right upper limb}} & \cdots \end{bmatrix}$$
 (3.48)
 $\mathbf{T}_{\text{right upper limb}} & \mathbf{F}_{\text{left lower limb}} & \mathbf{T}_{\text{left lower limb}} & \mathbf{F}_{\text{right lower limb}} & \mathbf{T}_{\text{right lower limb}} \end{bmatrix}$

From Eq. (3.3-3.7) and by time differentiating Eq. (3.16-3.19), and writing, e.g., $\mathbf{v}_{\text{torso}}^{CM} = \dot{\mathbf{r}}_{\text{torso}}^{CM}$, β is obtained from

$$v = \begin{bmatrix} \mathbf{v}_{\text{torso}}^{CM} & {}^{\mathcal{N}}\boldsymbol{\omega}^{\mathcal{T}} & \mathbf{v}_{\text{left upper limb}}^{CM} & {}^{\mathcal{N}}\boldsymbol{\omega}^{\mathcal{U}^{(L)}} & \mathbf{v}_{\text{right upper limb}}^{CM} & {}^{\mathcal{N}}\boldsymbol{\omega}^{\mathcal{U}^{(R)}} & \cdots & (3.49) \\ & & \mathbf{v}_{\text{left lower limb}}^{CM} & {}^{\mathcal{N}}\boldsymbol{\omega}^{\mathcal{L}^{(L)}} & \mathbf{v}_{\text{right lower limb}}^{CM} & {}^{\mathcal{N}}\boldsymbol{\omega}^{\mathcal{L}^{(R)}} \end{bmatrix}$$

$$= \beta(q, t) u.$$

The dynamical differential equations (see Eq. 3.46) can be written on the form

$$M\dot{u} = f(q, u). \tag{3.50}$$

Together with the kinematical differential equations (cf. Eq. 3.8)

$$\dot{q} = Ku, \tag{3.51}$$

and a description of the discrete jumps in the forcing, these constitute the complete set of equations of motion for the passive walker model described here. We continue by illustrating some typical gait motions of 2D and 3D passive walkers. Later (section 3.5), we will discuss bifurcations, existence and stability of recurrent gait motions under variations in system parameters.

3.4 Gait patterns

A repetitive gait for a walker is built up from a sequence of discrete events. A typical event sequence for one step of a 3D passive walker with two foot contact points per foot is given in Table 3.1. It is possible for some events to occur in reverse order

No.	Leg	Event	Function	Phase
1	Left	outer toe release	stance leg	double-support
2	Left	inner toe release	swing leg	single-support
3	Left	knee release	swing leg	single-support
4	Left	knee impact	swing leg	single-support
5	Left	outer toe impact	stance leg	double-support
6	Left	inner toe impact	stance leg	double-support
7	Right	outer toe release	stance leg	double-support
8	Right	inner toe release	swing leg	single-support
9	Right	knee release	swing leg	single-support
10	Right	knee impact	swing leg	single-support
11	Right	outer toe impact	stance leg	double-support
12	Right	inner toe impact	stance leg	double-support

Table 3.1: A gait sequence for a 3D walker with toe lines for one step.

or simultaneously. For instance, knee release could occur before the foot is entirely released from the ground. Suitable modifications apply in the case of 2D walkers.

As suggested in chapter 2.5, there is no reason to expect that recurrent gait will exist for a given choice of system parameters. That parameter choices (resembling those for an actual human) can nevertheless be found for which natural gait patterns are exhibited is an intriguing observation.

3.4.1 2D walkers

Figure 3.1 shows a typical period-1 gait. The hip angle (as well as all other state variables) can be mapped onto itself with a time shift of one period, approximately 1.5 seconds. In fact, for the majority of period-1 gaits observed in our analysis the period lies within 10 % of 1.5 seconds. In Figure 3.2, we illustrate a typical period-2 gait. In the upper panel it is almost impossible to see that the motion is not period-1, while the blow-up in the lower panel displays this clearly. This shows that we have to be careful when concluding from visual observation alone that a gait has a certain periodicity.

Figure 3.3 shows the time evolution of the left and right hip angles for a period-1 gait over one period. Since, the two curves can be mapped onto each other with a time shift of half the period, the gait is symmetric. In contrast to this, an asymmetric, limping period-1 gait is shown in Figure 3.4. The time evolutions of the hip angles can clearly not be mapped onto each other.

As indicated in the previous chapter, solution branches may terminate as a result of foot scuffing. Indeed, it is possible to show that the initial onset of foot scuffing, a grazing contact, may result in dramatic changes in stability and persistence of periodic solutions under further parameter variations. As an example of this, consider

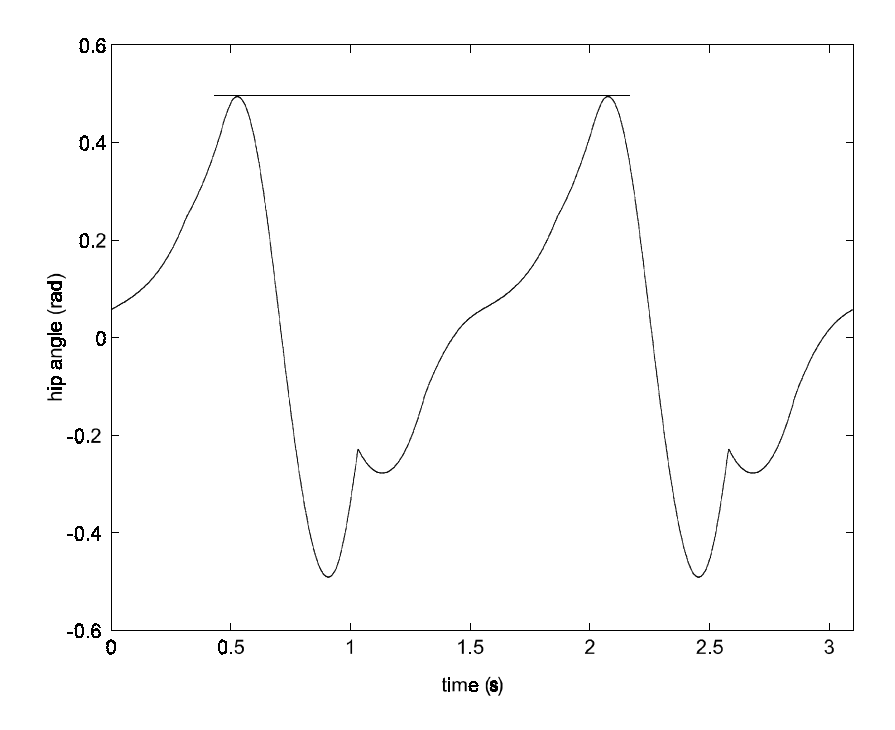


Figure 3.1: The hip angle as a function of time for a period-1 gait over two consecutive strides.

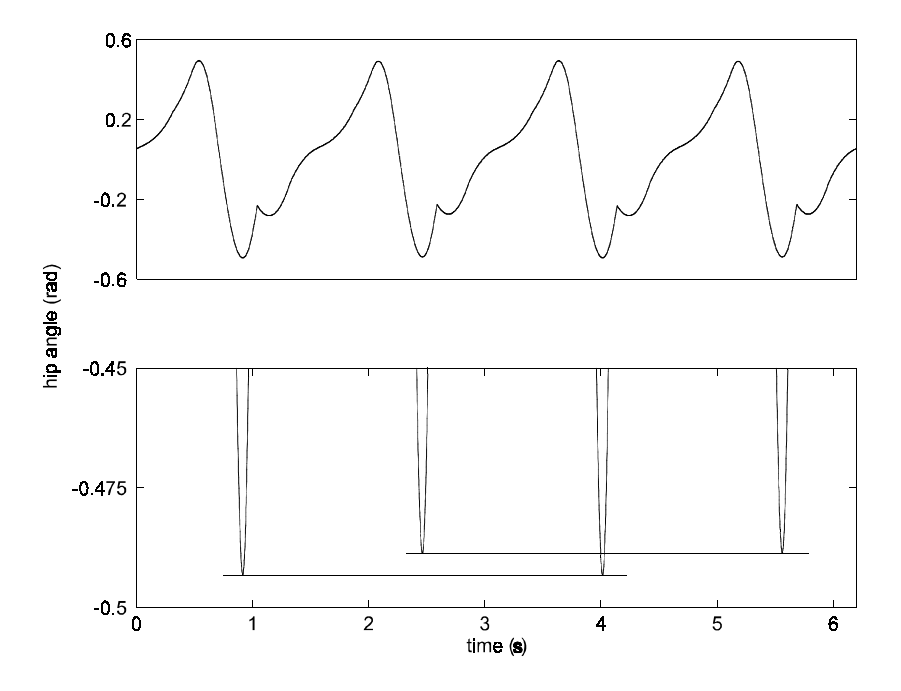


Figure 3.2: The hip angle as a function of time for a period-2 gait over four consecutive strides.

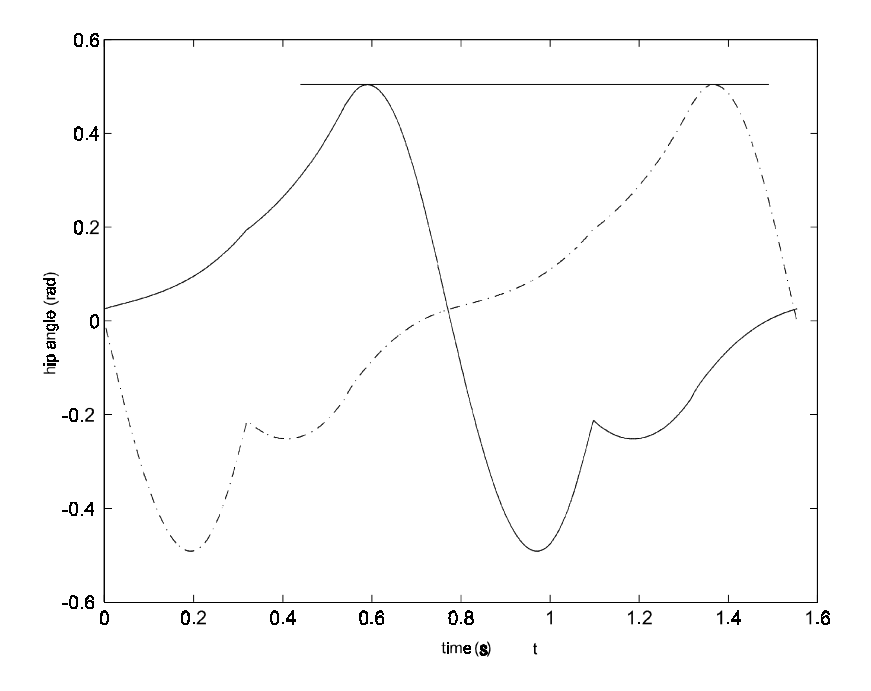


Figure 3.3: The left and right hip angles as a function of time for a symmetric period-1 gait over one stride.

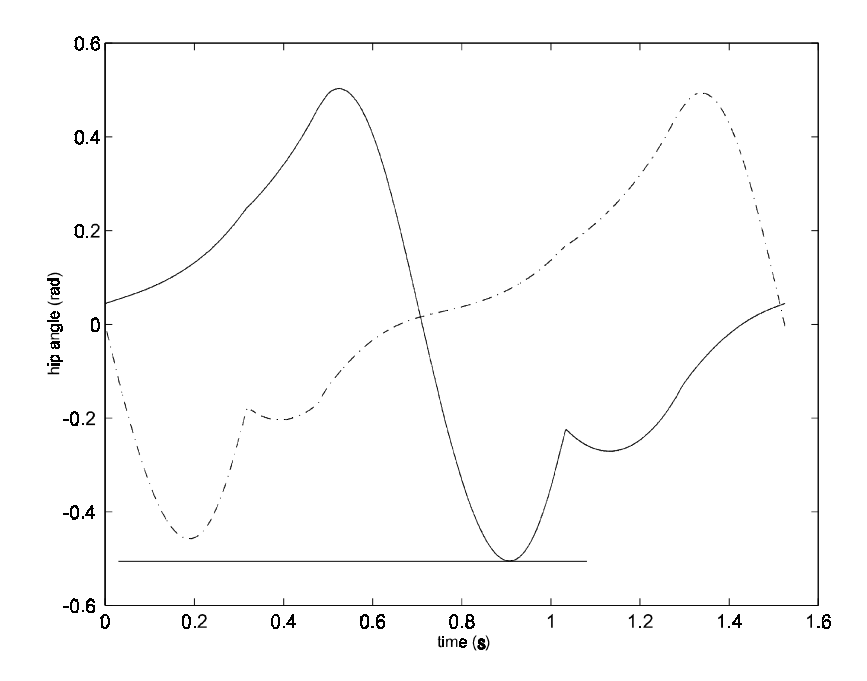


Figure 3.4: The left and right hip angles as a function of time for a asymmetric period-1 gait over one stride.

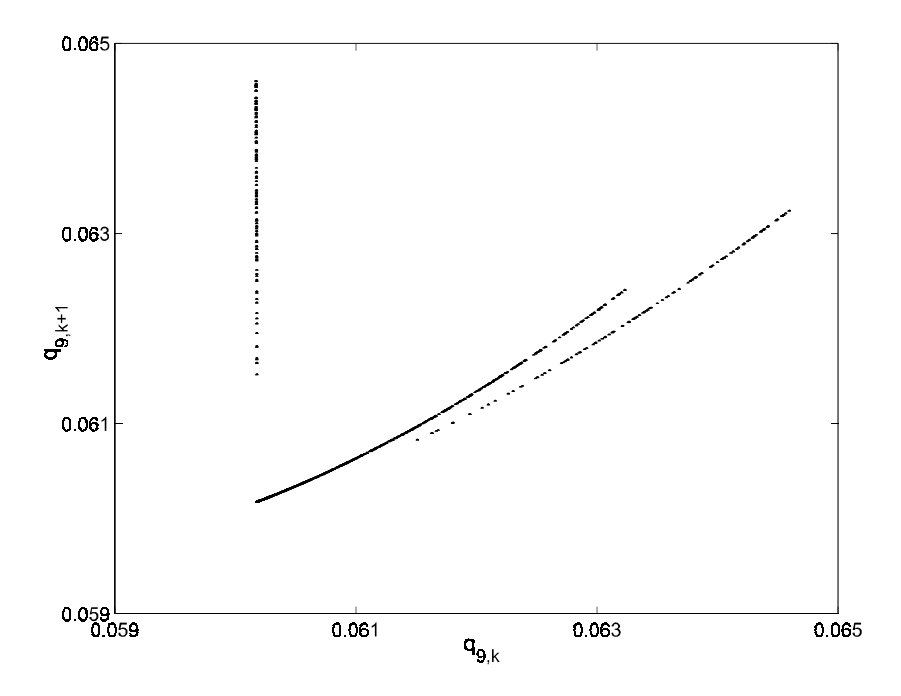


Figure 3.5: A delay plot for the hip angle q_9 showing an attractive chaotic motion with near-grazing impacts.

the limping gait (upper stable branch of Figure 3.8) at slope $\gamma=0.0609$ and change the slope slightly to $\gamma=0.06087$. Figure 3.5 is a delay plot of the hip angle at subsequent intersections with a Poincaré section. The almost vertical branch of the chaotic attractor corresponds to strides that include moments of foot scuffing. This type of diagram is characteristic of discontinuous dynamical systems near grazing, for example mechanical systems with impacts (Fredriksson et al. [14]). For such a system, Nordmark [38] shows that if the largest eigenvalue λ for the grazing motion is greater than 2/3, but less than 1, then the subsequent attractor is chaotic. In our case, the largest eigenvalue λ is 0.93644, confirming this prediction. We also note that the presence of two diagonal non-impacting branches of the attractor characterizes a system with several degrees of freedom (Fredriksson et al. [14]).

The different gaits presented above exemplify the majority of gaits in a 2D walker. Under different modeling choices, such as for the ground contact and in the knee joints, it may be possible to find chaotic gaits without foot scuffing, see e.g. Garcia et al. [16].

3.4.2 3D walkers

The inclusion of additional degrees of freedom naturally increases the complexity of the observed motion. While the gaits may be mainly 2D, 3D walkers can exhibit

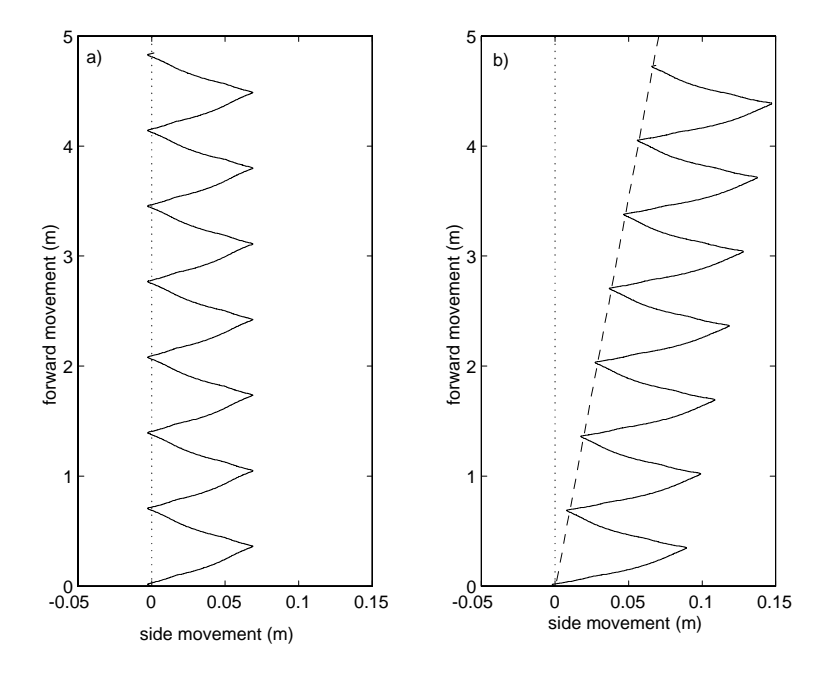


Figure 3.6: The vertical projection of the center of the hip line on the ground plane for two different 3D gaits.

side-to-side swaying and changes in gait heading. Figure 3.6 shows two different 3D gaits where the oscillations are largely due to side-to-side swaying. The motion in the right panel deviates from a nominal plane by approximately 1 degree.

An example of a quasiperiodic motion is shown in Figure 3.7. The figure also includes transient dynamics from an initial condition near an unstable periodic orbit at the center of the diagram.

3.5 Bifurcations and their effect on periodic gaits

In section 2.2, we introduced the concept of bifurcations in dynamical systems. Here we use the insights gained there together with the discussion about gait patterns in section 3.4. It is convenient to summarize the different changes in gait types that we observe under parameter variations.

When exploring the dynamical system of the passive walker, we have encountered five different bifurcations. The bifurcations that occur when one or more eigenvalues become one in magnitude are saddle-node/fold, pitchfork, period doubling/flip, and Hopf bifurcations. Sudden changes may also appear near grazing. Figure 3.8 is a projection of a bifurcation diagram for a 2D walker under varying inclination, illustrating a family of periodic solutions. This diagram will be discussed in detail in paper 1, but it gives a clear picture of some of the bifurcations.

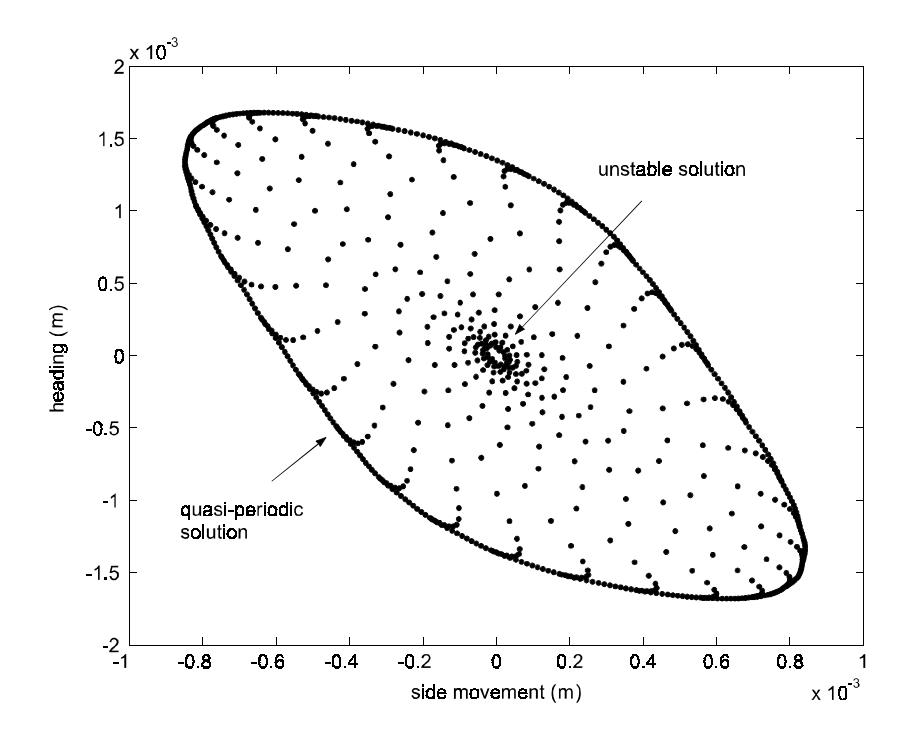


Figure 3.7: Motion towards a quasi-periodic solution at a Poincaré section.

In Table 3.2 and in the corresponding explanations 1. - 7., we have gathered the different bifurcation scenarios corresponding to variations in a parameter ν and a bifurcation at $\nu = \nu_0$. Notice also the references to the Roman numerals (bifurcations) I - IV in Figure 3.8.

Eigenvalue	Bifurcation	2D-gait	3D-gait
+1	Saddle-node/Fold	see 1.	see 1.
+1	Pitchfork	see 2.	see 2 . and 3 .
-1	Period doubling/Flip	see 4.	see 4.
$e^{\pm \frac{\pi}{2}ik}, k \neq 1, \dots, 4$	Hopf	see 5 .	see 6.
any	Grazing	see 7.	see 7.

Table 3.2: An overview of the different bifurcations and their impacts on bipedal passive walking. See also the explaining text labeled 1.- 8.

- 1. Two solutions, one stable and one unstable, exist for $\nu < \nu_0$ and no solutions exists for $\nu > \nu_0$. Compare with bifurcation I, where the solutions are symmetric.
- 2. For $\nu < \nu_0$, there is one symmetric solution, and for $\nu > \nu_0$, there are three solutions. The symmetric solution changes stability in the bifurcation. The

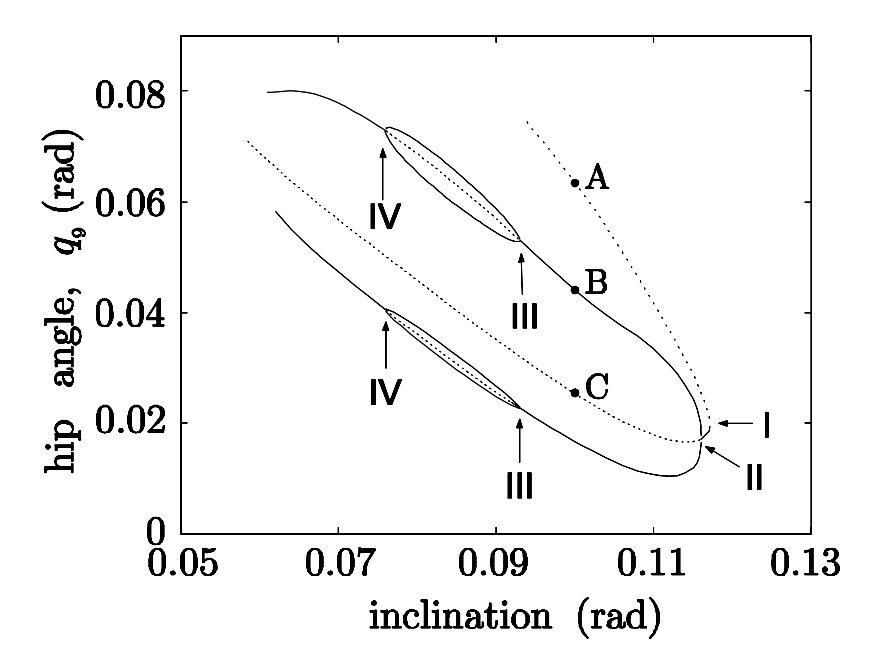


Figure 3.8: A projection of the bifurcation diagram for a 2D walker. The following bifurcations are represented: I - saddle-node/fold, II - pitch-fork, and III & IV - period-doubling/flip. The letters A and C indicate unstable symmetric gait and the letter B indicate stable limping gait.

two new branches correspond to asymmetric gait and have opposite stability from the symmetric motion. The two asymmetric solutions are mirror images of each other under a time shift of half a period. For symmetric 2D gaits, the asymmetric solution may still remain 2D. Compare with bifurcation II.

- 3. New solutions are born as in 2., but here an asymmetric gait straight down the plane exists for $\nu < \nu_0$ and two new asymmetric gaits walking on an angle relative to a nominal plane are born in the bifurcation.
- 4. As for the pitchfork bifurcation, three solutions become one or vice versa. The solution that exists alone always shows asymmetric walking and changes stability in the bifurcation. The new solution has twice the periodicity and the opposite stability of the original solution. Compare with bifurcations III and IV.
- 5. This type of bifurcation has not been reported.
- 6. A periodic solution changes stability as ν goes through ν_0 . On one side of the bifurcation a branch of quasiperiodic solutions appears. Compare with Figure 3.7.

7. A periodic orbit impinges tangentially on a discontinuity surface in state space as ν reaches ν_0 . Depending on the type of discontinuity, a further change in ν typically results in a rapid, and possible non-smooth, change in eigenvalues. The periodic solution may cease to exist or experience a quick succession of standard bifurcations. In the walker, this corresponds to one of the foot contact points just touching the ground prior to knee-locking. Compare with Figure 3.5.

Other combinations of the bifurcations above are certainly possible, but have not been observed.

As seen in this section, passive walkers can undergo a variety of different bifurcations where stability is lost. This lack of robustness under parameter variations suggest that additional control would need to be included in a robotic implementation of a passive walker to ensure a desirable recurrent motion. Some ideas for how to achieve this are presented in the following section.

3.6 Control of passive walkers

The whole idea with passive walkers is that they are able to exhibit sustained (stable or unstable) anthropomorphic gait in spite of being unactuated and relying only on gravity for energy input. It would be desirable to design a feedback-based control actuation that could affect the stability of a recurrent gait in a passive walker while involving no exchange of energy with the mechanism. One approach would be to make discrete changes to the foot contact point positions relative to the lower limb once every revolution whenever the corresponding foot is not touching the ground. This is very similar to introducing discrete changes in the orientation of a foot about an ankle joint keeping the ankle rigid at all other times. This has the effect of indirectly changing the timing and state of the mechanism at the subsequent impact of a foot contact point with the ground, thereby affecting the stability of the gait. This idea is successfully implemented in paper 6 (and derived in paper 5) where heavily unstable 2D and 3D walkers are stabilized.

One drawback with the control introduced in papers 5 and 6 is that it is very local and can only control for sufficiently small perturbations away from a reference trajectory. To overcome this, a model is developed in paper 7 involving the inclusion of muscles to the passive walker in order to achieve global stability and also to make it even more anthropomorphic.

3.7 Numerics

The following numerical methods have been used to produce the results described in this thesis:

3.7. NUMERICS 45

• Direct numerical integration – useful only for locating asymptotically stable gait.

- Parameter continuation a technique for mapping out solution branches independently of stability.
- Variational equations a mathematical tool for studying linear stability properties of periodic solutions and for implementing Newton-Raphson schemes for location periodic solutions.
- Numerical approximations of derivatives finite difference methods used in the normal-form calculations. (see appendix B)

The practical implementation is as follows.

Software The equations of motion (EOM) of the mechanisms studied in this thesis were derived using the Maple package Sophia, developed at the Department of Mechanics, KTH, originally by Martin Lesser and then extended by Anders Lennartsson (see Lesser [29], [42], and Lennartsson [28]). Sophia implements Kane's method (cf. Kane et al. [25]), which is based on d'Alemberts principle of virtual work (cf. section 2.3). Sophia also includes procedures for exporting the EOM as well as auxiliary functions for internal and external forces into C-code. This allows the user to interface with other applications.

In particular, simulations of the mechanisms have been carried out using Matlab. Matlab's built-in mex function, which uses a standard C-compiler, compiles the C-code for further use within the Matlab environment. For the stability calculations and parameter continuations we have used the possibility to export variational equations (VE) from Sophia to compatible C-code. See Appendix C for the maple code generating the EOM and VE.

All simulations, continuation algorithms, and normal-form calculations are programmed in and carried out with Matlab.

Typical sizes of C-files used here are about 240 kB for the EOM and 1400 kB for the variational equations including the EOM, while the sizes of the compiled files corresponding to the EOM and variational equations are about 195 kB and 850 kB, respectively.

Hardware The numerical computations in this thesis are performed on a Dell Dimension XPS 400 with a 400 MHz Pentium II processor 192 MB RAM and on a EV6 500 MHz processor with an available memory of 3GB RAM.

Cpu time While no detailed analysis has been carried out to determine the efficiency of the employed algorithms, for reference we mention that a bifurcation diagram, such as that in Figure 3.8 takes on the order of one day to compute.

Chapter 4

Discussion and outlook

This thesis describes the analysis of a number of nonsmooth dynamical systems originating in mechanical systems. From a mathematical perspective, the focus is on the development of tools for finding and studying certain motion characteristics, primarily the existence and robustness of recurrent motions. As an immediate application, we consider the study of two-legged passive walkers that exhibit a variety of recurrent gait-like motions. Specifically, we categorize the differences and similarities between two- and three-dimensional walkers, thereby verifying that even simple two-legged models may be used to investigate fundamental characteristics of human gait. The knowledge gained from the analysis of two-legged passive walkers could thus be used in many areas in industry and medicine.

To robotics, the passive component of sustained human gait—as exemplified by the model passive walkers—should be taken into account when studying the stability of walking as well as when developing more energy efficient control algorithms. One idea for such a control algorithm is to actively switch between control yielding static stability and that yielding dynamic stability, depending on the desired motion characteristics. A separate idea is to design the overall control strategy for a walking robot in a hierarchical structure, where the goal of low-level control could be the local stabilization of an already existing gait as suggested in this thesis, while next level of control could focus on global control, e.g., trajectory planning, avoiding obstacles, preventing the robot from falling, and so on. This would also be reflected in a distribution of actuators mimicking muscle activity.

The passive nature of the human gait apparatus is familiar to most physicians and others working with gait pathologies and gait analysis. In the biomedical industry, e.g., in the design of artificial leg prostheses, in analyzing gait data, and in creating computer-based models of human gait, this insight is of great importance.

Looking ahead, there are obvious benefits to be reaped to the areas of robotics, biomechanics, and medicine from finding a common ground from which to study bipedal walking. It is very likely that the aim for parts of the robotics community will be to construct robots that behave as closely to humans as possible and thereby

make their appearance more acceptable. For that purpose, it is necessary to understand the subtleties of human walking, considering the overall dynamics and the underlying muscular activity. For those working in biomechanics it will be (and already is) a significant challenge to overcome the differences between scientist working in mechanics and medicine. The differences have many layers, everything from different vocabulary to mathematical skills and understanding. It is, for example, reasonable to expect that great value is to be found in conveying to scientists in the medical sciences an understanding of how scientists and engineers working in mechanics model the world around us in general, and motion in particular.

Whatever the goals for the future are, there are still a great number of more specific, although quite ambitious, problems to be addressed. For instance, the topic of the present thesis—the analysis of nonsmooth dynamical systems—will be an even more important field in the future. The computational and analytical tools that will be the products of further study in this field will yield insight into the expected dynamical behavior of such systems and will generate new engineering intuition enabling a costand time-effective usage of more and more complex and comprehensive computer-based models of every-day mechanical systems.

Chapter 5

Summary of papers and authors contributions

Paper 1

Breaking Symmetries and Constraints: Transitions from 2D to 3D in Passive Walkers Petri Piiroinen (PP), Harry Dankowicz (HD), Arne Nordmark (AN)

The inherent dynamics of bipedal, passive mechanisms are studied to investigate the relation between motions constrained to two-dimensional planes and those free to move in a three-dimensional environment. In particular, we develop numerical and analytical techniques using dynamical-systems methodology to address the persistence and stability changes of periodic, gait-like motions due to the relaxation of configuration constraints and the breaking of problem symmetries. Symmetry properties of such mechanism are discussed and a few special symmetries are defined. Using these symmetries, we classify a number of different gaits. The results indicate the limitations of a two-dimensional analysis to predict the dynamics in the three-dimensional environment. For example, it is shown how the loss of constraints may introduce characteristically non-2D instability mechanisms, and how small symmetry-breaking terms may result in the termination of solution branches.

Implementations and computations are carried out by PP. The paper is written by PP with feedback from HD and AN.

Accepted for publication in Multibody System Dynamics, 2002

Paper 2

On a Normal-Form Analysis for a Class of Passive Bipedal Walkers Petri Piiroinen (PP), Harry Dankowicz (HD), Arne Nordmark (AN)

Paper 2 continues the work done in paper 1 and implements a center-manifold technique to arrive at a normal-form for the natural dynamics of a passive, bipedal rigid-body mechanism in the vicinity of infinite foot width and near-symmetric body geom-

etry. In particular, numerical schemes are developed for finding approximate forms of the relevant invariant manifolds and the near-singular dynamics on these manifolds. The normal-form approximations are found to be highly accurate for relative large foot widths with a range of validity extending to widths on the order of the mechanisms' height.

Implementations and computations are carried out by PP. The paper is written by PP with feedback from HD and AN.

Published in *International Journal of Bifurcation and Chaos*, Vol. 11, No. 9, pp 2411-2425, 2001

Paper 3

Low-velocity Impacts of Quasi-periodic Oscillations
Harry Dankowicz (HD), Petri Piiroinen (PP), Arne Nordmark (AN)

In this paper a method to predict the characteristics of system attractors that follow grazing intersections with a two-dimensional impacts surface is derived, where the original motion is a two-frequency quasiperiodic oscillation in a three dimensional state space. The alghorithm is based on the idea of discontinuity mappings and it is applied to an example model (the van-der-Pol oscillator) to illustrate the power of the method.

PP made all the figures in the paper, carried out all the implementations and numerics, and gave feedback throughout the work.

Published in Chaos, Solitons and Fractals 14, pp 241-255, 2002

Paper 4

Grazing Bifurcation of Initially Quasi-periodic System Attractors Harry Dankowicz (HD), Petri Piiroinen (PP), Arne Nordmark (AN)

Paper 4 further discusses the discontinuity mappings approach, rigorously derived in paper 3, to predict the characteristics of system attractors that undergo low-velocity impacts. Numerical observations from passive walkers are described and the method is applied to a circle mapping.

PP made all the figures in the paper, carried out all the implementations and numerics, and gave feedback throughout the work.

Published in proceedings of ASME 2001 DETC'01, Pennsylvania, 2001

Paper 5

Exploiting Discontinuities for Stabilization of Recurrent Motions Harry Dankowicz (HD), Petri Piiroinen (PP) In paper 5 a method is analytically derived to locally control dynamical system including discontinuities, by using the fact that it is possible to calculate the stability characteristics (Floquet multipliers) of periodic motions of such systems. When a periodic solution has been found the method makes it possible not only to stabilize heavily unstable dynamical systems but also to destabilize stable systems. The main advantage with this method is that the exact stability characteristics for the controlled system can be found, even without simulating it once, but only by using the local stability for a reference solution. The method is applied on a hopping robot and a Braille printer, where it is shown how the stability changes under variations of a control parameter. Numerical results are presented showing the basin of attraction for a specified set of control parameters as well as switching between different periodic motions.

PP made all the figures in the paper, carried out all the implementations and numerics, and gave feedback and suggestions on improvements throughout the work.

Accepted for publication in Nonlinear Dynamics, 2002

Paper 6

Low-Cost Control of Repetitive Gait in Passive Bipedal Walkers Petri Piiroinen (PP), Harry Dankowicz (HD)

In this paper, the control algorithm introduced in paper 5 is dereived and implemented for 2D and 3D passive walkers. The method is used to switch between different types of gait and also to stabilize heavily unstable motion.

All implementations and computations were carried out by PP, who also wrote the paper with feedback from HD.

Submitted to International Journal of Bifurcation and Chaos, 2002

Paper 7

Musculoskeletal Modeling of Two-Legged Bipedal Walkers Petri Piiroinen (PP)

This paper gives an idea on how the 3D passive walkers could be made more anthropomorphic by the addition of muscles and by increasing the total number of degrees of freedom. All sufficient parameters used for the upper and lower limbs, the different joints, the muscles, and the foot points are thoroughly introduced. Some thoughts on how to use an implementation of the extended walker is also given as well as possibilities for future development are suggested.

PP wrote the paper.

Acknowledgment

First of all I would like to thank my supervisor Dr. Harry Dankowicz. It has been a real pleasure to work with him and take part of his enthusiasm and never ending well of ideas. Even though we have been located at two different spots in the world, most of the time, we have had a close and fruitful collaboration. Another positive thing with Dr. Dankowicz is that he always had time for discussions and always tried to explain things, whatever the topic was. Thanks to him I also got the chance to go overseas and visit him at Virginia Tech, USA.

I would also like to thank Dr. Arne Nordmark who has been a good sounding board for my thoughts and questions. He has always generously shared his knowledge in mechanics, mathematics and numerical methods with me whenever I have been lost.

Many thanks goes to Prof. Martin Lesser and Dr. Hanno Essén for freely sharing their thoughts in science, politics, and philosophy. It has be a joy to listen to both of you.

The former graduate student in the theoretical and applied mechanics group Dr. Mats Fredriksson, Dr. Anders Lennartsson, Tekn. Lic. Gitte Ekdahl are acknowledged for making it very easy for me when I joined the group back in 1998. A special thanks goes to Dr. Jesper Adolfsson who initiated me into the field of passive walkers and also for sharing his knowledged in engineering and programming code. We got a very good start via the conference in München, including the visit at Hofbrauhaus.

The lunch gang has varied from time to time, but the laughs I have shared with, for instance, Per Olsson, Hans Silverhag, and Per Ekstrand have worked as a good and relaxing mental break

I would like to thank Lanie Gutierrez and MD Yvonne Haglund-Åkerlind at Astrid Lindgren Children Hospital at Karolinska Sjukhuset for demonstrating their gait lab and also for sharing their knowledge in clinical studies of human gait.

The time I spent at Virginia Tech was very enjoyable due to Colleen Shannon and David Ruppert. Hopefully you understood some of the "bad" jokes I spread around me, at the end.

To my former and present colleagues Gösta Wingårdh, Ola Widlund, Mats Lind, Tom Wright, Johan Eriksson, Daniel Ahlman, Anders Ahlström, and Kazuya Goto on the 8th floor I would like to express my gratitude. You have all made it a pleasure to go to KTH each day, and hopefully you feel the same.

My colleagues at the Department of Mechanics have definitely provided a very

stimulating research atmosphere and I am very fortunate to have met them all.

To my wonderful friends in MHFK(g) and DKV I would like to say: This thesis will not at all change the relation I have with you and the way I appreciate to be among you—it is always a pleasure!

Anna, thanks for everything and good luck in the future.

Finally, many thanks to my entire family that I have been neglecting lately, but you are often in my thoughts and I miss you all. Hopefully I will spend some more time with you in the future.

This work was supported by Swedish Foundation for Strategic Research (SSF) and Swedish Engineering Science Council (TFR).

Bibliography

- [1] J Adolfsson. Passive Control of Mechanical Systems Bipedal Walking and Autobalancing. PhD thesis, Royal Institute of Technology, Department of Mechanics, Sweden, 2001.
- [2] J Adolfsson, H Dankowicz, and A Nordmark. 3d passive walkers: Finding periodic gaits in the presence of discontinuities. *Nonlinear Dynamics*, 24:205–229, 2001.
- [3] M A Aizerman and F R Gantmakher. On the stability of periodic motions. *Journal of Applied Mathematics and Mechanics (translated from Russian)*, pages 1065–1078, 1958.
- [4] BIP. http://www.inrialpes.fr/bip/.
- [5] A Chatterjee and M Garcia. Small slope implies low speed in passive dynamic walking. Dynamics and Stability of Systems, 15(2):139–157, 1998.
- [6] M Coleman and A Ruina. An uncontrolled toy that can walk but cannot stand still. *Physical Review Letters*, 80(16):3658–3661, 1998.
- [7] M J Coleman, M Garcia, Mombaur K, and A Ruina. Prediction of stable walking for a toy that cannot stand. *Physical Review E*, 64(2), 2001.
- [8] S Collins, M Wisse, and A Ruina. A 3-d passive-dynamic walking robot with two legs and knees. *International Journal of Robotics Research*, 20(7):607–615, 2001.
- [9] R L Craik and C A Oatis, editors. *Gait Analysis: theory and application*. Mosby-Year Book, Inc., 1995.
- [10] H J Dankowicz. *Mechanics Problems and their solutions*. Dept. of Mechanics, KTH, Sweden, 1998.
- [11] H J Dankowicz, J Adolfsson, and A B Nordmark. Repetetive gait of passive bipedal mechanisms in a three-dimensional environment. *Journal of Biomechanical Engineer*ing, 123(1):40–46, 2001.
- [12] W T Dempster and G R L Gaughran. Properties of body segments based on size and weight. *American Journal of Anatomy*, 120:33–54.

56 BIBLIOGRAPHY

[13] A M Formal'sky. Ballistic Locomotion of a Biped. Design and Control of Two Biped Machines. CISM Advanced School on Modelling and Simulation of Human and Walking Robots Locomotion, Udine, 1996.

- [14] M H Fredriksson and A B Nordmark. On normal form calculations in impact oscillators. In *Proceedings of the Royal Society of London, series A, 456*, pages 315–329, 2000.
- [15] James R Gage, editor. Gait analysis in celebral palsy. Mac Keith Press, 1991.
- [16] M Garcia, A Chatterjee, and A Ruina. Efficiency, speed, and scaling of passive dynamical bipedal walking. *Dynamics and Stability of Systems*, 15(2):75–99, 2000.
- [17] M Garcia, A Chatterjee, A Ruina, and M Coleman. Passive-dynamic models of human gait. In *Proceedings of the Conference on Biomechanics and Neural Control of Human Movement*, pages 32–33, 1998.
- [18] J Guckenheimer. Bifurcation and degenerate decomposition in multiple time scale dynamical system. 2002.
- [19] J Guckenheimer and P Holmes. Nonlinear Oscillations, Dynamical Systems, and Bifurcations of Vector Fields. Springer-verlag, 1983.
- [20] R N Hinrichs. Regression equations to predict segmental moments of inertia from anthropometric measurements: An extension of the data of chandler et al. *Journal of Biomechanics*, 18(8):621–624, 1985.
- [21] R N Hinrichs. Adjustments to the segment center of mass proportions of clauser et al. Journal of Biomechanics, 23(9):949–951, 1990.
- [22] Honda. http://www.honda.co.jp/asimo/.
- [23] R K Jensen. Body segment mass, radius, and radius of gyration proportions of children. Journal of Biomechanics, 19(5):359–368, 1986.
- [24] R K Jensen. The growth of children's moment of inertia. *Medicine and Science in Sports and Exercise*, 18(4):440–445, 1986.
- [25] T R Kane and D A Levinsson. *Dynamics: Theory and Applications*. McGraw-Hill Book Company, 1985.
- [26] T Kapitaniak. Chaos for Engineers Theory, Application, and Control. Springer-Verlaag, 2000.
- [27] R Leine. Bifurcations in Discontinuous Mechanical Systems of Filippov-Type. PhD thesis, Teknische Universiteit Eindhoven, The Netherlands, 2000.
- [28] Anders Lennartsson. Efficient Multibody Dynamics. PhD thesis, Royal Institute of Technology, Department of Mechanics, Sweden, 1999.
- [29] M Lesser. The Analysis of Complex Nonlinear Mechanical Systems. World Scientific Publishing Co. Pte. Ltd, 1995.

BIBLIOGRAPHY 57

[30] T McGeer. Passive bipedal running. In *Proceedings of the Royal Society of London:* Biological Sciences, volume 240, pages 107–134, 1990.

- [31] T McGeer. Passive dynamic walking. International Journal of Robotics Research, 9: 62–82, 1990.
- [32] T McGeer. Passive walking with knees. In *Proceedings of the IEEE Conference on Robotics and Automation*, volume 2, pages 1640–1645, 1990.
- [33] MIT. Mit leg laboratory, http://www.ai.mit.edu/projects/leglab/home.html.
- [34] P C Müller. Calculations of lyapunov exponents for dynamical systems with discontinuities. *Chaos, Solitons and Fractals*, 5:1671–1681, 1995.
- [35] S Mochon and T McMahon. Ballistic walking: An improved model. *Mathematical Biosciences*, 52:241–260, 1980.
- [36] T A Mochon and G C Cheng. The mechanics of running: How does stiffness couple with speed? *Journal of Biomechanics*, 23:65–78, 1990.
- [37] M Nordin and M G Nordahl. An evolutinary architecture for a humanoid robot. *Preprint*.
- [38] A B Nordmark. Universal limit mapping in grazing bifurcations. *Physical Review E*, 55(1):266–270, 1997.
- [39] T S Parker and L O Chua. Practical Numerical Algorithms for Chaotic Systems. Springer-Verlag, New York, 1989.
- [40] P T Piiroinen. Passive walking: Transition from 2d to 3d, 2000.
- [41] Humanoid project at Chalmers. http://humanoid.fy.chalmers.se/.
- [42] Sophia. http://www.mech.kth.se/sophia.
- [43] S H Strogatz. Nonlinear Dynamics and Chaos. Addison-Wesley Publishing Company, 1994.
- [44] Vicon Motion Systems. http://www.vicon.com/.
- [45] M W Whittle. Gait Analysis an Introduction, 2nd ed. Butterwort Heinemann, Oxford, 1996.

58 BIBLIOGRAPHY

Appendix A

Physical quantities

The values of the parameters presented here are mainly used in paper 1 and 2. In the other papers some modifications have been done.

Constants

Gravity -9.81 m/s^2

Incline - varied

Masses

Torso - 0.8 kg

Upper legs -2.354 kg/each

Lower legs -1.013 kg/each

Toe point – 0 kg/each

Lengths

Torso (width) -0 m

Upper legs -0.35 m

Toe line - varied

Positions of mass center

Torso – in the midpoint between the hip joints.

Upper legs – $(0, 0, -0.09)_{\text{Upper leg}}$ relative the hip joints

Lower legs $-(0.0432, 0, -0.1663)_{Lower leg}$ relative the knee joints

Toe points $-(0.105, varied, -0.3132)_{Lower leg}$ relative the shank center of mass

The triplets correspond to the body fixed reference frame in which they are written. All values are given in meters.

Moments of inertia

 $Torso - (2, 2.2, 2.2, 0, 0, 0)_{Torso}$

Upper legs – $(0.008, 0.001, 0.01, 0, 0, 0)_{\text{Upper leg}}$

Lower legs $-(0.0393, 0.001, 0.01, 0, 0, 0)_{\text{Lower leg}}$

The numbers in the parentheses correspond to $(\mathbf{I}_{11}, \mathbf{I}_{22}, \mathbf{I}_{33}, \mathbf{I}_{12}, \mathbf{I}_{13}, \mathbf{I}_{23}) \text{ kgm}^2$.

Spring constants

Knee joints -50 N/m

Ground - 50 N/m

Damper constants

Hip joints - 0.04 Ns/m

Knee joints -20 Ns/m

Ground - 500 Ns/m

Appendix B

Numerical schemes

General formulas for the numerical differentiations in paper 2.

$$\frac{\partial \mathbf{u}}{\partial \varepsilon}(\mathbf{x}_0, \varepsilon_0, \mu_0) = \frac{1}{2h} \left[\mathbf{u}(\mathbf{x}_0, \varepsilon_0 + h, \mu_0) - \mathbf{u}(\mathbf{x}_0, \varepsilon_0 - h, \mu_0) \right]$$
(B.1)

$$\frac{\partial \mathbf{u}}{\partial \mathbf{x}}(\mathbf{x}_0, \varepsilon_0, \mu_0) \mathbf{x}_1 = \frac{1}{2h} \left[\mathbf{u}(\mathbf{x}_0 + h\mathbf{x}_1, \varepsilon_0, \mu_0) - \mathbf{u}(\mathbf{x}_0 - h\mathbf{x}_1, \varepsilon_0, \mu_0) \right]$$
(B.2)

$$\frac{\partial^2 \mathbf{u}}{\partial \varepsilon^2}(\mathbf{x}_0, \varepsilon_0, \mu_0) = \frac{1}{h^2} \left[\mathbf{u}(\mathbf{x}, \varepsilon_0 + h, \mu_0) - 2\mathbf{u}(\mathbf{x}_0, \varepsilon_0, \mu_0) + \mathbf{u}(\mathbf{x}_0, \varepsilon_0 - h, \mu_0) \right]$$
(B.3)

$$\frac{\partial^{2} \mathbf{u}}{\partial \varepsilon \partial \mu} (\mathbf{x}_{0}, \varepsilon_{0}, \mu_{0}) = \frac{1}{4h_{1}h_{2}} \begin{bmatrix} \mathbf{u}(\mathbf{x}_{0} + h_{1}\mathbf{x}_{1} + h_{2}\mathbf{x}_{2}, \varepsilon_{0}, \mu_{0}) - \mathbf{u}(\mathbf{x}_{0} + h\mathbf{x}_{0} - h\mathbf{x}_{1}, \varepsilon_{0}, \mu_{0}) - \mathbf{u}(\mathbf{x}_{0} + h_{2}\mathbf{x}_{0}, \mu_{0}) + \mathbf{u}(\mathbf{x}_{0} - h_{2}\mathbf{x}_{0}, \mu_{0}) - \mathbf{u}(\mathbf{x}_{0} + h_{2}\mathbf{x}_{0}, \mu_{0}, \mu_{0}) - \mathbf{u}(\mathbf{x}_{0} + h_{2}\mathbf{x}_{0}, \mu_{0}, \mu_{0}, \mu_{0$$

$$\frac{\partial^2 \mathbf{u}}{\partial \mathbf{x}^2} (\mathbf{x}_0, \varepsilon_0, \mu_0) \mathbf{x}_1 \mathbf{x}_2 = \frac{1}{4h_1 h_2} \begin{bmatrix} \mathbf{u}(\mathbf{x}, \varepsilon_0 + h_1, \mu_0 + h_2) - \mathbf{u}(\mathbf{x}_0, \varepsilon_0 + h_1, \mu_0 - h_2) - \\ \mathbf{u}(\mathbf{x}_0, \varepsilon_0 - h_1, \mu_0 + h_2) + \mathbf{u}(\mathbf{x}_0, \varepsilon_0 - h_1, \mu_0 - h_2) \end{bmatrix}$$
(B.5)

$$\frac{\partial^{3} \mathbf{u}}{\partial \varepsilon^{2} \partial \mu} (\mathbf{x}_{0}, \varepsilon_{0}, \mu_{0}) \mathbf{x}_{1} = \frac{1}{2h_{1}^{2} h_{2}} \begin{bmatrix}
\mathbf{u}(\mathbf{x}_{0}, \varepsilon_{0} + h_{1}, \mu_{0} + h_{2}) - 2\mathbf{u}(\mathbf{x}_{0}, \varepsilon_{0} + h_{2}, \mu_{0}) + \\
\mathbf{u}(\mathbf{x}_{0}, \varepsilon_{0} - h_{1}, \mu_{0} + h_{2}) - \mathbf{u}(\mathbf{x}_{0}, \varepsilon_{0} + h_{1}, \mu_{0} - h_{2}) + \\
2\mathbf{u}(\mathbf{x}_{0}, \varepsilon_{0}, \mu_{0} - h_{2}) - \mathbf{u}(\mathbf{x}_{0}, \varepsilon_{0} - h_{2}, \mu_{0} - h_{3})
\end{bmatrix}$$
(B.6)

$$\frac{\partial^{3} \mathbf{u}}{\partial \mathbf{x} \partial \varepsilon \partial \mu} (\mathbf{x}_{0}, \varepsilon_{0}, \mu_{0}) \mathbf{x}_{1} = \frac{1}{8h_{1}h_{2}h_{3}} \begin{bmatrix}
\mathbf{u}(\mathbf{x}_{0} + h_{1}\mathbf{x}_{1}, \varepsilon_{0} + h_{2}, \mu_{0} + h_{3}) - \\
\mathbf{u}(\mathbf{x}_{0} + h_{1}\mathbf{x}_{1}, \varepsilon_{0} + h_{2}, \mu_{0} - h_{3}) - \\
\mathbf{u}(\mathbf{x}_{0} + h_{1}\mathbf{x}_{1}, \varepsilon_{0} - h_{2}, \mu_{0} + h_{3}) + \\
\mathbf{u}(\mathbf{x}_{0} + h_{1}\mathbf{x}_{1}, \varepsilon_{0} - h_{2}, \mu_{0} - h_{3}) - \\
\mathbf{u}(\mathbf{x}_{0} - h_{1}\mathbf{x}_{1}, \varepsilon_{0} + h_{2}, \mu_{0} + h_{3}) + \\
\mathbf{u}(\mathbf{x}_{0} - h_{1}\mathbf{x}_{1}, \varepsilon_{0} + h_{2}, \mu_{0} - h_{3}) + \\
\mathbf{u}(\mathbf{x}_{0} - h_{1}\mathbf{x}_{1}, \varepsilon_{0} - h_{2}, \mu_{0} + h_{3}) - \\
\mathbf{u}(\mathbf{x}_{0} - h_{1}\mathbf{x}_{1}, \varepsilon_{0} - h_{2}, \mu_{0} - h_{3})
\end{bmatrix} \tag{B.7}$$

Appendix C

Maple/Sophia code

This Maple code is used for generating the equations of motion and variational equations for a passive 3D walker with knees.

```
Load Sophia library
> restart;
> read 'sophiaV5';
Kinematical differential equations
> &kde(10);
> dependsTime(seq(p.k,k=1..16));
> dependsTime(seq(theta.k,k=1..6));
Frame relations Rotation from inertial body N to upper body B
> chainSimpRot([N,T1,3,q6],[T1,T2,2,q5],[T2,B,1,q4]):
Rotation from intermeditiary frame T2 to upper leg UL1 to lower leg LL1 > chainSimpRot([T2,UL1,1,q7],[UL1,LL1,1,q8]):
Rotation from intermeditiary frame T2 to upper leg UL2 to lower leg LL2
> chainSimpRot([T2,UL2,1,q9],[UL2,LL2,1,q10]):
Rotation from lower leg LL1 \, foot \, F1 \,
> chainSimpRot([LL1,T3,3,theta1],[T3,T4,2,theta2],[T4,F1,1,theta3]):
Rotation from lower leg LL2 foot F2
> chainSimpRot([LL2,T5,3,theta4],[T5,T6,2,theta5],[T6,F2,1,theta6]):
Geometry
> rbody_hip_center:=N &ev [q1,q2,q3];
> r_torso_cm_rel:=B &ev [rx,ry,rz];
> rleg1_jointpos:=T2 &ev [rl11,0,0];
> rleg2_jointpos:=T2 &ev [rl21,0,0];
> rleg1_upper_cm_rel:= UL1 &ev [rl1u1,rl1u2,rl1u3];
> rleg2_upper_cm_rel:= UL2 &ev [rl2u1,rl2u2,rl2u3];
> rleg1_upper_jointpos_rel:= UL1 &ev [0,11u,0];
> rleg2_upper_jointpos_rel:= UL2 &ev [0,12u,0];
> rleg1_lower_cm_rel:= LL1 &ev [rl111,rl112,rl113];
> rleg2_lower_cm_rel:= LL2 &ev [rl2l1,rl2l2,rl2l3];
> rbody_cm:=mkc(rbody_hip_center,r_torso_cm_rel);
> rleg1upper_cm:=mkc(rbody_hip_center,rleg1_jointpos,rleg1_upper_cm_rel):
> rleg2upper_cm:=mkc(rbody_hip_center,rleg2_jointpos,rleg2_upper_cm_rel):
> rleg1lower_cm:=mkc(rbody_hip_center,rleg1_jointpos,rleg1_upper_jointpos_rel,rleg1_lower_cm_rel):
> rleg2lower_cm:=mkc(rbody_hip_center,rleg2_jointpos,rleg2_upper_jointpos_rel,rleg2_lower_cm_rel):
New kde's > v_body_hipcenter:= T2 &ev [u1,u2,u3]; > omega_body:=T2 &ev [u4,u5,u6];
> v_body_hipcenter_qt:= diffFrameTime(rbody_hip_center,N);
> omega_body_qt:=N &aV B;
Note that the kde for toe contact points are included
```

```
> ikde:={seq((T2 &to v_body_hipcenter &c i) = (T2 &to v_body_hipcenter_qt) &c i,i=1..3),
             seq((T2 &to omega_body &c i) = (T2 &to omega_body_qt) &c i,i=1..3),
             seq(p.(2*i-1).t=-q1t,i=1..8),
             seq(p.(2*i).t=-q3t, i=1..8),
             seq(theta.i.t=0,i=1..6):
> kde_new := simplify(solve(ikde, {seq(q.i.t,i=1..6)}
                                                 seq(p.i.t, i=1..16),
                                                 seq(theta.i.t,i=1..6)}) union
                                                {seq(q.i.t=u.i,i=7..10)}:
Velocities and angular velocities
> v_{body\_cm} := ccpt(map(Esimplify,subs(kde_new,cdft(rbody\_cm,N)))):
> vleg1upper_cm := ccpt(map(Esimplify,subs(kde_new,cdft(rleg1upper_cm,N)))):
> vleg2upper_cm := ccpt(map(Esimplify,subs(kde_new,cdft(rleg2upper_cm,N)))):
> vleg1lower_cm := ccpt(map(Esimplify,subs(kde_new,cdft(rleg1lower_cm,N)))):
> vleg1lower_cm := ccpt(map(Esimplify,subs(kde_new,cdft(rleg2lower_cm,N)))):
> vleg2lower_cm := ccpt(map(Esimplify,subs(kde_new,cdft(rleg2lower_cm,N)))):
> omega_leg1upper := &simp subs(kde_new,N &aV UL1):
> omega_leg1lower := &simp subs(kde_new,N &aV UL2):
> omega_leg1lower := &simp subs(kde_new,N &aV LL1):
> omega_leg2lower := &simp subs(kde_new,N &aV LL2):
Momentum and angular momentum
> pbody:=csm(m_body, v_body_cm):
> pleg1upper:=csm(ml1u,vleg1upper_cm):
> pleg2upper:=csm(ml2u,vleg2upper_cm):
> pleg1lower:=csm(ml11,vleg1lower_cm):
> pleg2lower:=csm(ml21,vleg2lower_cm):
> I_body:=EinertiaDyad(I_B11,I_B22,I_B33,I_B12,I_B13,I_B23,B):
> hbody:=I_body &o omega_body:
> I_leg1upper:=EinertiaDyad(I_LU111,I_LU122,I_LU133,I_LU112,I_LU113,I_LU123,UL1):
> hleg1upper:=I_leg1upper &o omega_leg1upper:
> I_leg2upper:=EinertiaDyad(I_LU211,I_LU222,I_LU233,I_LU212,I_LU213,I_LU223,UL2):
> hleg2upper:=I_leg2upper &o omega_leg2upper:
> I_leg1lower:=EinertiaDyad(I_LL111,I_LL122,I_LL133,I_LL112,I_LL113,I_LL123,LL1):
> hleg1lower:=I_leg1lower &o omega_leg1lower:
> I_leg2lower:=EinertiaDyad(I_LL211,I_LL222,I_LL233,I_LL212,I_LL213,I_LL223,LL2):
> hleg2lower:=I_leg2lower &o omega_leg2lower:
Timediff of Mom and ang. \ensuremath{\mathsf{mom}}
                  :=map(Esimplify,subs(kde_new,cdft(pbody,N))):
> ptbody
> ptleg1upper:=map(Esimplify,subs(kde_new,cdft(pleg1upper,N))):
> ptleg2upper:=map(Esimplify,subs(kde_new,cdft(pleg2upper,N))):
> ptleg1lower:=map(Esimplify,subs(kde_new,cdft(pleg1lower,N))):
> ptleg2lower:=map(Esimplify,subs(kde_new,cdft(pleg2lower,N))):
> htbody:=mkc( &simp subs(kde_new,N &fdt hbody) ):
> htleg1upper:=mkc( &simp subs(kde_new,N &fdt hleg1upper) ):
> htleg2upper:=mkc( &simp subs(kde_new,N &fdt hleg2upper) ):
> htleg1lower:=mkc( &simp subs(kde_new,N &fdt hleg1lower) ):
> htleg2lower:=mkc( &simp subs(kde_new, N &fdt hleg2lower) ):
Assembly of K velocity vector and tangent vector creation
> vK:=[v_body_cm, vleg1upper_cm, vleg2upper_cm, vleg1lower_cm, vleg2lower_cm,
> mkc(omega_body), mkc(omega_leg1upper), mkc(omega_leg2upper),
mkc(omega_leg1lower), mkc(omega_leg2lower) ]:
> tauK:=Kctau(vK,[seq(u.i,i=1..10)]):
Common stuff
Procedure for finding out what variables an expression depends on given a list of possible variables
> check_args:=proc(expr,args)
> local temp_args,i;
> temp_args:=[]:
> for i in args do
> if depends(expr,i) then temp_args:=[op(temp_args),i]; fi;
> od;
> RETURN(op(temp_args));
> end:
> args:=seq(q.i,i=1..10),seq(theta.i,i=1..6),seq(u.i,i=1..10);
First foot first toe 11
```

```
Position and velocity of toe11
> rtoe11:=&simp (N &to (rbody_hip_center &++ rleg1_jointpos &++ rleg1_upper_jointpos_rel &++
                         (LL1 &ev [0,111,0]) &++ (F1 &ev [xt11,yt11,zt11]))):
> vtoe11:=&simp (N &to subs(kde_new,N &fdt rtoe11)):
Find the variables that each coord. & vel. of the toepos depends on
> x11_args:=check_args((rtoe11 &c 1)-q1,[args]):
> y11_args:=check_args(rtoe11 &c 2,[args]):
> z11_args:=check_args((rtoe11 &c 3)-q3,[args]):
> vx11_args:=check_args(vtoe11 &c 1,[args]):
> vy11_args:=check_args(vtoe11 &c 2,[args]):
> vz11_args:=check_args(vtoe11 &c 3,[args]):
(N &ev [toefx(stat11,x11(x11_args),vx11(vx11_args),kX,dX,p1),
                                          toefy(stat11, y11(y11_args), vy11(vy11_args), kY, dY),
                                          toefz(stat11,z11(z11_args),vz11(vz11_args),kZ,dZ,p2)])):
Common subexpression used later in calculations
> toe11_list:=[x11=(rtoe11 &c 1)-q1,y11=rtoe11 &c 2,z11=(rtoe11 &c 3)-q3,
> vx11=vtoe11 &c 1,vy11=vtoe11 &c 2,vz11=vtoe11 &c 3,
                fx11=toefx(stat11,x11(x11_args),vx11(vx11_args),kX,dX,p1),
                fy11=toefy(stat11,y11(y11_args),vy11(vy11_args),kY,dY),
                fz11=toefz(stat11,z11(z11_args),vz11(vz11_args),kZ,dZ,p2), tx11=toe11_cmll1_cross_f &c 1, ty11=toe11_cmll1_cross_f &c 2,
                tz11=toe11_cmll1_cross_f &c 3]:
Substitutions used in stability calculations
    D[2] (toefx) (stat11,x11(x11_args),vx11(vx11_args),kX,dX,p1)=
    toefx_x(stat11,x11,vx11,kX,dX,p1),
D[3](toefx)(stat11,x11(x11_args),vx11(vx11_args),kX,dX,p1)=
      toefx_vx(stat11,x11,vx11,kX,dX,p1),
    D[2](toefy)(stat11,y11(y11_args),vy11(vy11_args),kY,dY) =
    toefy_y(stat11,y11,yy11,kY,dY),
D[3](toefy)(stat11,y11(y11_args),vy11(vy11_args),kY,dY)=
      toefy_vy(stat11,y11,vy11,kY,dY),
    D[2](toefz)(stat11,z11(z11_args),vz11(vz11_args),kZ,dZ,p2)=
       toefz_z(stat11,z11,vz11,kZ,dZ,p2),
    D[3] (toefz) (stat11,z11(z11_args), vz11(vz11_args), kZ, dZ,p2)=
       toefz_vz(stat11,z11,vz11,kZ,dZ,p2),
    D[6] (toefx) (stat11,x11(x11_args), vx11(vx11_args), kX, dX,p1)=
       toefx_p(stat11,x11,vx11,kX,dX,p1),
    D[6](toefz)(stat11,z11(z11_args),vz11(vz11_args),kZ,dZ,p2)=
      toefz_p(stat11,z11,vz11,kZ,dZ,p2),
     seq(diff(x11(x11_args),i)=dx11d.i,i=x11_args),
     seq(diff(vx11(vx11_args),i)=dvx11d.i,i=vx11_args),
     x11(x11_args)=x11,
     vx11(vx11_args)=vx11,
     seq(diff(y11(y11_args),i)=dy11d.i,i=y11_args),
     seq(diff(vy11(vy11_args),i)=dvy11d.i,i=vy11_args),
     y11(y11_args)=y11,
     vy11(vy11_args)=vy11,
     seq(diff(z11(z11_args),i)=dz11d.i,i=z11_args),
     seq(diff(vz11(vz11_args),i)=dvz11d.i,i=vz11_args),
     z11(z11 args)=z11,
     vz11(vz11_args)=vz11];
First foot second toe 12
> x12_args:=x11_args:
> y12_args:=y11_args:
> z12_args:=z11_args:
> x12_args:=vx11_args:
> vy12_args:=vy11_args:
> vz12_args:=vz11_args:
 from toe11 to toe12 sset:={
                                xt11=xt12,yt11=yt12,zt11=zt12,
rl111=rl111,rl112=rl112,rl113=rl113,
                                toefx(stat11,x11(x11_args))=toefx(stat12,x12(x12_args)),
                                toefy(stat11,y11(y11_args))=toefy(stat12,y12(y12_args)),
                                toefz(stat11,z11(z11_args))=toefz(stat12,z12(z12_args)), x11=x12,vx11=vx12, y11=y12,vy11=vy12,
```

```
z11=z12, vz11=vz12,
                                                                                                                                  stat11=stat12.
                                                                                                                                  p1=p3,p2=p4,
                                                                                                                                   seq(dx11d.x11_args[i]=dx12d.x12_args[i],i=1..nops([x12_args])),
                                                                                                                                   seq(dvx11d.vx11_args[i]=dvx12d.vx12_args[i],i=1..nops([vx12_args])),
                                                                                                                                   seq(dy11d.y11_args[i]=dy12d.y12_args[i],i=1..nops([y12_args])),
                                                                                                                                   seq(dvy11d.vy11\_args[i]=dvy12d.vy12\_args[i],i=1..nops([vy12\_args])),\\
                                                                                                                                   seq(dz11d.z11_args[i]=dz12d.z12_args[i],i=1..nops([z12_args]))
                                                                                                                                  seq(dvz11d.vz11_args[i]=dvz12d.vz12_args[i],i=1..nops([vz12_args])),
fx11=fx12,fy11=fy12,fz11=fz12,
                                                                                                                                  tx11=tx12,ty11=ty12,tz11=tz12}:
       rtoe12: =subs(from_toe11_to_toe12_sset,rtoe11)
> rtoe12:-subs(from_toe11_to_toe12_sset,rtoe11):
> vtoe12:=subs(from_toe11_to_toe12_sset,vtoe11):
> toe12_cmll1_cross_f:=subs(from_toe11_to_toe12_sset,toe11_cmll1_cross_f):
> toe12_list:=subs(from_toe11_to_toe12_sset,toe11_list):
> dset12:=subs(from_toe11_to_toe12_sset,dset11):
First foot third toe 13
Position & velocity of toe13
> rtoe13:=&simp (N &to (rbody_hip_center &++ rleg1_jointpos &++ rleg1_upper_jointpos_rel &++ (LL1 &ev [0,111,0]) &++ (F1 &ev [xt13,yt13,zt13]))):
> vtoe13:=&simp (N &to subs(kde_new,N &fdt rtoe13)):
 Find the variables that each coord. & vel. of the toepos depends on
  > x13_args:=check_args((rtoe13 &c 1)-q1,[args]):
  > y13_args:=check_args(rtoe13 &c 2,[args]):
  > z13_args:=check_args((rtoe13 &c 3)-q3,[args]):
 > vx13_args:=check_args(vtoe13 &c 1,[args]):
  > vy13_args:=check_args(vtoe13 &c 2,[args]):
 > vz13_args:=check_args(vtoe13 &c 3,[args]):
 Torque calculated as vector from cm of lower leg to contact point cross applied force > toe13_cmll1_cross_f:=&simp ((N &to ((LL1 &ev [0,111,0]) &++
                                                                                                                                         (F1 &ev [xt13,yt13,zt13]) &-
\tag{\text{\text{\text{\text{\text{\text{\text{\text{\text{\text{\text{\text{\text{\text{\text{\text{\text{\text{\text{\text{\text{\text{\text{\text{\text{\text{\text{\text{\text{\text{\text{\text{\text{\text{\text{\text{\text{\text{\text{\text{\text{\text{\text{\text{\text{\text{\text{\text{\text{\text{\text{\text{\text{\text{\text{\text{\text{\text{\text{\text{\text{\text{\text{\text{\text{\text{\text{\text{\text{\text{\text{\text{\text{\text{\text{\text{\text{\text{\text{\text{\text{\text{\text{\text{\text{\text{\text{\text{\text{\text{\text{\text{\text{\text{\text{\text{\text{\text{\text{\text{\text{\text{\text{\text{\text{\text{\text{\text{\text{\text{\text{\text{\text{\text{\text{\text{\text{\text{\text{\text{\text{\text{\text{\text{\text{\text{\text{\text{\text{\text{\text{\text{\text{\text{\text{\text{\text{\text{\text{\text{\text{\text{\text{\text{\text{\text{\text{\text{\text{\text{\text{\text{\text{\text{\text{\text{\text{\text{\text{\text{\text{\text{\text{\text{\text{\text{\text{\text{\text{\text{\text{\text{\text{\text{\text{\text{\text{\text{\text{\text{\text{\text{\text{\text{\text{\text{\text{\text{\text{\text{\text{\text{\text{\text{\text{\text{\text{\text{\text{\text{\text{\text{\text{\text{\text{\text{\text{\text{\text{\text{\text{\text{\text{\text{\text{\text{\text{\text{\text{\text{\text{\text{\text{\text{\text{\text{\text{\text{\text{\text{\text{\text{\text{\text{\text{\text{\text{\text{\text{\text{\text{\text{\text{\text{\text{\text{\text{\text{\text{\text{\text{\text{\text{\text{\text{\text{\text{\text{\text{\text{\text{\text{\text{\text{\text{\text{\text{\text{\text{\text{\text{\text{\text{\text{\text{\text{\text{\text{\text{\text{\text{\text{\text{\text{\text{\text{\text{\text{\text{\text{\text{\text{\text{\text{\text{\text{\text{\text{\text{\text{\text{\text{\text{\text{\text{\text{\text{\text{\text{\text{\text{\text{\text{\text{\text{\text{\text{\text{\text{\text{\text{\text{\text{\text{\text{\text{\text{\text{\text{\text{\text{\text{\text{\text{\text{\text{\text{\text{\text{\text{\
  Common subexpression used later in calculations
fy13=toefy(stat13,y13(y13_args),vy13(vy13_args),kY,dY),
                                                                    fz13=toefz(stat13,z13(z13_args),vz13(vz13_args),kZ,dZ,p6),
                                                                   tx13=toe13_cmll1_cross_f &c 1,
ty13=toe13_cmll1_cross_f &c 2,
                                                                    tz13=toe13 cmll1 cross f &c 3]:
 Substitutions used in stability calculations
  > dset13:=[
                 set13:=[
D[2](toefx)(stat13,x13(x13_args),vx13(vx13_args),kX,dX,p5)=toefx_x(stat13,x13,vx13,kX,dX,p5),
D[3](toefx)(stat13,x13(x13_args),vx13(vx13_args),kX,dX,p5)=toefx_vx(stat13,x13,vx11,kX,dX,p5),
D[2](toefy)(stat13,y13(y13_args),vy13(vy13_args),kY,dY)=toefy_y(stat13,y13,vy13,kY,dY),
D[3](toefy)(stat13,y13(y13_args),vy13(vy13_args),kY,dY)=toefy_vy(stat13,y13,vy13,kY,dY),
D[3](toefy)(stat13,y13(y13_args),vy13(vy13_args),kY,dY)=toefy_vy(stat13,y13,vy13,kY,dY),
                  \texttt{D[2]} \ (\texttt{toefz}) \ (\texttt{stat13}, \texttt{z13} \ (\texttt{z13\_args}) \ , \texttt{vz13} \ (\texttt{vz13\_args}) \ , \texttt{kZ}, \texttt{dZ}, \texttt{p6}) = \texttt{toefz\_z} \ (\texttt{stat13}, \texttt{z13}, \texttt{vz13}, \texttt{kZ}, \texttt{dZ}, \texttt{p6})
                  D[3] \, (\text{toefz}) \, (\text{stat13,z13(z13\_args),vz13(vz13\_args),kZ,dZ,p6}) \, \\ = \, \text{toefz\_vz(stat13,z13,vz13,kZ,dZ,p6)} \, , \\ = \, \text{toefz\_vz(stat13,z13,kZ,q2,kZ,p6)} \, , \\ = \, \text{toefz\_vz(stat13,z13,kZ,q2,kZ,q2,kZ,
                  \texttt{D[6]} \ (\texttt{toefx}) \ (\texttt{stat13}, \texttt{x13} \ (\texttt{x13\_args}) \ , \texttt{vx13} \ (\texttt{vx13\_args}) \ , \texttt{kX}, \texttt{dX}, \texttt{p5}) = \texttt{toefx\_p} \ (\texttt{stat13}, \texttt{x13}, \texttt{vx13}, \texttt{kX}, \texttt{dX}, \texttt{p5}) \ , \\ \texttt{vx13} \ (\texttt{vx13\_args}) \ , \texttt{vx13} \ (\texttt{vx13\_args}) \ , \texttt{vx13} \ (\texttt{vx13\_args}) \ , \\ \texttt{vx13} \ (\texttt{vx13\_args}) \ , \texttt{vx13} \ (\texttt{vx13\_args}) \ , \\ \texttt{vx13} \ (\texttt{vx13\_args}) \ , \texttt{vx13} \ (\texttt{vx13\_args}) \ , \\ \texttt{vx13\_args}) \ , \\ \texttt{vx13\_ar
                  seq(diff(x13(x13_args),i)=dx13d.i,i=x13_args),
                        seq(diff(vx13(vx13_args),i)=dvx13d.i,i=vx13_args),
                      x13(x13_args)=x13,
vx13(vx13_args)=vx13,
                        seq(diff(y13(y13_args),i)=dy13d.i,i=y13_args),
                        seq(diff(vy13(vy13_args),i)=dvy13d.i,i=vy13_args),
                       y13(y13_args)=y13,
vy13(vy13_args)=vy13,
seq(diff(z13(z13_args),i)=dz13d.i,i=z13_args),
                        seq(diff(vz13(vz13_args),i)=dvz13d.i,i=vz13_args),
                        z13(z13_args)=z13,
                        vz13(vz13_args)=vz13]:
 First foot second toe 14 > x14_args:=x13_args:
```

```
> y14_args:=y13_args:
> z14_args:=z13_args:
   vx14_args:=vx13_args:
vy14_args:=vy13_args:
   vz14_args:=vz13_args:
> from_toe13_to_toe14_sset:={
                                                            xt13=xt14,yt13=yt14,zt13=zt14,
rl111=rl111,rl112=rl112,rl113=rl113,
toefx(stat13,x13(x13_args))=toefx(stat14,x14(x14_args)),
                                                            toefy(stat13,y13(y13_args))=toefy(stat14,y14(y14_args)),
                                                            toefz(stat13,z13(z13_args))=toefz(stat14,z14(z14_args)),
                                                            x13=x14, vx13=vx14,
y13=y14, vy13=vy14,
                                                            z13=z14,vz13=vz14
stat13=stat14,
                                                            p5=p7,p6=p8,
seq(dx13d.i=dx14d.i,i=x14_args),
                                                            seq(dvx13d.i=dvx14d.i,i=vx14_args),
                                                            seq(dy13d.i=dy14d.i,i=y14_args),
                                                            seq(dvy13d.i=dvy14d.i,i=vy14_args),
                                                            seq(dz13d.i=dz14d.i,i=z14_args),
                                                            seq(dvz13d.i=dvz14d.i,i=vz14_args),
fx13=fx14,fy13=fy14,fz13=fz14,
                                                            tx13=tx14,ty13=ty14,tz13=tz14:
> rtoe14:=subs(from_toe13_to_toe14_sset,rtoe13)
> vtoe14:=subs(from_toe13_to_toe14_sset,vtoe13):
> toe14_cmll1_cross_f:=subs(from_toe13_to_toe14_sset,toe13_cmll1_cross_f):
> toe14_list:=subs(from_toe13_to_toe14_sset,toe13_list):
> dset14:=subs(from_toe13_to_toe14_sset,dset13)
Second foot first toe 21 > from_leg1_to_leg2:= \{q7=q9,q8=q10,u7=u9,u8=u10,theta1=theta4,theta2=theta5,theta3=theta6: > x21_args:=seq(subs(from_leg1_to_leg2,[x11_args])[i],i=1..nops([x11_args])):
> x21_args:-seq(subs(from_leg1_to_leg2, [x11_args])[i],i=1..nops([x11_args])):
> y21_args:-seq(subs(from_leg1_to_leg2, [y11_args])[i],i=1..nops([y11_args])):
> vx21_args:-seq(subs(from_leg1_to_leg2, [z11_args])[i],i=1..nops([vx11_args])):
> vx21_args:-seq(subs(from_leg1_to_leg2, [vx11_args])[i],i=1..nops([vx11_args])):
> vy21_args:-seq(subs(from_leg1_to_leg2, [vy11_args])[i],i=1..nops([vy11_args])):
> vz21_args:-seq(subs(from_leg1_to_leg2, [vz11_args])[i],i=1..nops([vz11_args])):
> from_toe11_to_toe21_sset:={
                                                           rt11=xt21,yt11=yt21,zt11=zt21,
rl111=rl2l1,rl112=rl2l2,rl113=rl2l3,
rl11=rl21,
                                                            l1u=l2u,
l1l=l2l,
                                                            toefx(stat11,x11(x11_args))=toefx(stat21,x21(x21_args)),
                                                            toefy(stat11,y11(y11_args))=toefy(stat21,y21(y21_args)),
                                                            toefz(stat11,z11(z11_args))=toefz(stat21,z21(z21_args)),
x11=x21,vx11=vx21,
y11=y21,vy11=vy21,
z11=z21,vz11=vz21,
stat11=stat21,
                                                            p1=p9,p2=p10,
                                                           property property seq(dx11d.x11_args[i]=dx21d.x21_args[i],i=1..nops([x21_args])), seq(dxx11d.x11_args[i]=dvx21d.vx21_args[i],i=1..nops([vx21_args])), dx11dq7=dx21dq9,dx11dq8=dx21dq10, dvx11dq7=dvx21dq9,dvx11du8=dx21du10, dvx11du7=dvx21du9,dvx11du8=dx21du10, dvx11du7=dvx21du9,dvx11du8=dvx21du10, seq(dy11d.vy11_args[i]=dvy21d.vy21_args[i],i=1..nops([y21_args])), seq(dvy11d.vy11_args[i]=dvy21d.vy21_args[i],i=1..nops([vy21_args])), dy11dq7=dvy21dq9,dvy11dq8=dvy21dq10, dvy11dq7=dvy21dq9,dvy11du8=dvy21dq10, dvy11du7=dvy21du9,dvy11du8=dvy21du10, seq(dz11d.z11_args[i]=dz21d.z21_args[i],i=1..nops([z21_args])), seq(dvy11d.vz11_args[i]=dvz21d.vz21_args[i],i=1..nops([z21_args])), seq(dvy11dv-dvy21du9,dvy11du8=dvy21du10, dvy11du7=dvz21dq9,dz11dq8=dvz21dq10, dz11dq7=dz21dq9,dz11dq8=dvz21dq10, dz11dq7=dz21du9,dz11du8=dz21du10, dvz11dq7=dvz21du9,dvz11du8=dvz21du10, fx11=fx21,fy11=fy21,fz11=fz21, tx11=tx21,ty11=ty21,tz11=tz21}:
                                                            seq(dx11d.x11_args[i]=dx21d.x21_args[i],i=1..nops([x21_args])),
                                                            tx11=tx21,ty11=ty21,tz11=tz21}:
> rtoe21:=subs(from_leg1_to_leg2,subs(from_toe11_to_toe21_sset,rtoe11)):
> vtoe21:=subs(from_leg1_to_leg2,subs(from_toe11_to_toe21_sset,vtoe11)):
> toe21_cml12_cross_f:=subs(from_leg1_to_leg2,subs(from_toe11_to_toe21_sset,toe11_cml11_cross_f)):
> toe21_list:=subs(from_leg1_to_leg2,subs(from_toe11_to_toe21_sset,toe11_list)):
> dset21:=subs(from_leg1_to_leg2,subs(from_toe11_to_toe21_sset,dset11)):
```

```
Second foot second toe 22
second Toot second toe
> x22_args:=x21_args:
> y22_args:=y21_args:
> z22_args:=z21_args:
> vx22_args:=vx21_args:
> vy22_args:=vy21_args:
> vz22_args:=vy21_args:
> vz22_args:=vz21_args:
 > from_toe21_to_toe22_sset:={
                                                                     xt21=xt22,yt21=yt22,zt21=zt22,
rl2l1=rl2l1,r2ll2=rl2l2,rl2l3=rl2l3,
                                                                     toefx(stat21,x21(x21_args))=toefx(stat22,x22(x22_args)),
                                                                     toefy(stat21,y21(y21_args))=toefy(stat22,y22(y22_args)),
                                                                    toefz(stat21,z21(z21_args))=toefz(stat22,z22(z22_args)), x21=x22,vx21=vx22, y21=y22,vy21=vy22, z21=z22,vz21=vz22, stat21=stat22,
                                                                     p9=p11,p10=p12,
                                                                     seq(dx21d.x21_args[i]=dx22d.x22_args[i],i=1..nops([x22_args])),
                                                                     seq(dvx21d.vx21_args[i]=dvx22d.vx22_args[i],i=1..nops([vx22_args])), seq(dy21d.y21_args[i]=dy22d.y22_args[i],i=1..nops([y22_args])),
                                                                     seq(dvy21d.vy21_args[i]=dvy22d.vy22_args[i],i=1..nops([vy22_args])),
                                                                     seq(dz21d.z21_args[i]=dz22d.z22_args[i],i=1..nops([z22_args])),
                                                                     seq(dvz21d.vz21_args[i]=dvz22d.vz22_args[i],i=1..nops([vz22_args])), fx21=fx22,fy21=fy22,fz21=fz22,
                                                                     tx21=tx22,ty21=ty22,tz21=tz22):
> rtoe22:=subs(from_toe21_to_toe22_sset,rtoe21):
> vtoe22:=subs(from_toe21_to_toe22_sset,vtoe21):
> toe22_cml12_cross_f:=subs(from_toe21_to_toe22_sset,toe21_cml12_cross_f):
> toe22_list:=subs(from_toe21_to_toe22_sset,toe21_list):
> dset22:=subs(from_toe21_to_toe22_sset,dset21);
Second foot second toe 23
> x23_args:=seq(subs(from_leg1_to_leg2, [x13_args])[i],i=1..nops([x13_args]));
> y23_args:=seq(subs(from_leg1_to_leg2, [y13_args])[i],i=1..nops([y13_args]));
> y2_args:-seq(subs(from_leg1_to_leg2,[z13_args])[i],i=1..nops([z13_args])):
> vx23_args:=seq(subs(from_leg1_to_leg2,[vx13_args])[i],i=1..nops([vx13_args])):
> vy23_args:=seq(subs(from_leg1_to_leg2,[vx13_args])[i],i=1..nops([vy13_args])):
> vz23_args:=seq(subs(from_leg1_to_leg2,[vz13_args])[i],i=1..nops([vz13_args])):
 > from toe13 to toe23 sset:={
                                                                    xt13=xt23,yt13=yt23,zt13=zt23,
rl111=rl211,rl112=rl212,rl113=rl213,
                                                                     rl11=rl21,
                                                                     11u=12u,
                                                                     111=121,
                                                                    toefy(stat13,y13(y13_args))=toefx(stat23,x23(x23_args)), toefy(stat13,y13(y13_args))=toefy(stat23,y23(y23_args)), toefz(stat13,z13(z13_args))=toefz(stat23,z23(z23_args)), x13=x23,vx13=vx23, y13=y23,vy13=vy23, z13=z23,vz13=vz23, stat13=stat23, p5=p13.n6=n14
                                                                     toefx(stat13,x13(x13_args))=toefx(stat23,x23(x23_args)),
                                                                     p5=p13,p6=p14,
                                                                     seq(dx13d.x13_args[i]=dx23d.x23_args[i],i=1..nops([x23_args])),
                                                                    seq(dx13d.x13_args[i]=dx23d.x23_args[i],i=1..nops([x23_args])),
seq(dx13d.vx13_args[i]=dvx23d.vx23_args[i],i=1..nops([vx23_args])),
seq(dy13d.vy13_args[i]=dy23d.vy23_args[i],i=1..nops([y23_args])),
seq(dvy13d.vy13_args[i]=dvy23d.vy23_args[i],i=1..nops([v23_args])),
seq(dx13d.z13_args[i]=dz23d.z23_args[i],i=1..nops([v23_args])),
                                                                    seq(dz13d.z13_args[i]=dz23d.z23_args[i],i=1..nops([z23_args])),
seq(dvz13d.vz13_args[i]=dvz23d.vz23_args[i],i=1..nops([vz23_args])),
dx13dq7=dx23dq9,dx13dq8=dx23dq10,
dvx13dq7=dvx23dq9,dvx13dq8=dvx23dq10,
dx13du7=dx23du9,dx13du8=dx23du10,
dvx13du7=dvx23dq9,dvx13du8=dvx23du10,
dvy13dq7=dy23dq9,dy13dq8=dy23dq10,
dvy13dq7=dy23dq9,dvy13dq8=dv23dq10,
dvy13dq7=dvy23du9,dvy13du8=dv23du10,
dvy13du7=dvy23du9,dvy13du8=dv23du10,
dvy13du7=dv23du9,dvy13du8=dv23du10,
dvx13du7=dv23du9,dvx13dq8=dz23dq10,
dvx13dq7=dz23dq9,dvx13dq8=dz23dq10,
dz13dq7=dz23du9,dz13dq8=dz23dq10,
dz13du7=dz23du9,dz13du8=dz23du10,
dz13du7=dz23du9,dz13du8=dz23du10,
dz13du7=dz23du9,dz13du8=dz23du10,
dz13du7=dz23du9,dz13du8=dz23du10,
dz13du7=dz23du9,dz13du8=dz23du10,
dz13du7=dz23du9,dz13du8=dz23du10,
fx13=fx23,fy13=fy23,fz13=fz23,
                                                                     fx13=fx23,fy13=fy23,fz13=fz23
                                                                     tx13=tx23,ty13=ty23,tz13=tz23:
> rtoe23:=subs(from_leg1_to_leg2,subs(from_toe13_to_toe23_sset,rtoe13)):
> vtoe23:=subs(from_leg1_to_leg2,subs(from_toe13_to_toe23_sset,vtoe13)):
> toe23_cmll2_cross_f:=subs(from_leg1_to_leg2,subs(from_toe13_to_toe23_sset,toe13_cmll1_cross_f)):
> toe23_list:=subs(from_leg1_to_leg2,subs(from_toe13_to_toe23_sset,toe13_list)):
```

```
> dset23:=subs(from_leg1_to_leg2,subs(from_toe13_to_toe23_sset,dset13)):
Second foot second toe 24
> x24_args:=x23_args:
> y24_args:=y23_args:
    z24_args:=z23_args:
vx24_args:=vx23_args:
vy24_args:=vy23_args:
vz24_args:=vz23_args:
> from_toe23_to_toe24_sset:={
                                                                                            xt23=xt24,yt23=yt24,zt23=zt24,
rl2l1=rl2l1,r2l12=rl2l2,rl2l3=rl2l3,
toefx(stat23,x23(x23_args))=toefx(stat24,x24(x24_args)),
                                                                                             toefy(stat23,y23(y23_args))=toefy(stat24,y24(y24_args)),
                                                                                            toefz(stat23,z23(z23_args))=toefz(stat24,z24(z24_args)),
                                                                                            x23=x24, vx23=vx24,
                                                                                            y23=y24, vy23=vy24
z23=z24, vz23=vz24
stat23=stat24,
                                                                                            p13=p15,p14=p16,
                                                                                             seq(dx23d.i=dx24d.i,i=x24\_args),
                                                                                            seq(dvx23d.i=dvx24d.i,i=vx24_args),
                                                                                             seq(dy23d.i=dy24d.i,i=y24_args),
                                                                                            seq(dvy23d.i=dvy24d.i,i=vy24_args),
                                                                                             seq(dz23d.i=dz24d.i,i=z24_args),
                                                                                            seq(dvz23d.i=dvz24d.i,i=vz24_args),
                                                                                            fx\dot{2}\dot{3}=fx24, fy23=fy24, f\dot{z}23=fz2\bar{4}
                                                                                            tx23=tx24,ty23=ty24,tz23=tz24:

/ rtoe24:=subs(from_toe23_to_toe24_sset,rtoe23):
/ vtoe24:=subs(from_toe23_to_toe24_sset,vtoe23]:
/ vtoe24:=subs(from_toe23_to_toe24_sset,toe23_cml12_cross_f):
/ toe24_cml12_cross_f:=subs(from_toe23_to_toe24_sset,toe23_list):
/ dset24:=subs(from_toe23_to_toe24_sset,dset23):
/ dset24:=subs(from_toe23_toe24_sset,dset23):
/ dset24:=subs(from_toe23_toe24_sset,dset23):
/ dset24:=subs(from_toe23_toe24_sset,dset23):
/ dset24:=subs(from_toe23_toe24_sset,dset23):
/ dset24:=subs(from_toe23_toe24_sset,dset23):
/ dset24:=subs(from_toe23_toe24_sset,dset23):
/ dset24:=subs(from_toe24_sset,dset23):
/ dset24:=subs(from_toe24_sset,dset23_toe24_sset,dset23_toe24_sset,dset23_toe2
Knee & Hip for leg 1 & 2
> knee1_list:=[Tleg11=knee(statk1,q8,u8,knee_k,knee_d,knee_d_reb)]:
> knee2_list:=[Tleg2l=knee(statk2,q10,u10,knee_k,knee_d,knee_d_reb)]:
             diff(knee(statk1,q8,u8,knee_k,knee_d,knee_d_reb),q8)
                              = knee_q(statk1,q8,u8,knee_k,knee_d,knee_d_reb),
             diff(knee(statk1,q8,u8,knee_k,knee_d,knee_d_reb),u8)
                            = knee_u(statk1,q8,u8,knee_k,knee_d,knee_d_reb)
             diff(knee(statk2,q10,u10,knee_k,knee_d,knee_d_reb),q10)
                                = knee_q(statk2,q10,u10,knee_k,knee_d,knee_d_reb),
            diff(knee(statk2,q10,u10,knee_k,knee_d,knee_d_reb),u10)
                                 = knee_u(statk2,q10,u10,knee_k,knee_d,knee_d_reb)]:
> hip1_list:=[Tleg1=hip(q4,q7,u4,u7,hip_k,hip_delta,hip_d)]:
> hip2_list:=[Tleg2=hip(q4,q9,u4,u9,hip_k,hip_delta,hip_d)]:
            \frac{1}{\text{diff}(\text{hip}(q4,q7,u4,u7,\text{hip\_k},\text{hip\_delta,hip\_d}),u4)} = \frac{1}{\text{hip\_u}_1(q4,q7,u4,u7,\text{hip\_k},\text{hip\_delta},\text{hip\_d})},
              \label{eq:diff_hip_qu_2} \text{diff} \left( \text{hip}(\vec{q}4, \vec{q}7, u4, u7, \text{hip}\_k, \text{hip}\_d \text{elta}, \text{hip}\_d \right), u7 \right) = \text{hip}\_u\_2 \\ (\vec{q}4, \vec{q}7, u4, u7, \text{hip}\_k, \text{hip}\_d \text{elta}, \text{hip}\_d), u7 \\ ) = \text{hip}\_u\_2 \\ (\vec{q}4, \vec{q}7, u4, u7, \text{hip}\_k, \text{hip}\_d \text{elta}, \text{hip}\_d), u7 \\ ) = \text{hip}\_u\_2 \\ (\vec{q}4, \vec{q}7, u4, u7, \text{hip}\_k, \text{hip}\_d \text{elta}, \text{hip}\_d), u7 \\ ) = \text{hip}\_u\_2 \\ (\vec{q}4, \vec{q}7, u4, u7, \text{hip}\_k, \text{hip}\_d \text{elta}, \text{hip}\_d), u7 \\ ) = \text{hip}\_u\_2 \\ (\vec{q}4, \vec{q}7, u4, u7, \text{hip}\_k, \text{hip}\_d \text{elta}, \text{hip}\_d), u7 \\ ) = \text{hip}\_u\_2 \\ (\vec{q}4, \vec{q}7, u4, u7, \text{hip}\_k, \text{hip}\_d \text{elta}, \text{hip}\_d), u7 \\ ) = \text{hip}\_u\_2 \\ (\vec{q}4, \vec{q}7, u4, u7, \text{hip}\_k, \text{hip}\_d \text{elta}, \text{hip}\_d), u7 \\ ) = \text{hip}\_u\_2 \\ (\vec{q}4, \vec{q}7, u4, u7, \text{hip}\_k, \text{hip}\_d \text{elta}, \text{hip}\_d), u7 \\ ) = \text{hip}\_u\_2 \\ (\vec{q}4, \vec{q}7, u4, u7, \text{hip}\_k, \text{hip}\_d \text{elta}, \text{hip}\_d), u7 \\ ) = \text{hip}\_u\_2 \\ (\vec{q}4, \vec{q}7, u4, u7, \text{hip}\_k, \text{hip}\_d \text{elta}, \text{hip}\_d), u7 \\ ) = \text{hip}\_u\_2 \\ (\vec{q}4, \vec{q}7, u4, u7, \text{hip}\_k, \text{hip}\_d \text{elta}, \text{hip}\_d \text{elta},
            diff(hip(q4,q9,u4,u9,hip_k,hip_delta,hip_d),q4) = hip_q_1(q4,q9,u4,u9,hip_k,hip_delta,hip_d), diff(hip(q4,q9,u4,u9,hip_k,hip_delta,hip_d),q9) = hip_q_2(q4,q9,u4,u9,hip_k,hip_delta,hip_d),
            diff(hip(q4,q9,u4,u9,hip_k,hip_delta,hip_d),u4) = hip_u_1(q4,q9,u4,u9,hip_k,hip_delta,hip_d),
diff(hip(q4,q9,u4,u9,hip_k,hip_delta,hip_d),u9) = hip_u_2(q4,q9,u4,u9,hip_k,hip_delta,hip_d)]:
Forces and torques
> Fbody:=N &ev [0, -m_body*g*cos(theta), -m_body*g*sin(theta)]:
> Tbody:=T2 &ev [Tleg1+Tleg2,0,0]:
> Fleg1upper:=N &ev [0,-ml1u*g*cos(theta),-ml1u*g*sin(theta)]:
> Tleg1upper:=T2 &ev [-Tleg1+Tleg11,0,0]:
> Fleg2upper:=N &ev [0,-ml2u*g*cos(theta),-ml2u*g*sin(theta)]:
> Tleg2upper:=T2 &ev [-Tleg2+Tleg21,0,0]:
 > Fleg1lower: =N &ev [fx11+fx12+fx13+fx14,
                                                                   fy11+fy12+fy13+fy14-ml11*g*cos(theta)
                                                                   fz11+fz12+fz13+fz14-ml11*g*sin(theta)]:
> Tlegilower:=(UL1 &ev [-Tlegil,0,0]) &++ (N &ev [tx11+tx12+tx13+tx14 ty11+ty12+ty13+ty14]
                                                                                                                                                                tz11+tz12+tz13+tz14]):
> Fleg2lower:=N &ev [fx21+fx22+fx23+fx24,
```

```
fy21+fy22+fy23+fy24-m121*g*cos(theta)
                                                                                                    fz21+fz22+fz23+fz24-ml21*g*sin(theta)]:
   > Tleg2lower:=(UL2 &ev [-Tleg21,0,0]) &++ (N &ev [tx21+tx22+tx23+tx24, ty21+ty22+ty23+ty24,
                                                                                                                                                                                                                                      tz21+tz22+tz23+tz24]):
   Kanes method
   https://documents.com/pkt.sc/pkt.sc/pkt.sc/pkt.sc/pkt.sc/pkt.sc/pkt.sc/pkt.sc/pkt.sc/pkt.sc/pkt.sc/pkt.sc/pkt.sc/pkt.sc/pkt.sc/pkt.sc/pkt.sc/pkt.sc/pkt.sc/pkt.sc/pkt.sc/pkt.sc/pkt.sc/pkt.sc/pkt.sc/pkt.sc/pkt.sc/pkt.sc/pkt.sc/pkt.sc/pkt.sc/pkt.sc/pkt.sc/pkt.sc/pkt.sc/pkt.sc/pkt.sc/pkt.sc/pkt.sc/pkt.sc/pkt.sc/pkt.sc/pkt.sc/pkt.sc/pkt.sc/pkt.sc/pkt.sc/pkt.sc/pkt.sc/pkt.sc/pkt.sc/pkt.sc/pkt.sc/pkt.sc/pkt.sc/pkt.sc/pkt.sc/pkt.sc/pkt.sc/pkt.sc/pkt.sc/pkt.sc/pkt.sc/pkt.sc/pkt.sc/pkt.sc/pkt.sc/pkt.sc/pkt.sc/pkt.sc/pkt.sc/pkt.sc/pkt.sc/pkt.sc/pkt.sc/pkt.sc/pkt.sc/pkt.sc/pkt.sc/pkt.sc/pkt.sc/pkt.sc/pkt.sc/pkt.sc/pkt.sc/pkt.sc/pkt.sc/pkt.sc/pkt.sc/pkt.sc/pkt.sc/pkt.sc/pkt.sc/pkt.sc/pkt.sc/pkt.sc/pkt.sc/pkt.sc/pkt.sc/pkt.sc/pkt.sc/pkt.sc/pkt.sc/pkt.sc/pkt.sc/pkt.sc/pkt.sc/pkt.sc/pkt.sc/pkt.sc/pkt.sc/pkt.sc/pkt.sc/pkt.sc/pkt.sc/pkt.sc/pkt.sc/pkt.sc/pkt.sc/pkt.sc/pkt.sc/pkt.sc/pkt.sc/pkt.sc/pkt.sc/pkt.sc/pkt.sc/pkt.sc/pkt.sc/pkt.sc/pkt.sc/pkt.sc/pkt.sc/pkt.sc/pkt.sc/pkt.sc/pkt.sc/pkt.sc/pkt.sc/pkt.sc/pkt.sc/pkt.sc/pkt.sc/pkt.sc/pkt.sc/pkt.sc/pkt.sc/pkt.sc/pkt.sc/pkt.sc/pkt.sc/pkt.sc/pkt.sc/pkt.sc/pkt.sc/pkt.sc/pkt.sc/pkt.sc/pkt.sc/pkt.sc/pkt.sc/pkt.sc/pkt.sc/pkt.sc/pkt.sc/pkt.sc/pkt.sc/pkt.sc/pkt.sc/pkt.sc/pkt.sc/pkt.sc/pkt.sc/pkt.sc/pkt.sc/pkt.sc/pkt.sc/pkt.sc/pkt.sc/pkt.sc/pkt.sc/pkt.sc/pkt.sc/pkt.sc/pkt.sc/pkt.sc/pkt.sc/pkt.sc/pkt.sc/pkt.sc/pkt.sc/pkt.sc/pkt.sc/pkt.sc/pkt.sc/pkt.sc/pkt.sc/pkt.sc/pkt.sc/pkt.sc/pkt.sc/pkt.sc/pkt.sc/pkt.sc/pkt.sc/pkt.sc/pkt.sc/pkt.sc/pkt.sc/pkt.sc/pkt.sc/pkt.sc/pkt.sc/pkt.sc/pkt.sc/pkt.sc/pkt.sc/pkt.sc/pkt.sc/pkt.sc/pkt.sc/pkt.sc/pkt.sc/pkt.sc/pkt.sc/pkt.sc/pkt.sc/pkt.sc/pkt.sc/pkt.sc/pkt.sc/pkt.sc/pkt.sc/pkt.sc/pkt.sc/pkt.sc/pkt.sc/pkt.sc/pkt.sc/pkt.sc/pkt.sc/pkt.sc/pkt.sc/pkt.sc/pkt.sc/pkt.sc/pkt.sc/pkt.sc/pkt.sc/pkt.sc/pkt.sc/pkt.sc/pkt.sc/pkt.sc/pkt.sc/pkt.sc/pkt.sc/pkt.sc/pkt.sc/pkt.sc/pkt.sc/pkt.sc/pkt.sc/pkt.sc/pkt.sc/pkt.sc/pkt.sc/pkt.sc/pkt.sc/pkt.sc/pkt.sc/pkt.sc/pkt.sc/pkt.sc/pkt.sc/pkt.sc/pkt.sc/pkt.sc/pkt.sc/pkt.sc/pkt.sc/pkt.sc/pkt.sc/pkt.sc/pkt.sc/pkt.sc/pkt.sc/pkt.sc/pkt
                                        \verb|mkc(Tbody)|, \verb|mkc(Tleg1upper)|, \verb|mkc(Tleg2upper)|, \verb|mkc(Tleg1lower)|| :
   > kane_eq:=map(simplify,ckane(tauK,pKt,RKt)):
   Export of dyn eqs to Mathlab
    Common subexpressions
  > common stdeaplessions
> cse:=[op(toe11_list),op(toe12_list),op(toe13_list),op(toe14_list),
> op(toe21_list),op(toe22_list),op(toe23_list),op(toe24_list),
> op(knee1_list),op(knee2_list),
                                        \verb"op"(hip1_list")", \verb"op"(hip2_list")"]":
   Translating differentiated functions into the appropriate c-function calls
  > uts := [u1t,u2t,u3t,u4t,u5t,u6t,u7t,u8t,u9t,u10t]:

> kde_new_ordered:=[seq(q.i.t=subs(kde_new,q.i.t),i=1..10),
  seq(p.i.t=subs(kde_new,p.i.t),i=1..16),

seq(p.i.t=subs(kde_new,p.i.t),i=1..16),

seq(theta.i.t=0,i=1..6)]:

> qts := [q1t,q2t,q3t,q4t,q5t,q6t,q7t,q8t,q9t,q10t,

p1t,p2t,p3t,p4t,p5t,p6t,p7t,p8t,p9t,p10t,p11t,p12t,p13t,p14t,p15t,p16t,
  pri,p2s,p3s,p4s,p3s,p0s,p1s,p1s,p1s,p1s,p1s,p1s
theta1t,theta2t,theta3t,theta4t,theta5t,theta6t]:
> vars:=[q1,q2,q3,q4,q5,q6,q7,q8,q9,q10,
    p1,p2,p3,p4,p5,p6,p7,p8,p9,p10,p11,p12,p13,p14,p15,p16,
    theta1,theta2,theta3,theta4,theta5,theta6,
    u1,u2,u3,u4,u5,u6,u7,u8,u9,u10]:
  > para:=[

> rx,ry,rz,

> rl11,rl21,

> rl1u1,rl1u2,rl1u3,

> rl2u1,rl2u2,rl2u3,
> r11u1,r11u2,r11u3,
> r12u1,r12u2,r12u3,
> 11u,12u,
> r1111,r1112,r1113,
> r1211,r1212,r1213,
> I_B11,I_B22,I_B33,I_B12,I_B13,I_B23,
> I_LU111,I_LU122,I_LU133,I_LU112,I_LU113,I_LU123,
> I_LU211,I_LU222,I_LU233,I_LU212,I_LU213,I_LU223,
> I_LL111,I_LL122,I_LL133,I_LL112,I_LL113,I_LL123,
> I_LL211,I_LL22,I_LL233,I_LL12,I_LL213,I_LL223,
> m_body,ml1u,ml2u,ml11,ml21,g,theta,
> kX,dX,kY,dY,kZ,dZ,
> knee_k,knee_d,knee_d_reb,
> hip_k,hip_delta,hip_d,
> statk1,statk2,
> xt11,yt11,zt11,stat11,
> xt12,yt12,zt12,stat12,
> xt13,yt13,zt13,stat13,
> xt14,yt14,zt14,stat14,
> xt21,yt21,zt21,stat21,
> xt22,yt22,zt22,stat22,
> xt23,yt23,zt23,stat23,
> xt24,yt24,zt24,stat24,
> rein_t nein2
   > xt24,yt24,zt24,stat24,
> poin1,poin2,
   > 111,121]:
> b:=[
                                              [y11=rtoe11 &c 2,y12=rtoe12 &c 2,y13=rtoe13 &c 2, y14=rtoe14 &c 2,y13=rtoe13 &c 2, y14=rtoe14 &c 2,y13=rtoe13 &c 2,y14=rtoe14 &c 2,y13=rtoe13 &c 2,y14=rtoe14 &c 2,y13=rtoe13 &c 2,y14=rtoe14 &c 2,y14=rtoe14
                                                  y21=rtoe21 &c 2,y22=rtoe22 &c 2,y23=rtoe23 &c 2, y24=rtoe24 &c 2],
                                              [y11,y12,y13,y14,y21,y22,y23,y24,q8,q10,q7,q9]
                                         [1,1,1,1,1,1,1,1,1,1,1,1],
[stat11,stat12,stat13,stat14,stat21,stat22,stat23,stat24,statk1,statk2,poin1,poin2]
   > ]:
> inc:='includes'=['','walker_3D_external.c','']:
> path:='':
   Simulation
   > exmex('walker_3D_8_ankle2',path,[[op(kde_new_ordered)]],[kane_eq,uts],[op(subs(dset,cse))],
                                         [op(qts),op(uts)], vars, parameters=para, 'v5'=['events'=b], inc);
```

```
Toeposfunc
    Toeposium:

> toe11 := matrix(1,3,[rtoe11 &c 1, rtoe11 &c 2, rtoe11 &c 3]):

> toe12 := matrix(1,3,[rtoe12 &c 1, rtoe12 &c 2, rtoe12 &c 3]):

> toe13 := matrix(1,3,[rtoe13 &c 1, rtoe13 &c 2, rtoe13 &c 3]):

> toe14 := matrix(1,3,[rtoe14 &c 1, rtoe14 &c 2, rtoe14 &c 3]):

> toe21 := matrix(1,3,[rtoe21 &c 1, rtoe21 &c 2, rtoe21 &c 3]):

> toe22 := matrix(1,3,[rtoe22 &c 1, rtoe22 &c 2, rtoe22 &c 3]):

> toe23 := matrix(1,3,[rtoe23 &c 1, rtoe23 &c 2, rtoe23 &c 3]):

> toe24 := matrix(1,3,[rtoe24 &c 1, rtoe24 &c 2, rtoe24 &c 3]):
     Export
   Export
> exmat('da_toe11_8_toe',path,toe11,vars,para,'matlab');
> exmat('da_toe12_8_toe',path,toe12,vars,para,'matlab');
> exmat('da_toe13_8_toe',path,toe13,vars,para,'matlab');
> exmat('da_toe14_8_toe',path,toe14,vars,para,'matlab');
> exmat('da_toe21_8_toe',path,toe21,vars,para,'matlab');
> exmat('da_toe22_8_toe',path,toe22,vars,para,'matlab');
> exmat('da_toe23_8_toe',path,toe23,vars,para,'matlab');
> exmat('da_toe24_8_toe',path,toe24,vars,para,'matlab');
    > exmat('da_T2toN_8_toe',path,Rmx(N,T2),vars,'matlab');
> exmat('da_UL1toT2_8_toe',path,Rmx(T2,UL1),vars,'matlab');
> exmat('da_UL2toT2_8_toe',path,Rmx(T2,UL2),vars,'matlab');
> exmat('da_LL1toUL1_8_toe',path,Rmx(UL1,LL1),vars,'matlab');
> exmat('da_LL2toUL2_8_toe',path,Rmx(UL2,LL2),vars,'matlab');
      > exmat('da_F1toLL1_8_toe',path,Rmx(LL1,F1),vars,'matlab');
     > exmat('da_F2toLL2_8_toe',path,Rmx(LL2,F2),vars,'matlab');
     Export of dynamical and variational eqs to matlab
      diffset=dset,'v5'=['events'=b],inc);
      Constructing the mapping matrices for discontinous forces % \left( 1\right) =\left( 1\right) \left( 1\right) \left(
     > qus:=[seq(q.i,i=1..10),seq(p.i,i=1..16),
seq(theta.i,i=1..6),seq(u.i,i=1..10)];
   seq(theta.i,i=1..6),so
> mxtoe11 := matrix(42,1,[]);
> mxtoe12 := matrix(42,1,[]);
> mxtoe13 := matrix(42,1,[]);
> mxtoe14 := matrix(42,1,[]);
> mxtoe21 := matrix(42,1,[]);
> mxtoe22 := matrix(42,1,[]);
> mxtoe23 := matrix(42,1,[]);
> mxtoe24 := matrix(42,1,[]);
> i:=1;
> for ii in qus do
> mxtoe11[i.1]:=diff(rtoe11
                         mxtoe11[i,1]:=diff(rtoe11 &c 2, ii);

mxtoe12[i,1]:=diff(rtoe12 &c 2, ii);

mxtoe13[i,1]:=diff(rtoe13 &c 2, ii);

mxtoe14[i,1]:=diff(rtoe14 &c 2, ii);
                           mxtoe14[1,1]:=diff(rtoe21 &c 2, i1);
mxtoe22[i,1]:=diff(rtoe22 &c 2, ii);
mxtoe22[i,1]:=diff(rtoe22 &c 2, ii);
mxtoe23[i,1]:=diff(rtoe23 &c 2, ii);
mxtoe24[i,1]:=diff(rtoe24 &c 2, ii);
i:=i+1;
                                             p9,p10,p11,p12,p13,p14,p15,p16,seq(theta.i,i=1..6),seq(u.i,i=1..10)]:
     > G14:=[seq(q.i,i=1..10),p1,p2,p3,p4,p5,p6,(rtoe14 &c 1)-q1,(rtoe14 &c 3)-q3,
                                            p9,p10,p11,p12,p13,p14,p15,p16,seq(theta.i,i=1..6),seq(u.i,i=1..10)]:
     > G21:=[seq(q.i,i=1..10),p1,p2,p3,p4,p5,p6,p7,p8,(rtoe21 &c 1)-q1,(rtoe21 &c 3)-q3,
                                            p11,p12,p13,p14,p15,p16,seq(theta.i,i=1..6),seq(u.i,i=1..10):
     > G22:=[seq(q.i,i=1..10),p1,p2,p3,p4,p5,p6,p7,p8,p9,p10,(rtoe22 &c 1)-q1,
                                               (rtoe22 &c 3)-q3,p13,p14,p15,p16,seq(theta.i,i=1..6),seq(u.i,i=1..10)]:
```